



HAL
open science

Virtual reconstruction of the skull of *Bernissartia fagesii* and current understanding of the neosuchian–eusuchian transition

Jeremy Martin, Thierry Smith, Celine Salaviale, Jérôme Adrien, Massimo Delfino

► To cite this version:

Jeremy Martin, Thierry Smith, Celine Salaviale, Jérôme Adrien, Massimo Delfino. Virtual reconstruction of the skull of *Bernissartia fagesii* and current understanding of the neosuchian–eusuchian transition. *Journal of Systematic Palaeontology*, 2020, pp.1-23. 10.1080/14772019.2020.1731722 . hal-02513657

HAL Id: hal-02513657

<https://hal.science/hal-02513657>

Submitted on 16 Nov 2020

HAL is a multi-disciplinary open access archive for the deposit and dissemination of scientific research documents, whether they are published or not. The documents may come from teaching and research institutions in France or abroad, or from public or private research centers.

L'archive ouverte pluridisciplinaire **HAL**, est destinée au dépôt et à la diffusion de documents scientifiques de niveau recherche, publiés ou non, émanant des établissements d'enseignement et de recherche français ou étrangers, des laboratoires publics ou privés.

Virtual reconstruction of the skull of *Bernissartia fagesii* and current understanding of the neosuchian–eusuchian transition

Jeremy E. Martin^{a,*}, Thierry Smith^b, Céline Salaviale^a, Jérôme Adrien^c and Massimo Delfino^{d,e}

^aUniv. Lyon, ENS de Lyon, Université Claude Bernard Lyon 1, CNRS, UMR 5276
Laboratoire de Géologie de Lyon: Terre, Planètes, Environnement, F-69342 46 Allée d'Italie,
Lyon, France, jeremy.martin@ens-lyon.fr;

^bRoyal Belgian Institute of Natural Sciences, Directorate Earth and History of Life, Rue
Vautier 29, B-1000 Brussels, Belgium;

^cUniversité de Lyon, INSA-Lyon, UMR CNRS 5510 MATEIS, 7 Avenue Jean Capelle,
69621, Villeurbanne Cedex, France, jerome.adrien@insa-lyon.fr;

^dDipartimento di Scienze della Terra, Università di Torino, Via Valperga Caluso 35, 10125
Torino, Italy ;

^eInstitut Català de Paleontologia Miquel Crusafont, Universitat Autònoma de Barcelona,
Edifici ICTAICP, Carrer de les Columnes s/n, Campus de la UAB, 08193 Cerdanyola del
Vallès, Barcelona, Spain

*Corresponding author

Since the description of *Isisfordia duncani*, a number of new extinct species and revisions of previous species have prompted a variety of contradicting phylogenetic hypotheses on the

topology of the Neosuchia. As a consequence, a consensus on the rooting of Eusuchia in relation to other neosuchian clades has not been reached and the origin of the group remains unsettled. Exemplifying this, *Bernissartia fagesii* from the Early Cretaceous of Belgium has long been considered a key taxon for understanding the origin of Eusuchia, but more recent hypotheses found support for a more basal position, as an ally to goniopholidids, paralligatorids or atoposaurids. Because many details of the anatomy of the type specimen are hidden by glue and sediment still adhering to the fossils, a number of characters are pending confirmation. Based on computed tomography data, we extract bones of the cranium and mandibles, describe new characters and re-evaluate anatomical details in the lectotype specimen. Our phylogenetic analysis confirms that *B. fagesii* is a derived neosuchian, unrelated to atoposaurids, goniopholidids and paralligatorids. We recover *B. fagesii* and *Koumpiodontosuchus aprosdokiti* in a basal position within Eusuchia, together with Suisuchidae, a group of gondwanan neosuchians containing *Suisuchus* and *Isisfordia*, which are here forming a polytomy with Hylaeochampsidae. The presence-absence of pterygoid-bound internal choanae cannot be used to fully resolve relationships at the neosuchian-eusuchian transition because of the variability of this character even at the familial level as recently reported within suisuchids and bernissartiids. There is no doubt that true eusuchians were present in Laurasia as early as the Early Cretaceous, the hylaeochampsid *Hylaeochampsia vectiana* being the oldest (Barremian) undoubted representative. But whether the Eusuchia were also present in southern landmasses depends on solving the phylogenetic position of suisuchids and other less known gondwanan forms within or outside Eusuchia.

Keywords: Eusuchia, Neosuchia, Cretaceous, Europe, phylogeny, ecology

Introduction

Semi-aquatic crocodylomorphs are ubiquitous in freshwater ecosystems since at least the Cretaceous. Hypotheses on the origin of modern eusuchian crocodylomorphs rely on a stable phylogenetic framework at the neosuchian–eusuchian transition. A consensus on the content forming the base of Eusuchia is in constant flux and the interrelationships of several neosuchian groups remain unsettled. Phylogenetic hypotheses about the origin and evolution of modern members have been intensely debated since the description of the Cretaceous *Isisfordia duncani* from Australia, originally interpreted as the oldest eusuchian representative (Salisbury *et al.* 2006). Although a number of taxa from Gondwana were at that time known from poorly preserved specimens (Stromer 1933; Gasparini & Buffetaut 1980; Michard *et al.* 1990), the discovery of *Isisfordia duncani* shifted the general paradigm about the origin of eusuchians from northern to southern landmasses. Recently, *I. duncani* has been re-interpreted as a derived neosuchian (Turner & Pritchard 2015) opening the way for a reassessment of other neosuchian lineages (Turner 2015). Yet, a consensus on neosuchian relationships remains fragile with several lineages, including susisuchids, goniopholidids, atoposaurids, paralligatorids, pholidosaurids, and dyrosaurids, characterized by labile phylogenetic positions (e.g. Leite & Fortier 2018). *Bernissartia fagesii* from the lower Cretaceous of Belgium has often been, and is still used as an outgroup taxon in phylogenetic analyses (e.g. Brochu 1999; Sookias 2019) but recent hypotheses do not confidently solve its phylogenetic position, discussing several alternatives (e.g. Turner 2015; Turner & Pritchard 2015). The uncertain phylogenetic position of *B. fagesii* partly arises from its possession of a mix of plesiomorphic and derived traits as recognized by previous authors (Buffetaut 1975; Norell & Clark 1990; Turner & Pritchard 2015) as well as from its state of preservation.

The type series of *B. fagesii* is represented by two specimens (IRSNB R46 and IRSNB R118) recovered in 1879 from the Barremian-Aptian coal mine at Bernissart (Dollo 1883)

from the same horizon as two specimens of the goniopholidid *Anteophthalmosuchus hooleyi* (Martin *et al.* 2016a) and many skeletons of the ornithopod *Iguanodon bernissartensis* (Godefroit *et al.* 2012). Noteworthy is that, contrary to previous assignments, one of the Lavalette historical drawings of the Bernissart crocodylomorphs probably does not correspond to Dollo's goniopholidid (Bultynck 1989; Fig. 2A in Martin *et al.* 2016a) but to *B. fagesii* (specimen IRSNB R46) before it was mounted for display. *B. fagesii* has been reported from several Cretaceous localities in Europe including England (Buffetaut & Ford 1979), Spain (Buscalioni *et al.* 1984; Buscalioni & Sanz 1990) and France (Mazin & Pouech 2008). Dollo (1883) described *B. fagesii* as a close ally to the Eusuchia. This view has been contradicted by Buffetaut (1975); then it was partly defended (Norell & Clark 1990; Salisbury *et al.* 2006) viewing *B. fagesii* as an advanced neosuchian; more recent studies (Turner 2015; Turner & Pritchard 2015) presented two alternative hypotheses, with *B. fagesii* either as an outgroup to the crown group or as a member of the Paralligatoridae.

The most comprehensive anatomical accounts of *B. fagesii* are those of Buffetaut (1975) and Norell & Clark (1990), both debating the nature of the choanae. Allegedly, several characters are poorly preserved due to the crushed nature of the delicate historical specimen, which is covered by a layer of sediment and glue.

In order to solve this problem, here we discuss new anatomical information derived from computed tomography (CT) data of the lectotype specimen IRSNB R46 (Fig. 1), a nicely preserved skull with mandibles. We explore its phylogenetic position and also take the opportunity to discuss the spatiotemporal distribution of Bernissartidae and their feeding ecology.

Material and methods

Computed tomography scan parameters

The skull and mandibles of IRSNB R46 (Dollo 1883) have been scanned at the X-ray facility of the Laboratoire Mateis (INSA, Lyon) at a voxel size of 39 μm . The specimen was scanned with a vtomex laboratory X-ray computed tomograph (GE Phoenix | X-Ray GmbH) equipped with a 160 kV nano-focus tube, a tungsten transmitting target, and a 1920 \times 1536 pixel Varian detector. Scanning parameters were set to 140 kV tube voltage and 90 μA current with a voxel size of 39 μm . A single scan consists of 1200 2D radiographs and an averaging 5 images at each step angle. The exposure time for one radiograph was 0,333 s. Three scans were performed in order to analyse the entire specimen. These parameters resulted in a measurement period of 2 hours. The volume was reconstructed in phoenix dataview (Version 2.1, GE Sensing & Inspection Technologies) using the conventional 2D filtered back projection algorithm. Volume rendering and processing of scans were completed with the Avizo software (version Avizo Lite 9.0.1)

Phylogenetic analysis

Following our new observations, *Bernissartia fagesii* was entirely re-coded in a previously published matrix (Turner & Pritchard 2015) incorporating three new characters and totalling 345 characters and 66 taxa (Appendix 1). Because the present study focuses on derived neosuchians, Notosuchia and Thalattosuchia were not included in the analysis. We decided to exclude *Pachycheilosuchus trinquei* and *Gilchristosuchus palatinus* due to their fragmentary nature, the first being represented by a composite skeleton (Rogers 2003); the second being represented by a partial skull table (Wu & Brinkman 1993). We coded the bernissartiid *Koumpiodontosuchus aprosdokiti* according to its recent description (Sweetman *et al.* 2014).

A phylogenetic analysis was performed under the software TNT version 1.1. (Goloboff *et al.* 2008). A traditional search included replicates of 1000 random addition sequences (Wagner trees) followed by two rounds of TBR branch-swapping (10 trees retained by replication), the later one executed using the most parsimonious trees obtained in the first search and stored in the RAM.

Character definitions

Pholidosaurus and *Sarcosuchus* were recoded as 49[0] according to previous observations of the cranioquadrate passage, which is open in these two taxa (Martin *et al.* 2016c). *Susisuchus anatoceps* was recoded as 49[2], as in *Isisfordia duncani*, following the observation provided in Salisbury *et al.* (2006). Following recent observations from Leite & Fortier (2018), codings for *Susisuchus anatoceps* were amended for the eusuchian type palate -43[1]- and procoelous condition in cervical vertebrae -92[1].

One state was added to character 207 [2: expanding on jugal as maxillojugal depression] in order to match previous work on the maxillary depression among goniopholidids and pholidosaurids (Martin & Buffetaut 2012).

Three new characters were added: character 343 (modified from character 414 in Martin *et al.*, 2016c): posterior margin of suborbital process of ectopterygoid in ventral view: straight or concave [0], convex [1]; character 344 (modified from character 52 in Brochu (1999): large, laterally displaced and adjoining maxillary and dentary alveoli holding double caniniform dentition: absent [0], present [1]; character 345: posterior margin of the pterygoid wing: mediolaterally oriented [0], or posterolaterally oriented being straight or concave [1].

Systematic palaeontology

Crocodylomorpha Walker, 1970

Mesoeucrocodylia Whetstone & Whybrow, 1983

Neosuchia Benton & Clark, 1988

Bernissartiidae Dollo, 1883

Bernissartia Dollo, 1883

Bernissartia fagesii Dollo, 1883

(Figs 1–10)

Lectotype. IRSNB R46, an articulated skeleton including a complete skull with mandibles.

Locality and Horizon. Coal mine of Bernissart, Belgium; Early Cretaceous, latest Barremian–earliest Aptian after Yans *et al.* (2012).

Revised diagnosis. Updated from Buffetaut (1975) and Norell & Clark (1990). *Bernissartia fagesii* is a small neosuchian with a total body length inferior to a meter and a mesorostrine skull with a rostrum to skull length ratio of 0.54. *B. fagesii* can be diagnosed by the following autapomorphies: presence of a peg on the lacrimal that interlocks with the maxilla; developed convex orbital margin of jugal. In addition, *B. fagesii* possesses the following combination of characters: nasals participating in the external nares; lacrimals slightly longer than the prefrontals; lacrimals contacting the nasals for a short distance; lacrimal with a smooth notch in its orbital margin; interorbital portion of frontal narrower than one orbital width; absence of periorbital ridge; quadratojugal excludes quadrate from posterodorsal margin of lower temporal fenestra; foramen aereum opens on the dorsomedial edge of the quadrate; quadratojugal hides quadrate in lateral view; laterally opened cranioquadrate groove; supratemporal fenestrae smaller than orbits; long squamosals building more than two-third the lateral margin of the skull table; squamosals with smooth posterior processes; frontoparietal suture within the level of the supratemporal fenestrae and participation of the frontal in them; small incisive foramen opening entirely into the premaxillae; narrow and elongated palatine

branches that barely enter into the maxillary palate; internal choanae bounded anteriorly by palatines and posteriorly by pterygoids; wide branches of the ectopterygoids with a straight suborbital margin; longer than wide suborbital fenestrae; lateral profile of upper and lower jaws sinusoidal; five premaxillary alveoli; sixteen maxillary alveoli including large and closely spaced alveoli 4 + 5 for caniniform dentition; twenty dentary alveoli including large and confluent dentary alveoli 3 + 4; tribodonty of last three maxillary and dentary teeth; last maxillary and dentary alveoli set in a groove; excavated pit at the premaxillary-maxillary suture for reception of caniniform dentary teeth; short mandibular symphysis encompassing the first five dentary alveoli; splenial modest participation into mandibular symphysis; presence of a bony shelf medial to the tribodont dentition in both maxillae and splenials; retroarticular process in a ventral position relative to the jaw joint; thin ventral margin of the angular for M. pterygoideus posterior; absence of external mandibular fenestra; amphicoelous cervical and thoracal vertebrae; biconvex first caudal vertebra; procoelous caudal vertebrae; dorsal osteoderms organised in two rows; double-keeled dorsal osteoderms; imbricated ventral osteoderms.

Description

General description and preservation. *Bernissartia fagesii* is a small taxon, the complete skeleton (IRSNB R46), as reconstructed, measuring a little more than 60 cm from the tip of the rostrum to the last preserved caudal vertebra. This total body length is within the range of other Cretaceous taxa known from complete skeletons that remain below or surpass a meter long such as *Isisfordia duncani*, *Susisuchus anatoceps*, *Pietraroiasuchus ormezanoi* or *Brillanceausuchus babouriensis* (Michard *et al.* 1990; Salisbury *et al.* 2003; Salisbury *et al.* 2006; Buscalioni *et al.* 2011). Several other Cretaceous taxa, known only from skulls, may

not have surpassed this size range (*Acynodon*, *Theriosuchus*) whereas goniopholidids and perhaps paralligatorids were substantially larger (Martin *et al.* 2016b) but not attaining the observed size of *Allodaposuchus* (Martin *et al.* 2016a).

Bernissartia fagesii has been previously described as having a brevirostrine skull but its rostrum to skull length ratio of 0.54 indicates a mesorostrine skull similar to that of *Allodaposuchus* (0.51 in the Velaux adult specimen) or *Diplocynodon* (*D. remensis* = 0.58) and slightly shorter than *Susisuchus anatoceps* (0.6), *Paralligator gradilifrons* (0.62), *I. duncani* (0.63) and *Pietraroiasuchus* (0.64). Goniopholidids have even longer rostrum (0.67 ref). On the other hand, brevirostrine taxa display a rostrum to skull length ratio inferior to 0.5 such as *Acynodon iberoccitanus* (0.4), *Koumpiodontosuchus aprosdokiti* (0.45) or *Iharkutosuchus makadii* (0.38). The rostrum proportions of *B. fagesii* depart from those of other typical ‘shell crushers’ in showing a slender rostrum. In *Bernissartia fagesii*, the rostrum is definitely not wide and short as in the hylaeochampsids *Acynodon*, *Allodaposuchus* or *Pietraroiasuchus*. In fact, its rostrum proportions are within the range of other mesorostrine forms such as *Isisfordia*, *Susisuchus*, *Koumpiodontosuchus* or *Paralligator*.

Digital removal of glue and sediment allows skull and mandibular ornamentation to be observed. The entire dorsal surface of the skull table, the quadratojugal, jugal, the bones forming the orbital margin as well as the median portion of the rostrum involving the nasal and medialmost parts of the maxilla are ornamented with marked ovoid pits. Such pits tend to be nearly circular and individualised on the squamosal, postorbital and lateral sides of the jugal; they are large and anastomosed on the quadratojugal and orbital margin of the jugal; they are shallow and take the form of grooves on the rostrum. Most of the dorsal and lateral surfaces of the premaxillae and maxillae are nearly smooth; deep circular foramina open in line just above the tooth row. In the mandible, ornamentation is contrasted between the dentary rami where furrows and foramina dominate, and the posterior region, which is

characterised by large anastomosed pits. Foramina densely cover the anterolateral and anteroventral portions of the dentary. Such foramina are sparsely distributed below the mandibular tooth row from the level of the sixth back to the posterior tooth row area. Pits are wider and more circular on the lateral surface of the surangular than on the angular, where they make deep furrows near its posteroventral margin. The posterior mandibular edge made by the surangular and angular is devoid of ornamentation.

The skull and mandible have been affected by crushing, as is often the case with bones embedded in clay. The CT scans allow observations of numerous cracks in the internal structure of the specimen, to the point that most elements of the braincase cannot be reconstructed to the exception of the inner ear (Fig. 8). The skull has clearly undergone a dorsoventral compression as is evidenced by the rostrum sitting at the same level as the skull table and with the prefrontal pillars penetrating and distorting the palatines in their anterior portion. Some lateromedial skewing is also apparent in the skull (Fig. 2I, J) and is obvious when comparing the left and right mandibular rami. In fact, the right mandible better preserves the original outline in lateral view whereas the left one has undergone deformation of the angular in two different parts (compare Fig. 2E and F).

Fenestrae and openings. The longer than wide external nares fully face dorsally and are delimited by the premaxillae and by the anterior nasal processes. Their posterior margin is imperfectly preserved because the paired nasals are partially displaced. The premaxillae contribute to the anterior and lateral contours of the external nares. These openings are slightly smaller than the supratemporal fenestrae. The small incisive foramen is almond-shaped and is contained within the palatal portion of the premaxillae, extending between the level of the second and fourth premaxillary alveoli. No antorbital fenestra or foramen could be identified. The orbits are delimited anteriorly by the lacrimals as a smooth notch; laterally by

the jugals; medially by the prefrontals and frontal; and posteriorly by the postorbitals. The orbital outline, especially the lateral margin, has suffered from dorsoventral compression. Here, the crushed jugal gives a false impression of a concave lateral margin. The undeformed orbits may have been oval being anteroposteriorly elongated. The lacrimal contributing to the orbital margin shows a smooth surface, corresponding to a sulcus. Because of deformation, this sulcus gives a false impression of being prominent on the right lacrimal, but the left one shows a best-preserved situation with a limited extent. The suborbital fenestrae are elongated and extend for nearly the entire palatine length, anteriorly up to the level of the tenth maxillary alveolus. They are delimited anteriorly and laterally by the maxillae and posteriorly by the ectopterygoids. It is unclear whether the pterygoid contribute slightly to their posteriormost margin because the bones are loosely connected. The right suborbital fenestra best preserves its lateral margin, which is slightly convex at the level of the largest maxillary alveolus. The posterolateral margin of the suborbital fenestra joins the midline of the skull along an oblique and straight margin of the ectopterygoid. The supratemporal fenestrae are ovoid being slightly longer than wide. The frontals and postorbitals make the anterior and anterolateral margins, respectively. The squamosals build the lateral and posterior margins while the parietals make the medial and contribute a little to the posteromedian margins. The internal supratemporal walls are vertical, except the anterior half of the parietal, which shows a smooth inclined surface. The supratemporal fenestrae are about half the size of the orbits. The orbitotemporal foramina could not be identified due to the presence of numerous fractures. The lower temporal fenestrae face dorsolaterally and are delimited ventrally by the jugals, posteriorly by the quadratojugals and dorsally by the squamosals and postorbitals. They are longer than high and extend along the anterior half of the skull table length. Little can be said about the outline of the foramen magnum due to bone fragmentation in the area. The exoccipitals forms its lateral margins and it is uncertain whether the supraoccipital

participates in the dorsal margin or whether the exoccipitals prevent such involvement. The ventral margin is made by the basioccipital condyle. An external mandibular fenestra is absent as evidenced from the sutural relationships of the surangulars, angulars and dentaries in the posterior margin of the lower jaw. The foramen intermandibularis oralis opens medially in the anterior portion of the splenial, at the level of the fifth dentary alveolus.

Rostrum. Both the left and right premaxillae are fractured but remain sutured to each other along the ventral margin and anterior to the external nares (Fig. 2). Each bone is longer than wide with a gently convex anterolateral contour. The dorsal surface is weakly ornamented; marked pits are visible just above the tooth row. The premaxillary dorsal process is partly eroded and delimits the external narial margin, which is bounded anteriorly and laterally by the premaxilla, and posteriorly by the nasal. An anteroposteriorly directed sulcus runs on the dorsal surface of the premaxilla, just lateral to the external nares. The posterior premaxillary process is long and not as wide as the anterior portion of the premaxilla; contrary to other derived neosuchians, this premaxillary process attains the suture with the maxilla well posterior to the premaxillary-maxillary notch. The posterior premaxillary process consists of a thin lamina that overlies the maxilla. As observed externally, the premaxillary-maxillary suture is perpendicular to the rostrum.

As observed in ventral view, the premaxillae give a semicircular outline to the anterior margin of the rostrum. The incisive foramen consists of a small, longer than wide, ovoid opening. It is completely enclosed by the premaxillae and opens away from the tooth row. The right and left premaxillae are in contact posterior to the incisive foramen through a long median palatal laminar suture, preventing any maxillary process to divide the premaxillae. The lingual premaxillary alveolar walls are damaged but the teeth are still in position and allow assessing alveolar relative dimensions. There are five individualised alveoli per

premaxilla; the first is separated from the second by a diastema; the third and fourth are the largest and separated from each other by a deep occlusal pit. The fifth premaxillary alveolus is the smallest and its posterior margin is close to the premaxillary-maxillary notch. The premaxilla nearly encompasses this notch, although the anteriormost maxillary process participates in the posteroventral margin of the notch. This notch accommodates the large fourth caniniform dentary tooth, as evidenced by the mandible on the mounted specimen (Figs. 2, 3). The premaxillary-maxillary notch marks the first festoon of the tooth row, giving a constricted outline to the upper jaw at this level. This circular notch is close to being excavated laterally, indicating that ontogenetically old specimens should present complete excavation of the notch. Here, on both sides of the skull, the premaxillae and maxillae possess bony projections that nearly meet along the lateral margin of the rostrum (Fig. 2). Therefore, when occluding in the premaxillary-maxillary notch, the enlarged dentary tooth crown becomes partly visible in lateral view. An oblique line of small foramina pierces the ventral surface of the premaxilla. Occlusal pits in the maxilla are obvious between the sixth and seventh, between the seventh and the eighth, and between the eighth and the ninth alveoli. The first two anterior pits are located in the interalveolar spaces and indicate an interdigitated occlusion (Figs. 2, 3). The last of these occlusal pits is slightly offset lingually. Faint occlusal pits can also be detected between the ninth back to the thirteenth alveoli.

The maxillae contribute to most of the rostrum. As evidenced from both sides, there are 16 maxillary alveoli per row. In lateral view, the maxillae display a marked double wave, attaining a maximum convexity at the level of the double caniniform dentition as well as at the level of the posterior molariform teeth. The maxillae do not suture medially on the dorsal surface, being separated by the nasals along an extensive suture. Although the ventral surface is heavily fractured, the maxillae seem to suture to each other from the premaxillary suture until the level of the eighth or ninth maxillary alveoli. In dorsal view, the maxillae have

extensive sutural contacts with the lacrimals and jugal along their posteromedian margins. The maxillae extend posteriorly below the entirety of the orbits but do not take part in those. Ventrally, the posteromedian maxillary suture of the palate appears separated by the anterior palatine processes, for a short distance. But this area is poorly preserved. The posterior part of the maxillae possesses a distinct median shelf that projects within the suborbital fenestra, at the level of the large molariform fourteenth alveolus. From this point, the posteromedian maxillary margin sutures extensively with the anterior ectopterygoid process. The last maxillary alveolus is close but does not contact the ectopterygoid nor the jugal. The jugal contributes to the posteriormost margin of the maxilla. The paired nasals can be observed in dorsal view where they extend for nearly the entire length of the rostrum. Their posterior extent, in front of the orbits connects with the anterior frontal process as well as with a long prefrontal process along their posteromedial margins. Anterior to the prefrontal contact, the nasals contact the lacrimal anterior processes for a short distance. Most of the lateral margins of the nasals contact the maxillae. The nasals become narrow at the level of the large caniniform maxillary alveoli. Anterior to this point, they become wide and contact the premaxillae where they participate in the posterior margin of the external nares. Here, they send a short spiny median process in the nares.

Periorbital area. The jugal extends along the lateral margin of the skull between the maxilla and the quadratojugal. Its anterior process projects ahead of the orbits reaching the level of the thirteenth maxillary alveolus. Here, the jugal extensively overlaps the posterior margin of the maxilla and sutures along its anteromedial margin onto a dorsally facing suture of the lacrimal. The jugal orbital margin consists of a long and concave tongue that delimits an external ornamented surface from a smooth internal surface. Posterior to the orbit, the jugal contribution to the postorbital bar is medially inset from the external surface of the jugal. Its

suture with the descending postorbital process is difficult to observe due to crushing and the presence of numerous cracks. The posterior jugal process is mediolaterally compressed and forms the ventral margin of the lower temporal fenestra. The jugal contacts the ascending process of the ectopterygoid below the level of the jugal contribution to the postorbital bar. No jugal foramen could be observed but this may be due to poor preservation. The lacrimal is a flat bone, longer than wide with an anterior region slightly narrower than its posterior region. It occupies the anterior orbital margin where it sends a posterolateral process within the orbit along the jugal. The lacrimal shares a long median suture with the prefrontal and, anteromedially, it contacts the nasal. Anteriorly and anterolaterally, the lacrimal sutures with the maxilla. Here above the suture, the dorsal surface of the lacrimal possesses an anteriorly projecting peg that interlocks with the maxilla (Fig. 4H, I). The prefrontal is an elongated bone wedging between the lacrimal and the anterior frontal process. An elevated rim delimits the ornamented dorsal surface from the smooth vertical orbital margin, which is pierced by a single foramina. Most of the lateral margin is dorsally covered by the lacrimal. The anteromedial process of the prefrontal projects anteriorly far, but not as far as the lacrimal. This process extensively contacts the frontal and the nasals medially. The prefrontal pillars descend ventrally from the orbital margin of the prefrontal to contact the palatines in their anterior region. The frontal bridges the skull table and the periorbital area. Its unpaired process contributes to the median orbital margin where it is rimmed by a thin crest. The frontal sends a long anterior process that slopes anterior to the orbits. This process accommodates the prefrontal and projects underneath the nasals for a short distance. No periorbital ridge or crest could be detected. In its posterior portion, the frontal sutures laterally with the postorbital and posteriorly with the parietal along an interdigitated suture. The frontoparietal suture is located within the first anterior half of the supratemporal fenestra. The frontal has a short participation in the anteromedial corner of the supratemporal fenestrae.

Here, the frontal sits over the capitate processes of the laterosphenoid and their horizontal suture is visible in the anterior part of the supratemporal fenestrae. In ventral view, the sulcus for the olfactory tract is well marked and the imprint corresponding the olfactory bulbs is wider than the interorbital space.

Skull table. The skull table is flat and devoid of a median crest on the frontoparietal midline. The frontoparietal suture is located between the supratemporal fenestrae and prevents a contact between the parietal and postorbital. The parietal retains the same width between the supratemporal fenestrae and in its posterior part. This width is about the same as the supratemporal fenestra width. The parietal delimits the posterior margin of the skull table and as observed in dorsal view, prevents the supraoccipital from participating in the skull table. The postorbital is restricted to the anterolateral corner of the skull table. Just below the level of the skull table, a large foramen opens on the anterolateral margin of the postorbital bar (Fig. 5J). Almost reaching this foramen, the squamosal projects far anteriorly as a strong acute process over the postorbital bar (Fig. 5J), which does not reach the orbital margin. The squamosal contributes to more than two third the length of the skull table. The squamosal projects posteriorly with the dorsal surface of the squamosal lobe being flat and unsculpted.

Palate. The palatal region of the skull underwent several breakages and bones are slightly displaced but maintain their original position. The left ectopterygoid is nearly complete and possesses a complex shape. The torsion of its main corpus has been attenuated by crushing. Its posterolateral flange is pointed and overlaps the pterygoid wing. Its posterior margin bears a notch. The main corpus is relatively wide and shows a foramen opening near the suture for the maxilla on its ventral side. In dorsal or ventral views, the ectopterygoid shows sutural contacts with the maxilla and pterygoid. Norell & Clark (1990) observed the lateral part of the

ectopterygoid as extending dorsally to contact the postorbital on the medial surface of the postorbital. The area is crushed but the left side does show instead that the ectopterygoid contacts the ventral surface of the jugal contribution to the postorbital bar, but not the postorbital itself, which is slightly more positioned dorsally (Fig. 6). A short ectopterygoid process extends along the medial surface of the jugal (Fig. 6). As noted previously by Buffetaut (1975) or Norell & Clark (1990), the left pterygoid appears to preserve the median suture contacting the right element, therefore confirming that the pterygoid is closed posterior to the choanae. The morphology of the pterygoid is best exemplified by the left element, which is almost complete and appears as a general triangle. The lateral margin of the pterygoid flange is obliquely oriented relative to the anteroposterior axis of the skull. It is extremely thick anteriorly, corresponding to the torus transiliens, which is expanded dorsally but not ventrally. Posterior to the torus transiliens, the lateral margin of the pterygoid flange projects posterolaterally as a thin lamina. Here, the posterior margin is thin and perpendicular with the anteroposterior axis of the skull. As preserved, the posteromedian margin of the pterygoid flange is at a level more anterior than the posterolateral margin. The ventral margin of the pterygoid wing is flat and a shallow notch along the lateral margin indicates the lateralmost limit of the suture with the ectopterygoid. The CT data also allow clarifications of some important anatomical traits of the palate. As such, the left pterygoid and palatine preserve a sutural contact and both contribute to the choanal opening (Figs. 2, 3); the palatine contributes to the anterolateral margins of the choana, as a thin lamina contacting ventrally the pterygoid. The anterior margin of the choana reaches the level of the suborbital fenestrae but does not penetrate far anteriorly within the interfenestral bars. The palatine bars are straight and parallel to each other for their entire length, which occupies all the median margin of the suborbital fenestrae (Figs. 2, 6). The left palatine is the less fractured. As observed in ventral view, both palatines very slightly expand laterally into the maxillae where their anteriormost

extent reaches the level of the 10th maxillary alveolus. The internal part of the palatines is hollow, connecting the internal choanae to the external nares as a closed duct. Numerous breaks do not allow to securely assess what bone contributes to the dorsal wall of this choanal duct. As observed by Norell and Clark (1990), the prefrontal pillars do meet the palatines at about one third the distance from their anterior margin. This is well visible due to crushing, where the right vertical pillar deforms the right palatine.

Braincase. The braincase is heavily fractured, hampering an inspection of the endocranial cavity and of the orbitotemporal foramen. Nevertheless, the exit foramina for cranial nerve XII, the carotid artery, and the vagal foramen are visible on the medial margin of the right exoccipital (Fig 8). As evidenced from the left side, the cranioquadrate passage is laterally open (Fig. 2 and Fig. 7G, H). This passage runs along the ventromedial margin of the exoccipital and only the exoccipital contributes to it. The posterior margin of the external otic aperture is delimited by a wide concave margin of the squamosal and exoccipital. The quadratojugal covers the lateral margin of the quadrate. On the posterodorsal corner of the lower temporal fenestra, the quadratojugal prevents the quadrate from participating in the lower temporal fenestra. The quadratojugal ascending process is best seen from the left side, but its dorsalmost tip is damaged and it is uncertain if it contacts the squamosal or the postorbital. The quadrate builds the ventral margin of the external otic aperture. Along the dorsal margin, the quadrate surface hosts one depression (Fig. 7D), as originally identified by Norell & Clark (1990). This depression is not perforated although it is topologically similar to preotic sinuses; but other specimens would be required to investigate the relevance of this morphology. The left quadrate condyle is complete and the foramen aereum opens on the dorsomedial corner of quadrate (Fig. 7D–F). Muscle insertion scars are visible on the ventral surface of the quadrate branch (Fig. 7C). Here, a faint crest A of Iordansky (1973) runs along

the quadrate-quadratojugal suture. The crest B of Iordansky (1973) is more developed and runs obliquely in the middle of the posterior surface.

The supraoccipital is strongly developed above the foramen magnum and bears a strong vertical median keel (Fig. 5). The basioccipital contributes to the occipital condyle but the underlying basioccipital plate is destroyed. The ventralmost process of the basisphenoid, as preserved, wedges between the pterygoid plates as a concave structure. Its dorsal portion is inflated and preserves the Eustachian canals. The median one is the largest and the paired lateral foramina are located close to it near the posterior margin of the bone. The laterosphenoid preserves the capitate process, which is wider than long and contacts the frontal and laterally part of the postorbital as a rugose tubercle. On the lateral margin of the laterosphenoid, the cotylar crest is not developed. The trigeminal foramen is not preserved so it is not possible to assess whether a laterosphenoid bridge was present.

Due to heavy breakage in the endocranial cavity, (Fig. 8A), the endosseous labyrinth could be partially reconstructed for the right side only. The cochlea could not be located but a partial vestibular system was reconstructed including parts of the lateral and anterior semicircular canals as well as the sacculus (Fig. 8B–G). The lateral semicircular canal is only preserved in its anterior region where it connects to the anterior ampulla together with the anterior semicircular canal. Although, the curvature of the lateral semicircular canal around the sacculus cannot be assessed precisely, its orientation suggests a significant curvature (Fig. 8D and G). Curved lateral semicircular canals have been described in modern eusuchians and may indicate sensitivity (Brusatte *et al.* 2016). In lateral view, the straight but not curved anterior semicircular canal of *B. fagesii* resembles the general pyramidal appearance of other semicircular canals in *Crocodylus johnstoni*, *Pelagosaurus* and other crocodylomorphs (Pierce *et al.* 2017). As observed in lateral view, the angle between the lateral and anterior semicircular canals is about 47°; whereas it is between 50° and 60° in modern eusuchians (see

Fig. 8 in Brusatte *et al.* 2016). Although the anterior ampulla is dorsoventrally expanded in modern eusuchians, here it seems laterally bulging. Also, the lateral ampulla is distinctly inflated, more so than in modern eusuchians, which would again support sensitivity to angular motion (Sipla & Spoor 2008).

Mandible. In dorsal or ventral view, the mandible is V-shaped, matching the triangular outline of the skull (Fig. 2). The right dentary is damaged anteriorly but the left dentary is complete and includes a total of 18 alveoli (Fig. 10). The dentary is a long rod that makes about three quarters of the entire mandible length. In lateral view, the ventral surface of the dentary is flat and contrasts with the sinusoidal dorsal margin. As for the upper jaw, the dentary displays a typical double wave with maximum heights attained at the level of the dentary alveoli 3+4 and at the level of the twelfth dentary alveolus. The dentary symphyseal portion is spatulate and incorporates the first four alveoli. The splenial modestly participates in the mandibular symphysis. In dorsal or ventral view, the dentary narrows from the level of the fifth to tenth alveoli. From the fourteenth alveolus backward, the splenial contributes to the lingual wall of the dentary alveoli. Along the lateral side of the dentary, the bone is vertical but near its posterior end, it is slightly bulged at the level of the last dentary alveoli. In lateral view, the dentary makes a large contact with the angular and dorsally, contacts the surangular along a less extensive suture. The splenial prevents any contribution of the dentary to the lingual cavity. The first dentary alveolus is damaged but the left tooth is preserved in position and shows a procumbent geometry. The second alveolus is set apart and much smaller than the first one. The double caniniform dentary teeth are as large as the first tooth and set in alveoli 3+4, which are confluent and raised above the tooth row. Dentary alveoli 5 to 9 are small, set apart and open on a concave area of the tooth row. The thecodont implantation prevails for the first fourteenth alveoli. From the fifteenth to the last dentary

alveolus, all teeth are set in a groove. Occlusal pits could not be detected in the dentary. Lingual to the molariform dentition, the splenial is distinctly enlarged, forming a shelf. A coronoid seems present as evidenced from the right mandible in medial view between the surangular and the dentary. Because of preservational reasons, it is not possible to provide more morphological details. The angular best preserves its general shape on the right mandible. It occupies the lower half of the posterior margin of the mandible. The surangular-angular suture runs nearly horizontally back to the tip of the mandible. Both angular and surangular hide the articular and retroarticular process in lateral view. As observed in lateral view, the posteroventral margin of the angular is convex; its posterodorsal margin is devoid of ornamentation. As seen in ventral view, the angular consists of a mediolaterally thin ridge, corresponding to the attachment of *M. pterygoideus posterior*. Still in ventral view, the angular sends an anterior process between the dentary and splenial. Medially, the posterior wall of the angular accommodates the descending process of the articular. According to the left mandible, the surangular has a horizontal dorsal margin. This margin is simple with no obvious muscle scars and is mediolaterally thin. The combined height of the surangular and angular is about twice that of the dentary ramus. The relation between the surangular and dentary is poorly preserved and it is not possible to assess their sutural pattern. Nevertheless, the surangular does not reach the level of the posterior dentary tooth row. In lateral view, the posterior part of the surangular slopes ventrally by sending a posterior process that follows and covers the medially placed retroarticular process. The articular sutures to the medial side of the surangular. In lateral view, only the posterior buttress of the glenoid fossa is visible. The glenoid fossa faces anterodorsally and possesses two hemi-fossae of equal dimensions, poorly distinct from each other by an anterior pointed process. In front of the lateral hemifossa, the anterior surface of the descending articular process is concave and contacts the surangular and eventually the angular at its ventral tip. The retroarticular process projects

posteriorly and sits in a lower position than the articular glenoid fossa. In dorsal or ventral view, the retroarticular process consists of a thin lamina that also projects medially and serves as an obvious attachment for *M. depressor mandibulae*.

Dentition. The dentition of *Bernissartia fagesii* is heterodont of the tribodont type with blunt and rounded posterior crushing teeth (Buffetaut & Ford 1979; Ósi 2013). All teeth present a mesiodistal carina and finely wrinkled enamel characterised by vertical ridges. From the front to the back of the upper or lower tooth rows, one can observe a progressive change in tooth morphology (Fig. 10). Here, the crown progressively diminishes in height and increases in mesiodistal length. Crowns of the premaxillary teeth, maxillary teeth 1–6 and dentary teeth 1–6 are of the conical type. Crowns of the maxillary teeth 7–13 and dentary teeth 7–16 are lanceolate, i.e. with a tooth crown that is triangular in labial or lingual view. Finally, the posteriormost teeth corresponding to maxillary teeth 14 and 15 as well as dentary teeth 17–19 are bulbous. Those bulbous crowns are mesiodistally longer than high and labiolingually thick. Finally, the last tooth of each tooth row possesses a small rounded crown that is as long as high. This tooth is about three times smaller than the penultimate tooth. Complete tooth rows are represented by the right upper row, totaling five premaxillary and sixteen maxillary teeth and by the left lower row, totaling twenty dentary teeth. As in extant forms, the roots are curved lingually with their lingual surface being slightly depressed, whereas their labial surface is convex. The crowns are close to each other, especially in the posterior part of the tooth row but do not seem to be in contact. The roots of the maxillary teeth 13–16 do however contact each other. Although less marked in the anterior conical teeth, all teeth present a constriction between the root and the crown. Replacement teeth can be observed as bud crowns on almost every tooth position. These buds develop within the base of roots of

functional teeth. Here, the lingual surface of the functional root shows the typical U-shaped resorption pattern (Poole 1961).

Phylogenetic results

We recovered ten MPTs with a length of 1045 steps (CI = 0.332; RI = 0.663; Fig. 11). Several neosuchians lineages successively fall stem-ward to the Eusuchia with a monophyletic group that includes Goniopholididae, Pholidosauridae + Dyrosauridae, then of Paralligatoridae, then of *Wannchampsus*, and finally a paraphyletic atoposaurid group (Fig. 11).

Bernissartia fagesii is the sister taxon of *Koumpiodontosuchus aprosdokiti*, supporting a bernissartiid clade (Sweetman *et al.* 2014) that is nested within Eusuchia. The Bernissartiidae are in a sister position with the Susisuchidae (i.e. *Susisuchus anatoceps* and *Isisfordia duncani*), and both form a polytomy with the Hylaeochampsidae. Although Hylaeochampsidae is not monophyletic here, Allodaposuchidae (*Allodaposuchus*, *Agaresuchus*, *Lohuecosuchus*) form a separate lineage from *Acynodon*, *Iharkutosuchus* and *Hylaeochampsia*. All of the above-mentioned taxa including Bernissartiidae, are closely related, forming a sister group to the crown group, all of which represent the Eusuchia. Inactivating character 178 concerning the lateral contour of the snout yields similar but slightly different results: the Bernissartiidae form a clade with Susisuchidae, with both clades being sister group to the crown group.

Discussion

The palate of *Bernissartia*

The description of *Bernissartia fagesii* Dollo (1883), from the Early Cretaceous of Belgium, followed nearly a decade the description of another hallmark taxon, *Hylaeochampsia vectiana* Owen (1874), from the Wealdian of England. Until recently, both European taxa were

deemed important for the comprehension of the origin of modern eusuchians (see discussion in Pol *et al.* 2009) with *B. fagesii* considered as a derived neosuchian and *H. vectiana* as the basalmost eusuchian (Buffetaut 1975; Clark 1986; Clark & Norell 1992). For this reason, the position of the choanal opening within the palate and of the vertebral morphology have been central in previous discussions on the affinities of *Bernissartia fagesii* and derived neosuchians (e.g. Buffetaut 1975; Norell & Clark 1990; Pol *et al.* 2009; Sweetman *et al.* 2014). Here, we will discuss the morphology of the internal choanae thanks to the new observations allowed by CT data.

Unlike in derived eusuchians, the internal choanal opening of *B. fagesii* is not pterygoid-bound because the palatine contributes to the anterolateral margins of the choana, as a thin lamina connecting ventrally to the pterygoid. The pterygoid hosts most of the choanal recess, extending for most of the median margin of the pterygoidean plate (Fig. 6A). There is no evidence of a recess but the area is poorly preserved. Pterygoid-palatine-bound choanal configuration is similar to that recently reinterpreted for *Isisfordia duncani* (Turner & Pritchard 2015) as well as a common feature of many neosuchians including *Theriosuchus pusillus* or *Paralligator gradilifrons* (Clark 1986; Turner 2015). Nevertheless, the anterior reach of the choana in *Bernissartia fagesii* is short, unlike in goniopholidids, pholidosaurids, *T. pusillus* or *Rugosuchus nonganensis* where it expands frankly within the suborbital fenestrae. The condition in *B. fagesii* is similar to that of *P. gradilifrons* (Turner 2015) where the choana stops roughly at the level of the suborbital fenestra. Whether it is also similar to *I. duncani* as recently reinterpreted (Turner & Pritchard 2015) should be tested using CT data.

Our phylogenetic results support a variable position of the choanal opening in the palate among basal eusuchians, as exemplified here by Bernissartiidae and Susisuchidae, which both contain taxa with pterygoid-bound choanae (Sweetman *et al.* 2014; Leite & Fortier 2018) or with choanae extending into the palatines (Turner & Pritchard 2015; this

study). Nevertheless, the condition recently described for *Susisuchus* by Leite & Fortier (2018) requires independent validation in view of the flattened preservation of the specimen. In such a case where the internal choanae open in an anterior position within the palate, cracks could be easily mistaken for the palatine-pterygoid suture, rendering observations difficult to interpret. A similar issue has been recently discussed in the case of *Isisfordia duncani* (compare descriptions in Salisbury *et al.* 2006 with Turner & Pritchard 2015). Basal eusuchians such as hylaeochampsids and members of the crown group offer a palatal configuration less prone to confusion: they possess pterygoid-bound choanae, but those open in a middle or posterior position within the pterygoids (Clark & Norell 1992; Brochu 1999; Martin *et al.* 2007; Delfino *et al.* 2008a, b; Ósi, 2008; Martin *et al.* 2016a).

In the present phylogeny, the pterygoid-bound configuration of the internal choanae in *Susisuchus* and *Koumpiodontosuchus* may contribute in uniting bernissartiids and susisuchids into Eusuchia. This recovered topology contrasts with a recent study using the same datamatrix, and placing susisuchids stem-ward to goniopholidids (Turner 2015; Turner & Pritchard 2015). Indeed, uncertainties remain as concerns the proper extent of the internal choanae in *Isisfordia*, *Susisuchus* and *Koumpiodontosuchus* and new interpretations, for example based on CT data, may help refine the proposed phylogenetic hypothesis. In addition, it is also now recognised that the position of the choanae and the morphology of the vertebrae have evolved multiple times in different neosuchian lineages (Turner & Buckley 2008; Pol *et al.* 2009; Sweetman *et al.* 2014; Leite & Fortier 2018). Although pterygoid-bound choanae do not necessarily characterise eusuchians, according to our results, the participation of the palatine in the choanae does not necessarily disqualify an assignment to basal eusuchians either. Pterygoid-bound choanae were reported in *Mahajangasuchus insignis*, a neosuchian close to Peirosauridae from the Maastrichtian of Madagascar (Turner &

Buckley 2008), and as discussed by these authors, there is a strong functional link between platyrostry, tensile stress on the palate and its configuration as well as feeding style.

***Bernissartia* and its position among derived neosuchians**

The phylogenetic results presented herein should be regarded with caution until anatomical clarifications can be brought in a number of derived neosuchians and basal eusuchians. Other relevant Cretaceous forms, here mentioned from older to younger deposits, are known only from fragmented remains and include *Unasuchus reginae* from the Barremian of Spain (Brinkmann 1992) known from cranial and mandibular elements; *Turcosuchus okani* from the ?Barremian of Turkey (Jouve *et al.* 2019) known from a partial mandible and postcranial elements; ‘*Crocodylus*’ *cantabrigiensis* from the Albian Greensands of Great Britain (Seeley 1874) reported from procoelous vertebrae; *Aegyptosuchus peyeri* from the Cenomanian of Egypt (Stromer 1933) known from a skull table and discussed as a possible ally to the enigmatic *Stomatosuchus inermis* from the same formation (Pol *et al.* 2009; see also Sereno & Larsson 2011 and Holliday & Gardner 2012 about stomatosuchid affinities); *Gilchristosuchus palatinus* from the Santonian or Campanian of Alberta (Wu & Brinkman 1993) known from a skull table; and *Dolichochoampsa minima* from the Maastrichtian of Argentina (Gasparini & Buffetaut 1980) known from several skull fragments including a braincase and mandibles. Recent reappraisal of the type specimen of *Brillianceausuchus babouriensis* from the Barremian-Aptian of Cameroon (Michard *et al.* 1990) led Tennant *et al.* (2016) to interpret it as a paralligatorid, a view not supported by the results of Kuzmin *et al.* (2018). Two articulated individuals of *Pietraroiiasuchus ormezanoi* from the Albian of Italy were described by Buscalioni *et al.* (2011) who proposed a close relationship with *Pachycheilosuchus trinquei* from the Barremian of Texas, a taxon known from limited cranial remains (Rogers 2003). Future work on the undescribed neosuchian from the Barremian of Las Hoyas, Spain

(see codings in Buscalioni *et al.* 2011) should also prove useful. Indeed, *Hylaeochampsia vectiana* was described from an incomplete skull (Clark & Norell 1992) and several features remain unknown such as the dentition and mandible. Another potentially important taxon, *Portugalosuchus azenhae* was recently described from the Cenomanian of west-central Portugal (Mateus *et al.* 2018) and preserves the perirobital area, skull table and palate. The internal choanae are pterygoid-bound and placed in a posterior position, similarly to eusuchians such as hylaeochampsids or members of the crown group. Therefore, the above-mentioned taxa represent a potential source for exploring and re-evaluating the evolutionary history of derived neosuchians. For the time being, the position of *B. fagesii* within Neosuchia is discussed in the context of recent finds.

Previous studies have recovered *B. fagesii* to be nested among or at least closely positioned relative to various neosuchian lineages such as goniopholidids, paralligatorids, atoposaurids, susisuchids or hylaeochampsids (e.g. Norell and Clark 1990; Salisbury *et al.* 2006; Turner 2015; Turner & Pritchard 2015; Kuzmin *et al.* 2018), illustrating our lack of resolution over the position of *B. fagesii* but also between those different neosuchian lineages. Here, we recover *B. fagesii* as a member of Eusuchia close to *Koumpiodontosuchus* and susisuchids.

Indeed, *B. fagesii* retains plesiomorphic traits such as the palatine-pterygoid complex involved in the internal choanae (see discussion above) or the open cranioquadrate passage. The latter one's presence has been described in both non-eusuchians and basal eusuchians as well. For example, an open cranioquadrate passage is observed in various goniopholidids (e.g. Salisbury *et al.* 1999; Martin *et al.* 2016b), hylaeochampsids (Clark & Norell 1992; Martin 2007; Delfino *et al.* 2008b; Martin *et al.* 2016a), paralligatorids (Turner 2015) and perhaps in atoposaurids where it is poorly preserved (Martin *et al.* 2014b; Schwarz *et al.* 2017). This contrasts with the condition in the susisuchid *Isisfordia duncani*, where the cranioquadrate

passage is fully enclosed in the quadrate (Salisbury *et al.* 2006). The condition observed in *B. fagesii* also differs from the condition in dyrosaurids (e.g. Brochu *et al.* 2002) or from derived eusuchians where the cranioquadrate passage is fully enclosed by the exoccipital and the quadrate.

We do not recover *B. fagesii* as a member of Paralligatoridae. Turner (2015) underlined several characters uniting *Theriosuchus* and Paralligatoridae, including a slightly sculpted surface of the squamosal lobe showing a prominent depressed area just anterior to the lobe (see also Pol *et al.* 2009); the presence of an orbitonasal sulcus; a midline ridge on the dorsal surface of the frontal and parietal; and a sharp ridge along the lateral surface of the angular. None of these characters are observed in *B. fagesii*. Paralligatoridae are further diagnosed by the three synapomorphies (Kuzmin *et al.* 2018), but to the exception of the absence of participation of the supraoccipital to the dorsal surface of the skull table, *B. fagesii* does not share longitudinal keels restricted to the posterior edge of dorsal osteoderms, nor posteriorly flaring interfenestral bar between suborbital fenestrae. So, whatever the relationships of Paralligatoridae with Atoposauridae (e.g. Turner, 2015; Tennant *et al.* 2016; Kuzmin *et al.* 2018), *B. fagesii* cannot be assigned to either lineage.

B. fagesii is not a close ally of Goniopholididae. That Goniopholididae share with *B. fagesii* the enlarged double caniniform alveoli for dentary alveoli 3 and 4 is a symplesiomorphy also observed in derived eusuchians such as *Leidyosuchus*, *Borealosuchus* or *Diplocynodon* (e.g. Brochu 1999; Delfino & Smith 2012; Martin *et al.* 2014a). Goniopholididae, differ, among other characters from *B. fagesii* in having the nasals excluded from the external nares (Salisbury *et al.* 1999; Andrade & Hornung 2011); in possessing a complex pattern of periorbital ridges (Andrade & Hornung 2011); a straight dentary tooth row (Martin *et al.* 2016b, c); the anterolateral processes of the postorbital that project close to the

orbital margin of the jugal (e.g. Salisbury & Naish 2011) or in displaying strong anterolateral processes on wider than long dorsal osteoderms (e.g. Martin *et al.* 2016b, c).

Our phylogenetic results and anatomical observations do not support a close affinity between *Bernissartia fagesii* and some non-eusuchian neosuchian lineages. Here, we recover a basal neosuchian position for Paralligatoridae close to a polyphyletic Atoposauridae as in a recent work (Tennant *et al.* 2016). As explained above on the basis of anatomical differences, there is no evidence to relate *B. fagesii* to other neosuchian lineages such as Goniopholididae, Paralligatoridae or Atoposauridae.

Regarding the affinities of *Bernissartia fagesii* with proper eusuchians, our results may appear surprising in view of the close relationships recovered with susisuchids and hylaeochampsids. The rostrum of crocodylomorphs is highly plastic with several known cases of cranial convergence in distantly related lineages (Brochu 2001). As presently recovered under one hypothesis here, the close relationship between *B. fagesii* and susisuchids is probably a bias related to snout profile or the possession of a rectilinear tooth row, a condition shared between Susisuchidae and more derived members of the Hylaeochampsidae such as *Acynodon* or *Iharkutosuchus* (e.g. Martin 2007; Ősi 2008; Jouve *et al.* 2019). Both taxa also share nasals that participate in the posterior margin of the external nares, the relatively elongate rostrum and the general sutural relationships of the peri-orbital and skull table areas. Nevertheless, notable differences between susisuchids and hylaeochampsids include tooth row outline, alveolar count, heterodonty, and configuration of the cranioquadrate passage. Contrary to susisuchids, the mandible of *B. fagesii* is not rectilinear but shows the double-wave lateral profile matching the premaxillary-maxillary tooth row, a feature commonly observed among derived eusuchians. Moreover, contrary to susisuchids, *B. fagesii* is markedly heterodont displaying caniniform dentition including confluent anterior dentary alveoli, as well as tribodont posterior teeth. *B. fagesii* has less alveolar positions in the maxilla

(18) than do *Susisuchus* or *Isisfordia duncani* (about 20) (Salisbury *et al.* 2006; Leite & Fortier 2019). Finally, *B. fagesii* retains a plesiomorphic character with the open cranioquadrate groove, which is closed in *Isisfordia duncani* (Salisbury *et al.* 2006) and unknown in *S. anatoceps* (Salisbury *et al.* 2003). For the above reasons, it does not seem reasonable to view *B. fagesii* as a susisuchid or as a form close to it. Similarly, removing susisuchids from the analysis results in bernissartiids falling crownward along the stem of the crown group due to the possession of a double wave in the tooth row, a feature widely encountered among members of the crown group, except longirostrine forms. Other traits of *B. fagesii* such as the possession of enlarged posterior teeth; a medially expanded shelf of the splenial; a quadratojugal forming the posterior corner of the infratemporal fenestra; a jugal bar inset from the lateral surface of the skull; a tetraserial arrangement of the dorsal armour, are also shared with *Acynodon* and basal alligatoroids.

Nevertheless, *B. fagesii* is also characterised by a primitive trait: the insertion of M. pterygoideus posterior along the posteroventral margin of the angular, which is similar to what is observed in neosuchians such as goniopholididae (Martin *et al.* 2016b), pholidosauridae (Martin *et al.* 2016c) or Paralligatoridae (e.g. *P. gradilifrons* in Turner 2015, Fig. 5F) where the lateral surface is fully ornamented and the medial surface lacks a developed insertion area. The angular is poorly known in atoposaurids but some specimens might indicate that the situation is similar to other non-eusuchian neosuchians (see Schwarz-Wings *et al.* 2017). On the other hand, in members of the crown group the insertion area is particularly developed medially with a large process; moreover, the insertion area also spreads as a smooth surface over the lateral edge of the angular (e.g. Martin *et al.* 2014a, Fig. 8).

A close relationship between *B. fagesii* and Hylaeochampsidae will have to be tested in future works. The absence of an external mandibular fenestra may represent an apomorphy of Bernissartidae + Hylaeochampsidae with *Acynodon*, *Allodaposuchus* and *Iharkutosuchus*

lacking such a fenestra (Martin *et al.* 2016a). The mandible is unknown in *Hylaeochampsia* but another possible eusuchian, *Unasuchus reginae*, also lacks such an external mandibular fenestra (Brinkmann 1992) and was recently recovered as a member of the Hylaeochampsidae (Jouve *et al.* 2019). All other eusuchians from the crown group possess an external mandibular fenestra and its reported presence in the susisuchid *I. duncani* (Salisbury *et al.* 2006) is at odds with our results placing Susisuchidae (presence / absence of the external mandibular fenestra is unknown in *S. anatoceps*; Salisbury *et al.* 2003) with Hylaeochampsidae and Bernissartidae. However, according to Leite & Fortier (2018), an external mandibular fenestra is absent in *S. anatoceps*.

Despite sharing several features, *B. fagesii* also differs in a number of characters with Hylaeochampsidae, beginning with the configuration of the internal choanae in the palate (see previous discussion above). Other differences include the participation of the nasals in the external nares or the position of the foramen aereum on the quadrate. On the distal margin of the quadrate, the foramen aereum is clearly visible and opens on the mediodorsal margin of the medial hemicondyle as in *Paralligator gradilifrons* and crocodyloids. This foramen is dorsally placed in *Allodaposuchus* (Delfino *et al.* 2008a; Martin *et al.* 2016a) and also among alligatoroids but not in crocodyloids (Brochu 1999).

Our phylogenetic analysis recovers *B. fagesii* as a member of the Eusuchia, in a clade containing *Susisuchus*, *Isisfordia*, *Koumpiodontosuchus*, *Acynodon*, *Hylaeochampsia*, *Iharkutosuchus* and Allodaposuchidae. Contrary to members of the crown group, hylaeochampsids, bernissartids and susisuchids evolved with various configurations of the choanae, the cranioquadrate passage, or the vertebrae, characters that may no longer be used in the definition of the Eusuchia. Our results support the hypothesis of a lineage of endemic basal eusuchians that populated the European archipelago during the Cretaceous. Indeed, the position of susisuchids from southern landmasses with hylaeochampsids and bernissartiids

from Europe requires further investigation, notably by retrieving new specimens from the field including Cretaceous forms from Gondwana such as *Aegyptosuchus*, *Brillanceausuchus*, *Dolichochampsia* and *Stomatosuchus*.

Spatiotemporal distribution of Bernissartiidae

A review of the distribution of *Bernissartia fagesii* was provided by Buffetaut & Ford (1979) who largely based their identifications on isolated teeth and carefully referred those to bernissartids. Since then, rare but nearly complete cranial remains are providing a clearer picture. Notably, the recent description of *Koumpiodontosuchus aprosdokitii* from the Barremian of the Isle of Wight (UK) by Sweetmann *et al.* (2014) highlights that the tribodont dentition is not only present in *Bernissartia fagesii* but in another genus of similar age. The distribution of *Bernissartia fagesii* on the basis of isolated teeth should be taken with caution until teeth of both taxa are compared. Given the phylogenetic topology recovered here, it seems safe for the time being to refer isolated tribodont teeth from the Jurassic and Cretaceous of Europe to Bernissartiidae indet. Reports of teeth assigned to *Bernissartia* sp. from the Kimmeridgian of Guimarota, Portugal (Brinkmann 1989), from the Berriasian of the Purbeck Limestone Group, UK (Salisbury 2002), from the Berriasian of Cherves-de-Cognac, France (Mazin & Pouech, 2008), from the Berriasian of Denmark (Schwarz-Wings *et al.* 2009) are all significantly older than the complete skull from the Barremian of the Isle of Wight (Sweetmann *et al.* 2014) or from the complete specimen referred herein (see also Buffetaut 1975; Norell & Clark, 1990). Cranial remains have yet to be reported from Berriasian deposits so as to clarify relationships with younger recognised taxa such as *Bernissartia fagesii* and *Koumpiodontosuchus aprosdokitii*. Clarifying the age of the skull of *Bernissartia fagesii* that was reported from a wide temporal gap covering the Berriasian (?) – lower Aptian of Galve in Teruel, Spain (Buscalioni *et al.* 1984; Buscalioni & Sanz 1990) will be helpful in that regard.

That bernissartiids were common components of Barremian environments of Western Europe is now ascertained by their occurrence at different localities in Spain (Brinkmann 1992; Buscalioni *et al.* 2008).

Bernissartiid teeth have also been reported outside Europe from the Albian of the Trinity Formation of Texas (Langston 1974; Thurmond 1974) or from the Albian-Cenomanian of the Cedar Mountain Formation of Utah (Cifelli *et al.* 1999). Isolated tribodont teeth were also attributed to ?*Bernissartia* from the Middle and Upper Saurian Beds at Tendaguru, Tanzania, which were dated to the Late Kimmeridgian and post-Tithonian–pre-Valanginian, respectively (Heinrich *et al.* 2001). Although it may be possible that the group occurs elsewhere, this record should be re-evaluated because of convergent forms with tribodont teeth are known to exist (see below). For now, current evidence restricts the occurrence of Bernissartiidae to a Kimmeridgian–Aptian interval. The occurrence of *Bernissartia fagesii* itself is restricted to the late Barremian–early Aptian of Belgium. This range may be expanded with future discoveries.

Interestingly, as noted previously by several authors, bernissartiids often co-occur in the same deposits with goniopholidids and pholidosaurids (e.g. Salisbury 2002; Mazin & Pouech 2008; Schwarz-Wings *et al.* 2009) implying spatial and/or niche partitioning to explain such a high local crocodylomorph biodiversity (Martin *et al.* 2016c). Aspects of the feeding ecology of *B. fagesii* are discussed below.

Diet of *Bernissartia* and other tribodont forms

The distinctive morphology of the dentition of *Bernissartia fagesii* has widely been considered in relation to feeding preferences for hard-shelled organisms. Buffetaut & Ford (1979) did not favour a diet of turtles due to the small size of *B. fagesii*. Arguments in favour or against chelinivory among blunt-toothed crocodylomorphs have often been discussed with

indirect evidences (e.g. Carpenter & Lindsey 1980; Bartels 1984) that do not satisfactorily support any hypothesis. A recent study of various traces on a pleurosternid shell provides evidence for such chelonivorous habits in the large generalist-morphotype genus *Goniopholis* (Gônet *et al.* 2019). Therefore, blunt posterior teeth are not essential for subduing hard-shelled preys and modern species with a generalist appearance do also feed on turtles when they are available. As regards *B. fagesii*, Buffetaut & Ford (1979) considered a specialised diet toward mollusc-eating in view of the presence in the Wealdian of the Isle of Wight of various freshwater invertebrates including lamellibranchs, gastropods and planorbids, a hypothesis shared by Sweetmann *et al.* (2014) regarding the diet of the other bernissartid *Koumpiodontosuchus aprosdokitii*. Although this might be possible, *B. fagesii* is not as brevirostrine as other small eusuchians such as *Acynodon* (e.g. Martin 2007; Delfino *et al.* 2008b) or *Gnathusuchus*, the latter being interpreted as a mollusc-crusher as evidenced from punctured molluscs found in the same deposits (Salas-Gismondi *et al.* 2015).

Another indicator of diet is body size, because diet changes through ontogeny as observed for a variety of modern species (Cott 1961; Magnusson *et al.* 1987 and references in Grigg & Kirshner 2015). Accordingly, diet in crocodylians can be directly related to body size increase grading from insects, amphibians, crustaceans and/or molluscs to fishes, reptiles, birds and mammals. The frequency histograms realised on the proportions of food items retrieved from the stomach contents of *Crocodylus niloticus* can be useful (Fig. 34 in Cott 1961). They reveal that for a body length of less than a meter, i.e. corresponding to that of *Bernissartia fagesii*, a high proportion of insects and crustaceans are recovered as dietary items. Does that mean that *B. fagesii* was exclusively relying on such organisms? The question remains open until direct evidence becomes available. Nevertheless, it should be remembered that modern crocodylians are opportunistic and will feed on what is available to them (see discussion in Grigg & Kirshner 2015) and there is no reason to think otherwise for

extinct species. In fact, the anterior conical teeth in *B. fagesii* allow capturing any type of prey within the limits of mouth holding. The closest modern analogue to *B. fagesii* is *Osteolaemus tetraspis* from equatorial forests of Africa, which displays posterior blunt dentition and does not surpass 2 meters in total body length. Its diet has been described as opportunistic with stomach contents containing primarily crustaceans, insects, amphibians and small mammals (Pauwels *et al.* 2007; Shirley *et al.* 2016). Again in the case of *B. fagesii*, it is difficult to evaluate the diet of an extinct taxon when stomach content is absent but *O. tetraspis* might be a good approximation for the diet of *B. fagesii*.

All eusuchians with a tribodont dentition do not surpass 2 meters in total body length. Those include Cretaceous but also Paleogene and Neogene forms (e.g. review in Ősi *et al.* 2013). If tribodontology is constrained by resource abundance and body size, ontogenetic growth trajectories may help understand the independent occurrence of the tribodont dentition in distant neosuchian lineages.

Conclusions

Details of the cranial anatomy of *Bernissartia fagesii* are now available thanks to CT data performed on the best-preserved specimen (IRSNB R46). This will serve as a basis to compare and explore the phylogenetic affinities of Cretaceous representatives of the neosuchian-eusuchian transition. Our exploratory phylogenetic analysis recovers *B. fagesii* as a basal eusuchian, close to Hylaeochampsidae in a context where a consensus over the relationships of the different neosuchian lineages has not been achieved yet. Although such results should be critically reevaluated under the light of new discoveries and additional phylogenetic codings, we also point out an important result in recovering no support for a relationship of *B. fagesii* with Atoposauridae, Paralligatoridae or Goniopholididae. Although

not resolvable here, the phylogenetic position of *B. fagesii* might still lie somewhere among derived non-eusuchian neosuchians or close to basal eusuchians. From a palaeoecological point of view, the tribodont dentition of *B. fagesii* is reminiscent of other small forms from different ages and provenances, highlighting repeated occurrences during the evolutionary history of eusuchians. As indicated by its small size, *B. fagesii* may have regularly fed on small invertebrates, insects and crustaceans but also small vertebrates such as frogs or lizards. Many Cretaceous eusuchians reached a relatively small body size (circa 1 m) at adulthood. The evolutionary significance of tribodonty and small body size will have to be explored under the light of ecological and developmental constraints.

Acknowledgements

The authors thank A. Folie and M. Haemelinck (RBINS, Brussels) for access to the mounted specimen IRSNB R46. CT scanning of specimen IRSNB R46 was funded by Laboratoire de Géologie de Lyon: Terre, Planète, Environnements (UMR CNRS 5276). This research was supported by Synthesys Project BE-TAF-2788 (to JEM) and BE-TAF-6142 (to MD) funded by the European Commission (<http://www.synthesys.info/>). We thank the two anonymous reviewers and editor P. M. Barrett for their careful reading and constructive remarks.

References

Adams, T. L., Noto, C. R. & Drumheller, S. 2017. A large neosuchian crocodyliform from the Upper Cretaceous (Cenomanian) Woodbine Formation of North Texas. *Journal of Vertebrate Paleontology*, **37**, e1349776.

- de Andrade, M. B. & Hornung, J. J.** 2011. A new look into the periorbital morphology of *Goniopholis* (Mesoeucrocodylia: Neosuchia) and related forms. *Journal of Vertebrate Paleontology*, **31**, 352–368.
- Bartels, W. S.** 1984. Osteology and systematic affinities of the horned alligator *Ceratosuchus* (Reptilia, Crocodylia). *Journal of Paleontology*, **58**, 1347–1353.
- Brinkmann, W.** 1992. Die Krokodilier-Fauna aus der Unter-Kreide (Ober-Barremium) von Uña (Provinz, Cuenca, Spanien). *Berliner Geowissenschaftliche Abhandlungen, Reihe E, Band, 5*, 1–123.
- Brochu, C. A.** 1999. Phylogenetics, taxonomy, and the historical biogeography of Alligatoroidea. *Society of Vertebrate Paleontology Memoir*, **6**, 19, 9–100.
- Brochu, C. A.** 2001. Crocodylian snouts in space and time : phylogenetic approaches toward adaptive radiation. *American Zoologist*, **41**, 564–585.
- Brochu, C. A., Bouare, M. L., Sissoko, F., Roberts, E. M. & O’Leary, M. A.** 2002. A dyrosaurid crocodyliform braincase from Mali. *Journal of Paleontology*, **76**, 1060–1071.
- Brusatte, S. L., Muir, A., Young, M. T., Walsh, S., Steel, L. & Witmer, L. M.** 2016. The braincase and neurosensory anatomy of an Early Jurassic marine crocodylomorph: implications for crocodylian sinus evolution and sensory transitions. *The Anatomical Record*, **299**, 1511–1530.
- Buffetaut, E.** 1975. Sur l'anatomie et la position systématique de *Bernissartia fagesii* Dollo, L., 1883, crocodylien du Wealdien de Bernissart, Belgique. *Bulletin de l’Institut royal des Sciences Naturelles de Belgique*, **51**, 1–20.
- Buffetaut, E. & Ford, R. L. E.** 1979. The crocodylian *Bernissartia* in the Wealden of the Isle of Wight. *Palaeontology*, **22**, 905–912.

- Bultynck, P.** 1989. Bernissart et les Iguanodons. French version by F. Martin and P. Bultynck. Edition de l'institut royal des Sciences naturelles de Belgique, Brussels, 115 p.
- Buscalioni, A. D. & Sanz, J. L.** 1990. The small crocodile *Bernissartia fagesii* from the Lower Cretaceous of Galve (Teruel, Spain). *Bulletin de l'Institut royal des Sciences Naturelles de Belgique*, **60**, 129–150.
- Buscalioni, A. D., Buffetaut, E. & Sanz, J. L.** 1984. An immature specimen of the crocodylian *Bernissartia* from the Lower Cretaceous of Galve (Province of Teruel, Spain). *Palaeontology*, **27**, 809–813.
- Buscalioni, A. D., Frenegeal, M. A., Bravo, A., Poyato-Ariza, F. J., Sanchíz, B., Báez, A. M., Cambra Moo, O., Martín Closas, C., Evans, S. E. & Marugán Lobón, J.** 2008. The vertebrate assemblage of Buenache de la Sierra (Upper Barremian of Serranía de Cuenca, Spain) with insights into its taphonomy and palaeoecology. *Cretaceous Research*, **29**, 687–710.
- Buscalioni, A. D., Piras, P., Vullo, R., Signore, M. & Barbera, C.** 2011. Early eusuchia crocodylomorpha from the vertebrate-rich Plattenkalk of Pietraroia (Lower Albian, southern Apennines, Italy). *Zoological Journal of the Linnean Society*, **163**, S199–S227.
- Carpenter, K. & Lindsey, D.** 1980. The dentary of *Brachychampsia montana* Gimore (Alligatorinae; Crocodylidae), a Late Cretaceous turtle-eating alligator. *Journal of Paleontology*, **54**, 1213–1217.
- Clark, J. M.** 1986. Phylogenetic relationships of the crocodylomorph archosaurs. Unpublished Ph.D. dissertation. University of Chicago, 556 p.
- Clark, J. M. & Norell, M. A.** 1992. The Early Cretaceous crocodylomorph *Hylaeochampsia vectiana* from the Wealden of the Isle of Wight. *American Museum Novitates*, **3032**, 1–19.

- Cifelli, R. L., Nydam, R. L., Weil, A., Eaton, J. G., Kirkland, J. I. & Madsen, S. K.** 1999. Medial Cretaceous vertebrates from the Cedar Mountain Formation, Emery County, Utah : the Mussentuchit local fauna. In D. D. Gillette : Vertebrate Paleontology in Utah. Miscellaneous Publication 99-1, Utah Geological Survey: 219–242.
- Cott, H. B.** 1961. Scientific results of an enquiry into the ecology and economic status of the Nile Crocodile (*Crocodylus niloticus*) in Uganda and Northern Rhodesia. *Transactions of the Zoological Society of London*, **29**, 211–356.
- Delfino, M., Codrea, V., Folie, A., Dica, P., Godefroit, P. & Smith, T.** 2008a. A complete skull of *Allodaposuchus precedens* Nopcsa, 1928 (Eusuchia) and a reassessment of the morphology of the taxon based on the Romanian remains. *Journal of Vertebrate Paleontology*, **28**, 111–122.
- Delfino, M., Martin, J. E. & Buffetaut, E.** 2008b. A new species of *Acynodon* (Crocodylia) from the Upper Cretaceous (Santonian-Campanian) of Villaggio del Pescatore, Italy. *Palaeontology*, **51**, 1091–1106.
- Delfino, M. & Smith, T.** 2012. Reappraisal of the morphology and phylogenetic relationships of the middle Eocene alligatoroid *Diplocynodon deponiae* (Frey, Laemmert, and Riess, 1987) based on a three-dimensional specimen. *Journal of Vertebrate Paleontology*, **32**, 1358–1369.
- Dollo, L.** 1883. Première note sur les crocodiliens de Bernissart. *Bulletin de l'Institut royal des Sciences Naturelles de Belgique*, **2**, 309–340.
- Gasparini, Z. & Buffetaut, E.** 1980. *Dolichochampsa minima*, n.g.n.sp., a representative of a new family of eusuchian crocodiles from the Late Cretaceous of northern Argentina. *Neues Jahrbuch für Geologie und Paläontologie Monatshefte*, **1980**, 257–271.
- Godefroit, P., Yans, J. & Bultynck, P.** 2012. Bernissart and the Iguanodonts: historical perspective and new investigations; pp. 3–20 in P. Godefroit (ed.), Bernissart Dinosaurs

- and Early Cretaceous Terrestrial Ecosystems. Indiana University Press, Bloomington, Indiana.
- Goloboff, P. A., Farris, J. S. & Nixon, K. C.** 2008. TNT, a free program for phylogenetic analysis. *Cladistics*, **24**, 774–786.
- Gônet, J., Rozada, L., Bourgeais, R. & Allain, R.** 2019. Taphonomic study of a pleurosternid turtle shell from the Early Cretaceous of Angeac-Charente, southwest France. *Lethaia*, doi: 10.1111/let.12309.
- Grigg, G. & Kirshner, D.** 2015. Biology and evolution of crocodylians. Csiro Publishing 672 p.
- Heinrich, W. D., Bussert, R., Aberhan, M., Hampe, O., Kapilima, S., Schrank, E., Schultka, S., Maier, G., Msaky, E., Sames, B. & Chami, R.** 2001. The German–Tanzanian Tendaguru Expedition 2000. *Fossil Record*, **4**, 223–237.
- Holliday, C. M. & Gardner, N. M.** 2012. A new eusuchian crocodyliform with novel cranial integument and its significance for the origin and evolution of Crocodylia. *PLoS ONE*, **7**, e30471.
- Iordansky, N. N.** 1973. The skull of the Crocodylia: pp. 201–262 in: Gans C. & Parson T.S. (eds.), *Biology of the Reptilia*, Vol. 1, Morphology A, Academic Press, London and New York.
- Jouve, S., Sarigül, V., Steyer, J.-S. & Sen, S.** 2019. The first crocodylomorph from the Mesozoic of Turkey (Barremian of Zonguldak) and the dispersal of the eusuchians during the Cretaceous. *Journal of Systematic Palaeontology*, **17**, 111–128.
- Kuzmin, I. T., Skutschas, P. P., Boitsova, E. A. & Sues, H.-S.** 2018. Revision of the large crocodyliform *Kansajsuchus* (Neosuchia) from the Late Cretaceous of Central Asia. *Zoological Journal of the Linnean Society*, **185**, 335–387.
- Langston, W.** 1974. Nonmammalian Comanchean tetrapods. *Geoscience and Man* **8**, 77–102.

- Leite, K. J. & Fortier, D. C.** 2018. The palate and choanae structure of the *Susisuchus anatoceps* (Crocodyliformes, Eusuchia): phylogenetic implications. *PeerJ*, **6**, e5372.
- Magnusson, W. E., da Silva, E. V. & Lima, A. P.** 1987. Diets of Amazonian crocodylians. *Journal of Herpetology*, **21**, 85–95.
- Martin, J. E.** 2007. New material of the Late Cretaceous globidontan *Acynodon iberoccitanus* (Crocodylia) from southern France. *Journal of Vertebrate Paleontology*, **27**, 362–372.
- Martin, J.E. & Buffetaut, E.** 2012. The maxillary depression of Pholidosauridae: an anatomical study. *Journal of Vertebrate Paleontology*, **32**, 1442–1446
- Martin, J. E., Smith, T., de Lapparent de Broin, F., Escuillié, F. & Delfino, M.** 2014a. Late Palaeocene eusuchian remains from Mont de Berru, France, and the origin of the alligatoroid *Diplocynodon*. *Zoological Journal of the Linnean Society*, **172**, 867–891.
- Martin, J. E., Rabi, M., Csiki-Sava, Z. & Vasile, S.** 2014b. Cranial morphology of *Theriosuchus sympiestodon* (Mesoeucrocodylia, Atoposauridae) and the widespread occurrence of *Theriosuchus* in the Late Cretaceous of Europe. *Journal of Paleontology*, **88**, 444–456.
- Martin, J. E., Delfino, M. Garcia, G., Godefroit, P., Berton, S. & Valentin, X.** 2016a. New specimens of *Allodaposuchus precedens* from France: intraspecific variability and the diversity of European Late Cretaceous eusuchians. *Zoological Journal of the Linnean Society*, **176**, 607–631.
- Martin, J. E., Delfino, M. & Smith, T.** 2016b. Osteology and affinities of Dollo's goniopholidid (Mesoeucrocodylia) from the Early Cretaceous of Bernissart, Belgium. *Journal of Vertebrate Paleontology*, **36**, e1222534.

- Martin, J. E., Raslan-Loubatié, J. & Mazin, J. M.** 2016c. Cranial anatomy of *Pholidosaurus purbeckensis* from the Lower Cretaceous of France and its bearing on pholidosaurid affinities. *Cretaceous Research*, **66**, 43–59.
- Mateus, O., Puértolas-Pascual, E. & Callapez, P. M.** 2018. A new eusuchian crocodylomorph from the Cenomanian (Late Cretaceous) of Portugal reveals novel implications on the origin of Crocodylia. *Zoological Journal of the Linnean Society*, **186**, 501–528.
- Mazin, J. M. & Pouech, J.** 2008. Crocodylomorph microremains from Champblanc (Berriasian, Cherves-de-Cognac, Charente, France). Mid-Mesozoic Life and Environments. *Documents du Laboratoire de Géologie de Lyon*, **164**, 65–67.
- Michard, J. G., de Broin, F., Brunet, M. & Hell, J. F.** 1990. Le plus ancien crocodilien néosuchien spécialisé à caractères ‘eusuchiens’ du continent africain (Crétacé inférieur, Cameroun). *Comptes Rendus de l’Académie des Sciences, Paris*, **311**, 365–371.
- Montelfreto, F. C., Larsson, H. C., de França, M. A. & Langer, M.** 2013. A new neosuchian with Asian affinities from the Jurassic of northeastern Brazil. *Naturwissenschaften*, **100**, 835–841.
- Norell, M. A., & Clark, J. M.** 1990. A reanalysis of *Bernissartia fagesii*, with comments on its phylogenetic position and its bearing on the origin and diagnosis of the Eusuchia. *Bulletin de l’Institut royal des Sciences Naturelles de Belgique*, **60**, 115–128.
- Noto, C. R., Drumheller, S. K., Adams, T. L. & Turner, A. H.** 2019. An Enigmatic Small Neosuchian Crocodyliform from the Woodbine Formation of Texas. *The Anatomical Record*, <https://doi.org/10.1002/ar.24174>
- Ósi, A.** 2013 Cranial osteology of *Iharkutosuchus makadii*, a Late Cretaceous basal eusuchian crocodyliform from Hungary. *Neues Jahrbuch für Geologie und Paläontologie-Abhandlungen*, **248**, 279–299.

- Ósi, A.** 2013 The evolution of jaw mechanism and dental function in heterodont crocodyliforms. *Historical Biology*, **26**, 1–137.
- Pauwels, O. S. G., Barr, B., Sanchez, M. L. & Burger, M.** 2007. Diet records for the dwarf crocodile, *Osteolaemus tetraspis* in Rabi oil fields and Loango National Park, southwestern Gabon. *Hamadryad*, **31**, 258–264.
- Pierce, S. E., Williams, M. & Benson, R. B.** 2017. Virtual reconstruction of the endocranial anatomy of the early Jurassic marine crocodylomorph *Pelagosaurus typus* (Thalattosuchia). *PeerJ*, **5**, e3225.
- Pol, D., Turner, A. H. & Norell, M. A.** 2009. Morphology of the Late Cretaceous crocodylomorph *Shamosuchus djadochtaensis* and a discussion of neosuchian phylogeny as related to the origin of Eusuchia. *Bulletin of the American Museum of Natural History*, **324**, 1–103.
- Poole, D. F. G.** 1961. Notes on tooth replacement in the Nile crocodile *Crocodilus niloticus*. *Proceedings of the Zoological Society of London*, **136**, 131–140.
- Rogers, J. V.** 2003. *Pachycheilosuchus trinquei*, a new procoelous crocodyliform from the lower Cretaceous (Albian) Glen Rose Formation of Texas. *Journal of Vertebrate Paleontology*, **23**, 128–145.
- Salas-Gismondi, R., Flynn, J. J., Baby, P., Tejada-Lara, J., Wesselingh, F. P. & Antoine, P. -O.** 2015. A Miocene hyperdiverse crocodylian community reveals peculiar trophic dynamics in proto-Amazonian mega-wetlands. *Proceedings of the Royal Society B*, **282**, 20142490.
- Salisbury, S. W.** 2002. Crocodylians from the Lower Cretaceous (Berriasian) Purbeck Limestone Group of Dorset, southern England. *Special Papers in Palaeontology*, **68**, 121–144.

- Salisbury, S. W., Willis, P. M. A., Peitz, S. & Sander, P. M.** 1999. The crocodylian *Goniopholis simus* from the lower Cretaceous of north-western Germany. *Special Papers in Palaeontology*, **60**, 121–148.
- Salisbury, S. W., Frey, E., Martill, D. M. & Buchy, M. C.** 2003. A new crocodylian from the Lower Cretaceous Crato Formation of north-eastern Brazil. *Palaeontographica Abteilung A Palaeozoologie-Stratigraphie*, **270**, 3–47.
- Salisbury, S. W., Molnar, R. E., Frey, E. & Willis, P. M.** 2006. The origin of modern crocodyliforms: new evidence from the Cretaceous of Australia. *Proceedings of the Royal Society of London B*, **273**, 2439–2448.
- Salisbury, S. W. & Naish, D.** 2011. Crocodylians ; pp. 305-369 in D. J. Batten (ed.), English Wealden fossils, The Palaeontological Association, London.
- Schwarz-Wings, D., Rees, E. & Lindgren, J.** 2009. Lower Cretaceous mesoeucrocodylians from Scandinavia (Denmark and Sweden). *Cretaceous Research*, **30**, 1345–1355.
- Schwarz-Wings, D., Raddatz, M. & Wings, O.** 2017. *Knoetschkesuchus langenbergensis* gen. nov. sp. nov., a new atoposaurid crocodyliform from the Upper Jurassic Langenberg Quarry (Lower Saxony, northwestern Germany), and its relationships to *Theriosuchus*. *PLoS ONE*, **12**, e0160617.
- Seeley, H. G.** 1874. On cervical and dorsal vertebrae of *Crocodylus cantabrigiensis* (Seeley) from the Cambridge Upper Greensand. *Quarterly Journal of the Geological Society*, **30**, 693–695.
- Sereno, P. C. & Larsson, H. C.** 2009. Cretaceous crocodyliforms from the Sahara. *Zookeys*, **28**, 1–143.
- Shirley, M. H., Burtner, B., Oslisly, R., Sebag, D. & Testa, O.** 2016. Diet and body condition of cave-dwelling dwarf crocodiles (*Osteolaemus tetraspis*, Cope 1861) in Gabon. *African Journal of Ecology*, **55**, 411–422.

- Sipla, J. S. & Spoor, F.** 2008. The physics and physiology of balance; pp. 227–232 in J. G. M. Thewissen and S. Nummela (eds.), *Sensory evolution on the threshold, adaptations in secondarily aquatic vertebrates*. University of California Press.
- Sookias, R. B.** 2019. Exploring the effects of character construction and choice, outgroups and analytical method on phylogenetic inference from discrete characters in extant crocodylians. *Zoological Journal of the Linnean Society*, doi.org/10.1093/zoolinnea
- Stromer, E.** 1933. Wirbeltierreste der Baharije-Stufe. 12. Die procoelen Crocodylia. *Akademie der Wissenschaften, Mathematisch-Naturwissenschaftliche Abteilung*, **15**, 1–5.
- Sweetman, S. C., Pedreira-Segade, U. & Vidovic, S. U.** 2014. A new bernissartiid crocodyliiform from the Lower Cretaceous Wessex Formation (Wealden Group, Barremian) of the Isle of Wight, southern England. *Acta Palaeontologica Polonica*, **60**, 257–268.
- Tennant, J. P., Mannion, P. D. & Upchurch, P.** 2016. Evolutionary relationships and systematics of Atoposauridae (Crocodylomorpha: Neosuchia): implications for the rise of Eusuchia. *Zoological Journal of the Linnean Society*, **177**, 854–936.
- Thurmond, J. T.** 1974. Lower vertebrate faunas of the Trinity division in north-central Texas. *Geoscience and Man*, **8**, 103–129.
- Turner, A. H. & Pritchard, A. C.** 2015. The monophyly of Susisuchidae (Crocodyliformes) and its phylogenetic placement in Neosuchia. *PeerJ*, **3**, e759.
- Turner, A. H. & Buckley, G. A.** 2008. *Mahajangasuchus insignis* (Crocodyliformes: Mesoeucrocodylia) cranial anatomy and new data on the origin of the eusuchian-style palate. *Journal of Vertebrate Paleontology*, **28**, 382–408.
- Turner, A. H.** 2015. A review of *Shamosuchus* and *Paralligator* (Crocodyliformes, Neosuchia) from the Cretaceous of Asia. *PLoS One*, **10**, e0118116.

Yans, J., Dejax, J., & Schnyder, J. 2012. On the age of the Bernissart iguanodonts. In: P. Godefroit (Ed.), *Bernissart Dinosaurs and Early Cretaceous Terrestrial Ecosystems* (p. 79-86). (Life of the Past). Indiana (USA): Indiana University Press.

Wu, X-C. & Brinkman, D. B. 1993. A new crocodylomorph of “mesosuchian” grade from the upper Cretaceous upper Milk River Formation, southern Alberta. *Journal of Vertebrate Paleontology*, **13**, 153–160.

Figure Captions

Figure 1. The lectotype specimen of *Bernissartia fagesii* (IRSNB R46) from the Barremian–Aptian of Bernissart, Belgium. **A**, articulated skeleton in dorsal view; **B**, photograph of skull in dorsal view compared with a **C**, virtual reconstruction using CT data. Note that virtually adjusting contrasts allows reconstructing the specimen without glue or sediment. This also permits fine observations of anatomical details otherwise obscured by glows or poorly resolved contrasts from the darkness of the specimen.

Figure 2. 3D surface rendering of the skull of *Bernissartia fagesii* (IRSNB R46) in **A**, dorsal; **B**, ventral; **C**, left lateral; **D**, right lateral views; and associated left mandible in **E**, lateral; **F**, medial views; associated right mandible in **G**, lateral; **H**, medial views and of both associated mandibles in **(I, J)** occlusal views, as well as the skull in **K**, anterior and **L**, occipital views. Abbreviations: agf, articular glenoid fossa; an, angular; art, articular; boc, basioccipital; ch, choana; cqq, cranioquadrate groove; den, dentary; ec, ectopterygoid; en, external nares; ep, excavation pit; exo, exoccipital; fa, foramen aereum; fio, foramen intermandibularis oralis; fr, frontal; if, incisive foramen; j, jugal; l, lacrimal; ltf, lower temporal fenestra; mx, maxilla; n, nasal; mmf, medial mandibular fenestra; op, occlusal pit; or, orbit; p, parietal; pa, palatine; po, postorbital; pmx, premaxilla; pob, postorbital bar; pfr, prefrontal; pt, pterygoid; q, quadrate;

qj, quadratojugal; ra, retroarticular process; san, surangular; sof, suborbital fenestra; sp, splenial; sq, squamosal; sym, symphysis; tt, torus transiliens of pterygoid; P1-5, premaxillary alveolar or tooth count; m1-16, maxillary alveolar or tooth count; d1-d20, dentary alveolar or tooth count. [planned for full page width]

Figure 3. Line drawings of the skull of *Bernissartia fagesii* (IRSNB R46) in **A**, dorsal; **B**, ventral; **C**, occipital; **D**, right lateral views; and associated right mandible in **E**, lateral views. See Figure 2 for abbreviations. Line drawing in **C** is not to scale and has been slightly augmented for clarity.

Figure 4. Bones from the antorbital area of *Bernissartia fagesii* (IRSNB R46). Left prefrontal in **A**, dorsal; **B**, lateral; **C**, ventral and **D**, anterior views. Left lacrimal in **E**, dorsal; **F**, lateral; **G**, ventral and **H–I**, anterior views. The view in **I** is an enlargement of the view in **H** and is not to scale. Frontal in **J**, dorsal; **K**, left lateral; **L**, ventral and **M**, anterior views. Left jugal in **N**, dorsal; **O**, lateral and **P**, ventral views. Abbreviations: lp, lacrimal peg; fo, foramen; orn, orbital notch; pp, prefrontal pillar; s.mx., suture for maxilla; s.pfr., suture for prefrontal.

Figure 5. Elements of the skull table of *Bernissartia fagesii* (IRSNB R46) as observed in dorsal (**A–D**), ventral (**E–H**) and right lateral (**I–K**) views with right postorbital (**A**, **E**, **J**), right squamosal (**B**, **F**, **I**), right laterosphenoid (**C**, **G**) and right parietal (**D**, **H**, **K**). The supraoccipital is presented in **L**, posterior and **M**, right lateral views. The arrow in **K** points to a fracture running through the deformed parietal. Abbreviations: cp, capitate process; fo, foramen; on, otic notch; s.sq., suture for squamosal.

Figure 6. 3D surface rendering of left palatal elements of *Bernissartia fagesii* (IRSNB R46) in **A**, ventral; **B**, dorsal and **C**, left lateral views. The anterior direction is indicated by the arrow. Abbreviations: chd, choanal depression on pterygoid; fo, foramen; mxs, maxillary suture of the ectopterygoid; pa, palatine; papt, palatine-ptyerygoid suture; pep, posterior ectopterygoid process; pts, pterygoid suture of the ectopterygoid; tt, torus transiliens.

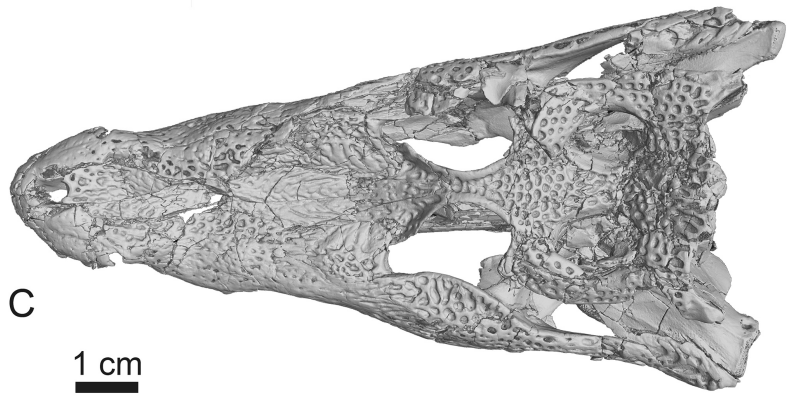
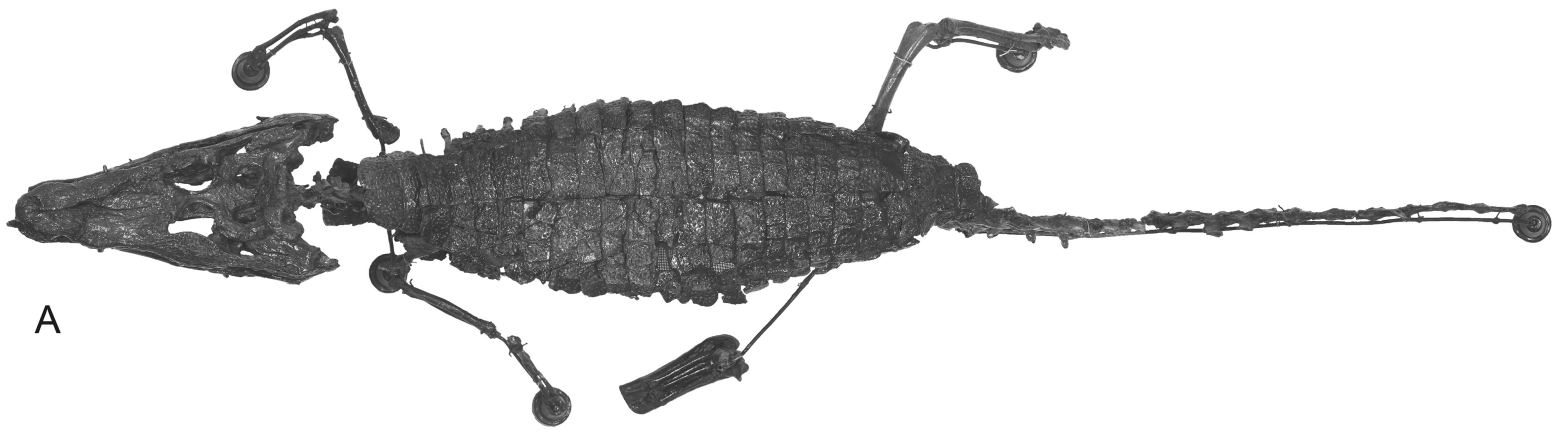
Figure 7. 3D surface rendering of braincase elements of *Bernissartia fagesii* (IRSNB R46) including the left quadratojugal in **A**, ventral and **B**, dorsal views; the left quadrate in **C**, ventral; **D**, dorsal; **E**, medial and **F**, posterior views; the left partially preserved exoccipital in **G**, anterior and **H**, posterior views; the right exoccipital in **I**, ventral view; the occipital condyle in **J**, right lateral; **K**, ventral and **L**, dorsal views; the basisphenoid in **M**, dorsal and **N**, ventral views. Abbreviations: cA–cB, crests A and B of Iordansky (1973); cqg, cranioquadrate groove; fa, foramen aereum; fc, opening for carotid artery; fv, opening for vagal foramen; ioa, internal otic aperture; meu, median Eustachian opening; on, otic notch; qd, quadrate depression; s.exo, suture for exoccipital; s.q, suture for quadrate; XII, opening for cranial nerve XII

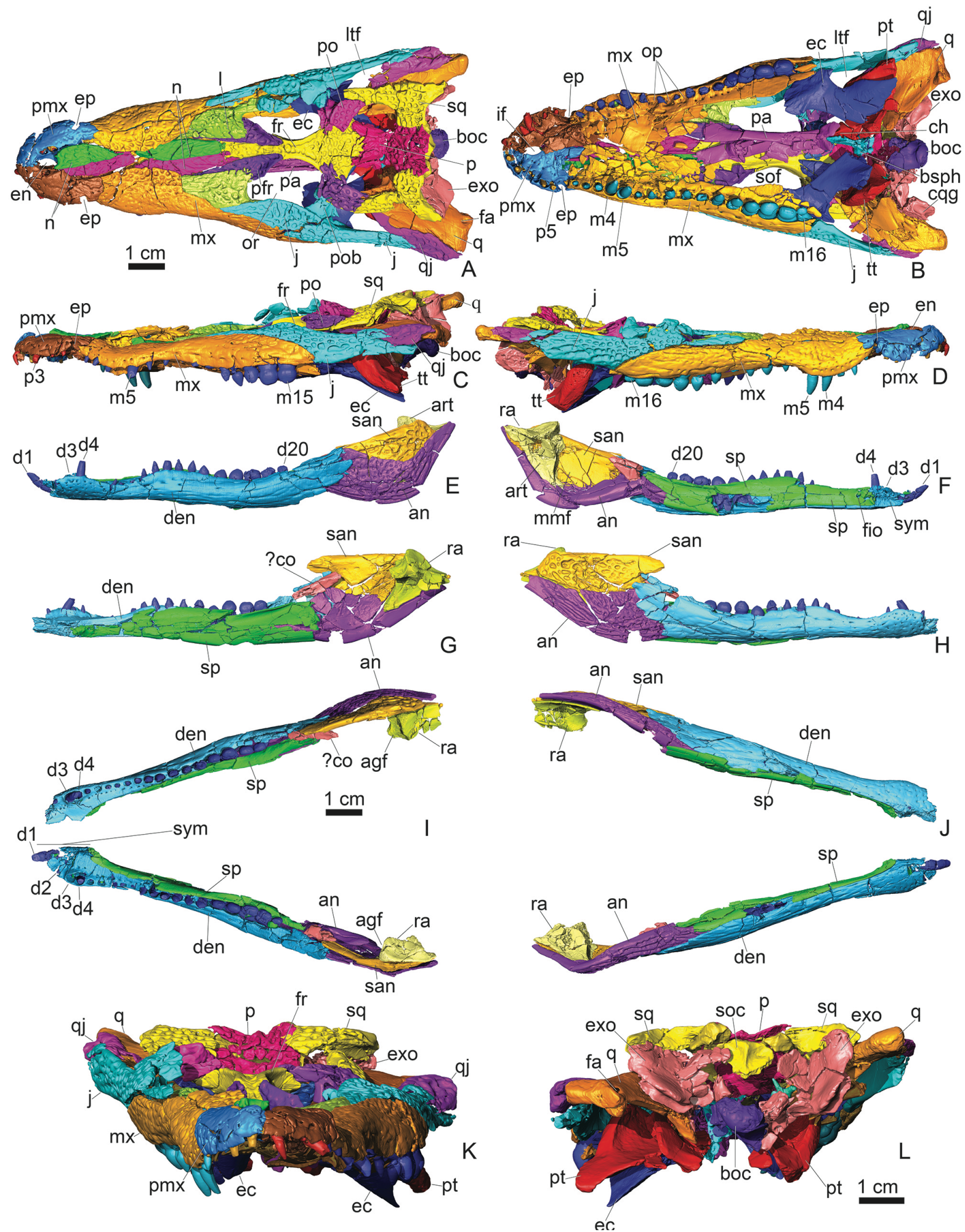
Figure 8. **A**, Transverse tomography through the skull of *Bernissartia fagesii* (IRSNB R46) illustrating the state of preservation of the inner parts of the skull at slice 2589/3105 with part of the right labyrinth identified. 3D surface rendering of the right vestibular system in **B**, medial; **C**, lateral; **D**, dorsal; **E**, ventral; **F**, posterior and **G**, anterior views. Abbreviations : aa, anterior ampulla; asc, anterior semicircular canal; la, lateral ampulla; lsc, lateral semicircular canal; sac, sacculus; q, quadrate.

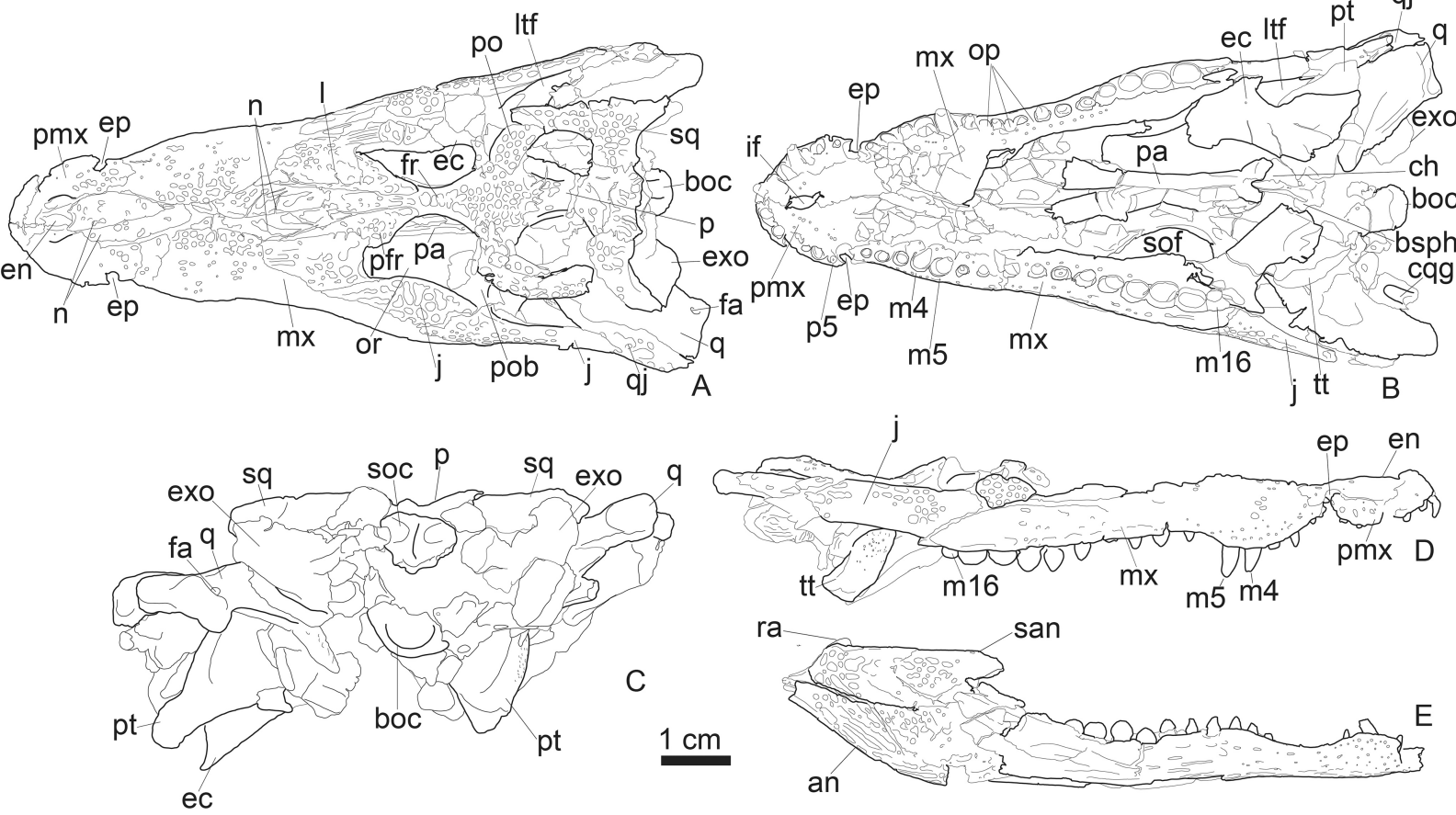
Figure 9. Bones of the mandible of *Bernissartia fagesii* (IRSNB R46). Right dentary in **A**, medial and **B**, occlusal views as well as in **C**, a close-up view of its anterior portion. Right angular in **D**, lateral; **E**, medial and **F**, posterior views. Right surangular in **G**, lateral; **H**, medial and **I**, posterior views. Right articular in **J**, dorsal; **K**, lateral; **L**, anterior and **M**, medial views.

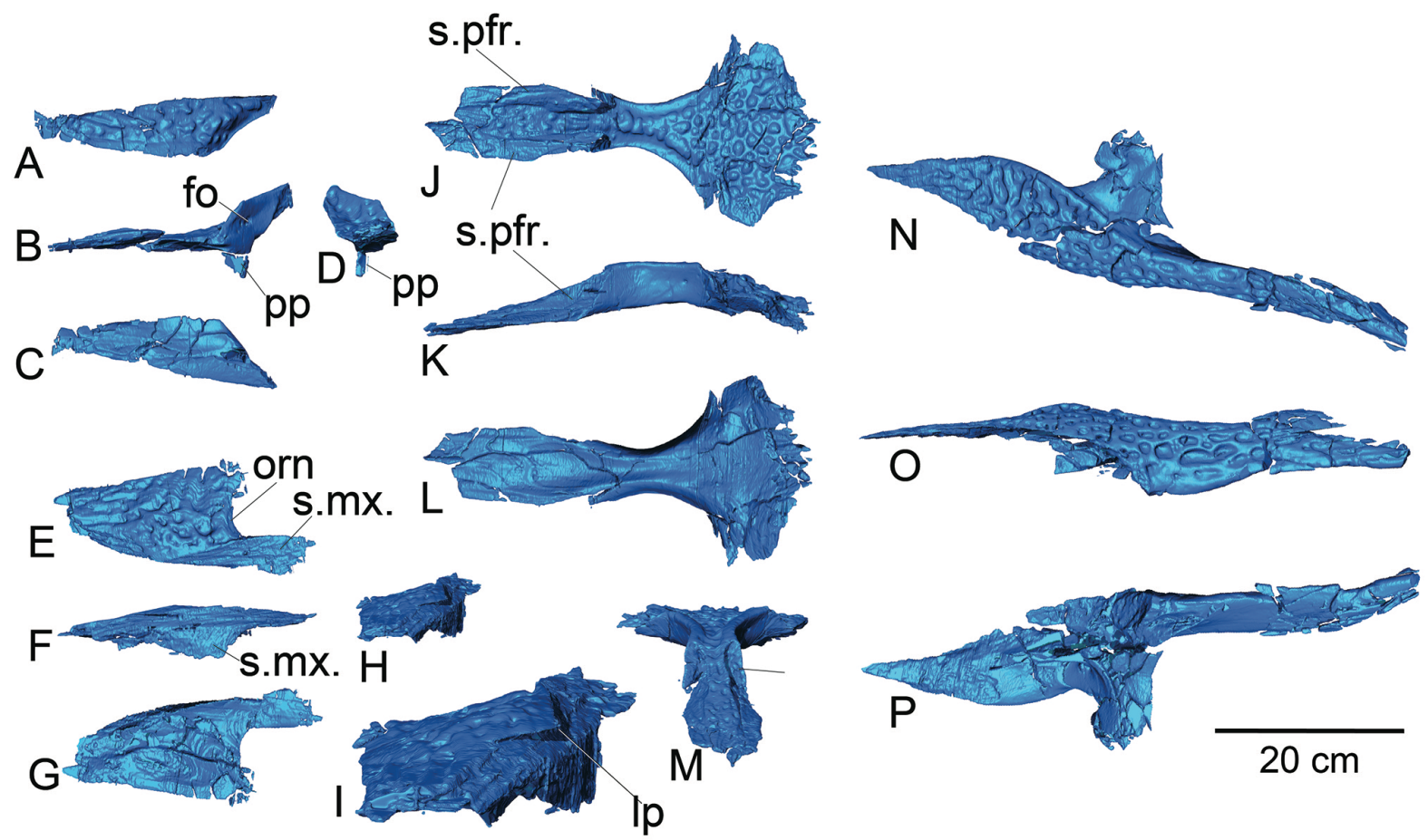
Figure 10. The dentition of *Bernissartia fagesii* (IRSNB R46) as revealed through transparent CT reconstructions of the skull and mandible in **A**, left lateral; **B**, ventral; **C**, right lateral views. Enlargement and details of the extracted right maxillary tooth row in **D**, medial and **E**, lateral views as well as the extracted right dentary tooth row in **F**, medial and **G**, lateral views.

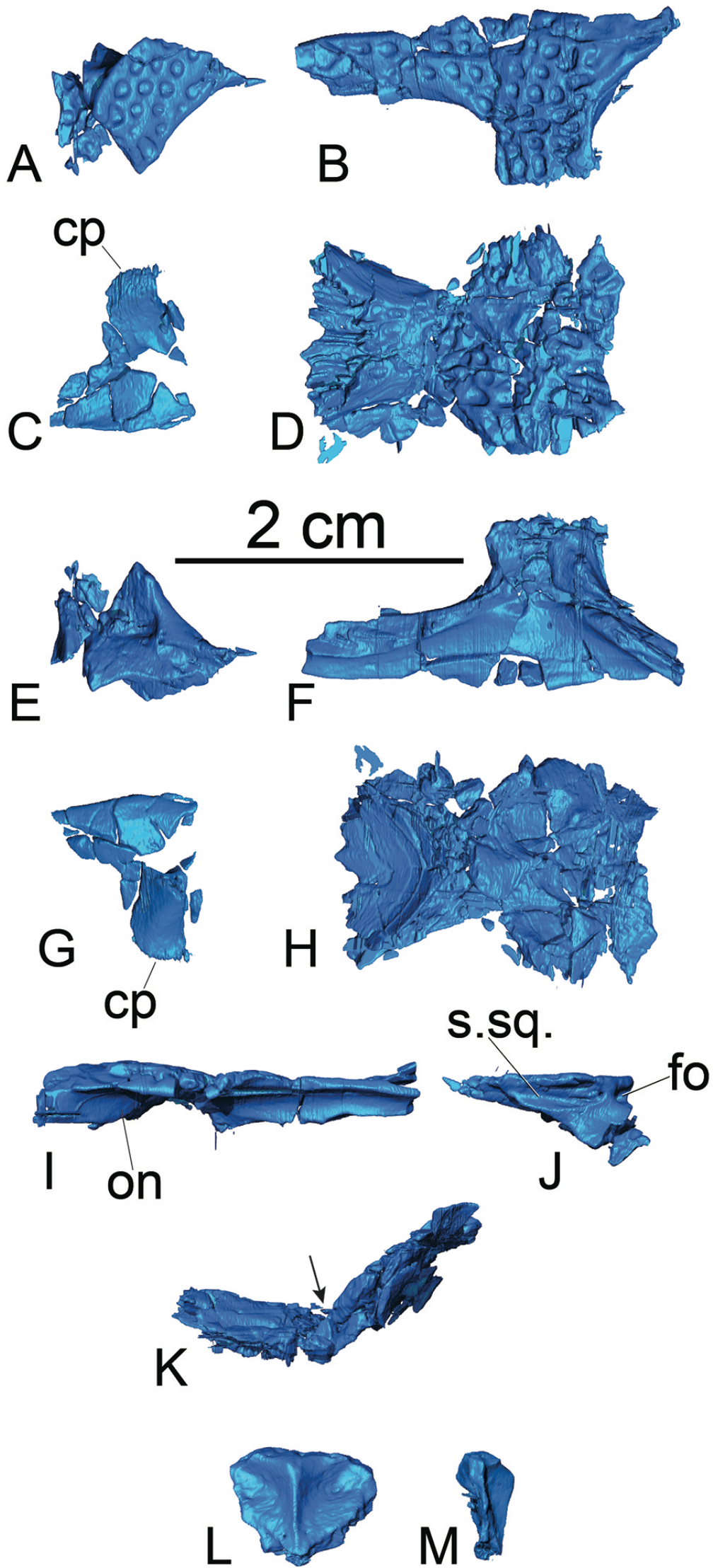
Figure 11. Stratigraphically calibrated strict consensus tree of derived neosuchians as recovered in this work including the relationships of Paralligatoridae, Goniopholididae, Pholidosauridae, Hylaeochampsidae and the crown clade. Note that Atoposauridae are not monophyletic. Numbers refer to Bremer support indices.

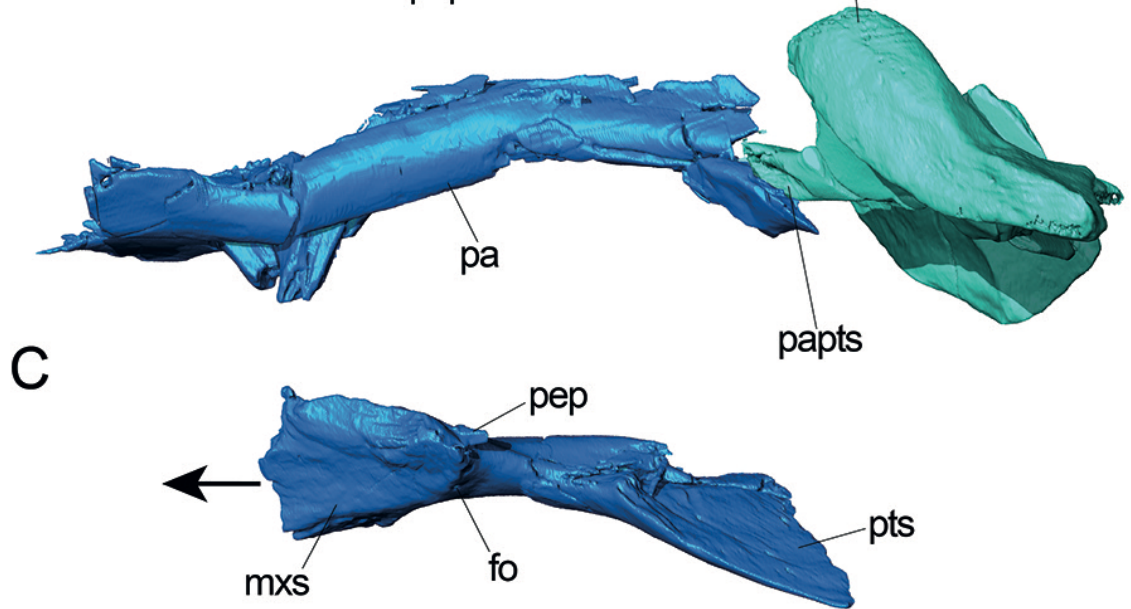
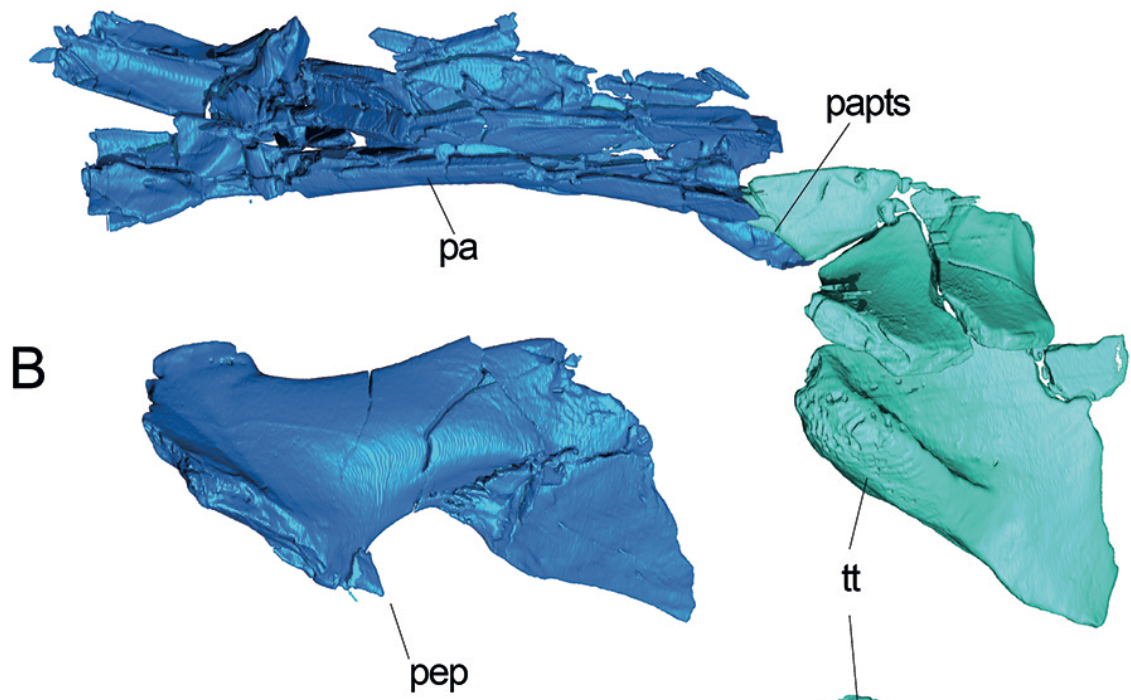
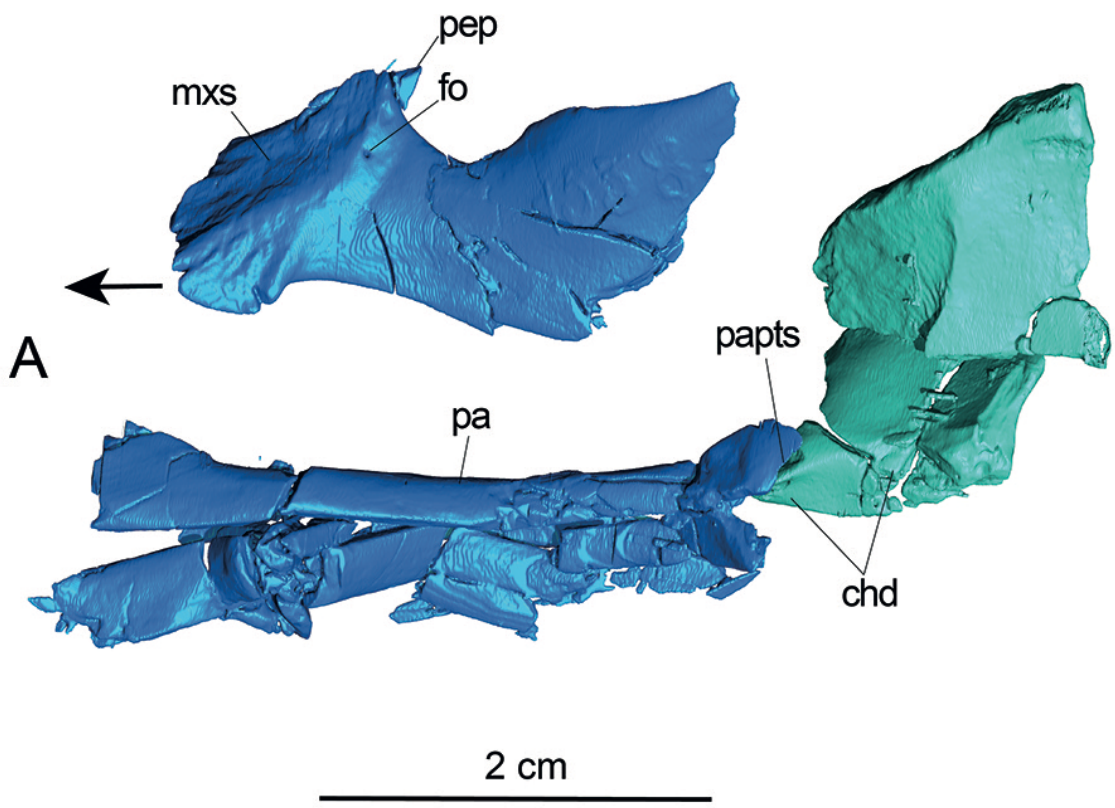


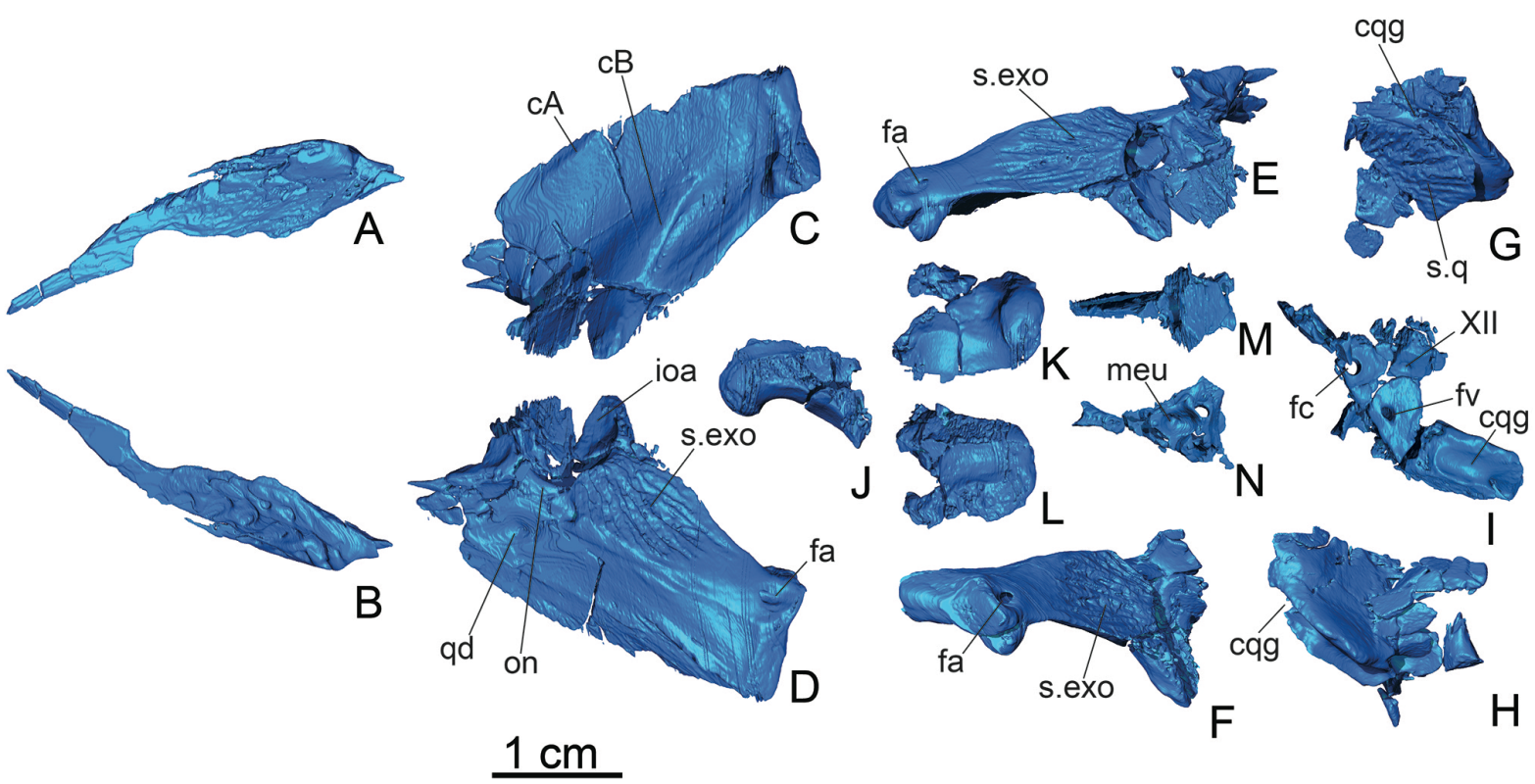


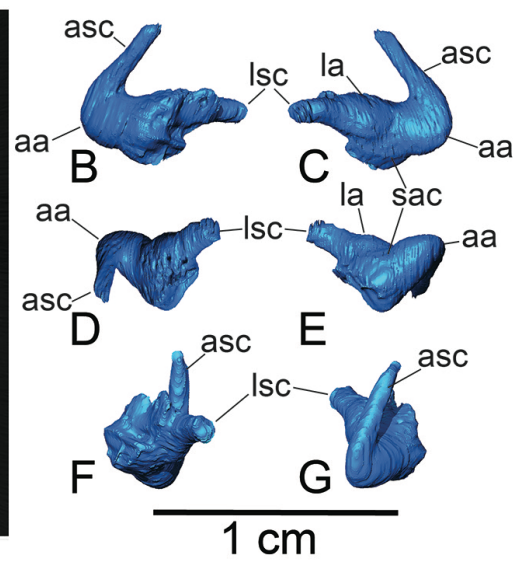
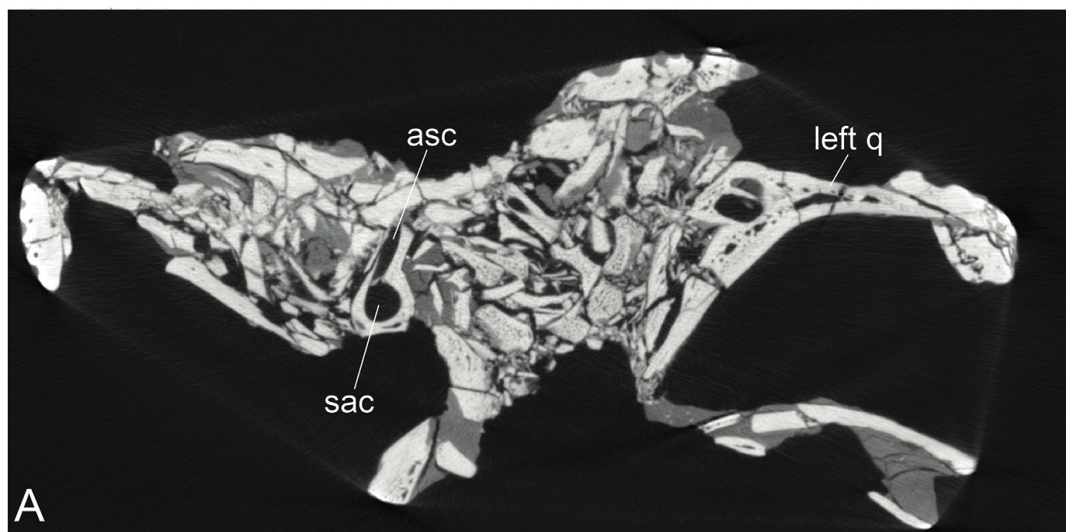


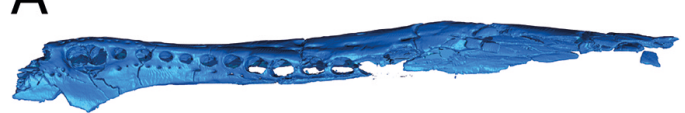
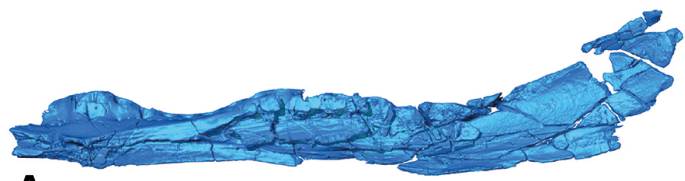




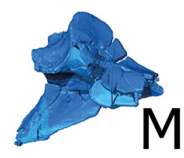
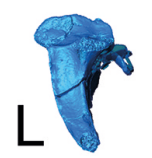
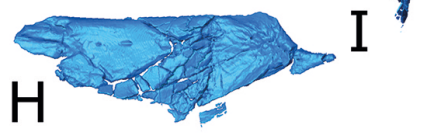
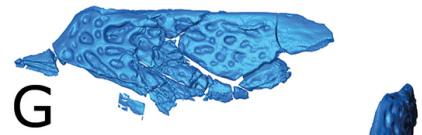
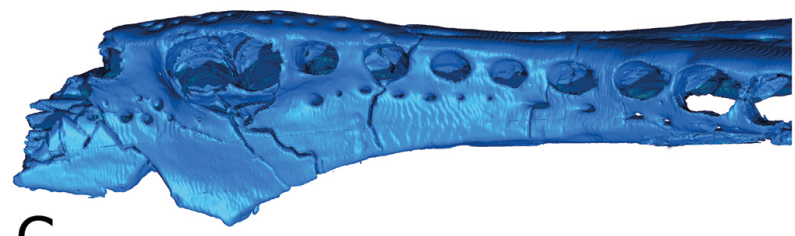
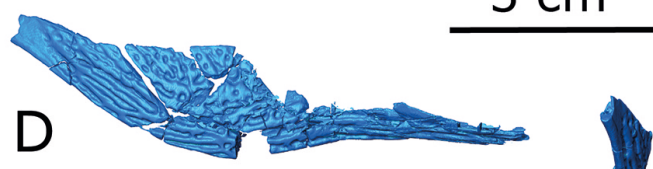


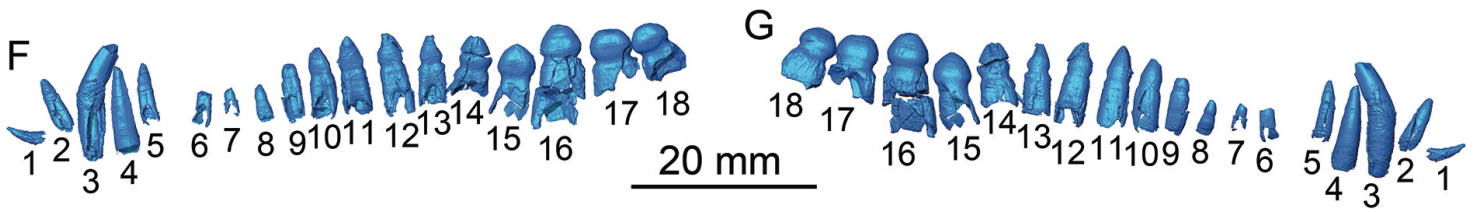
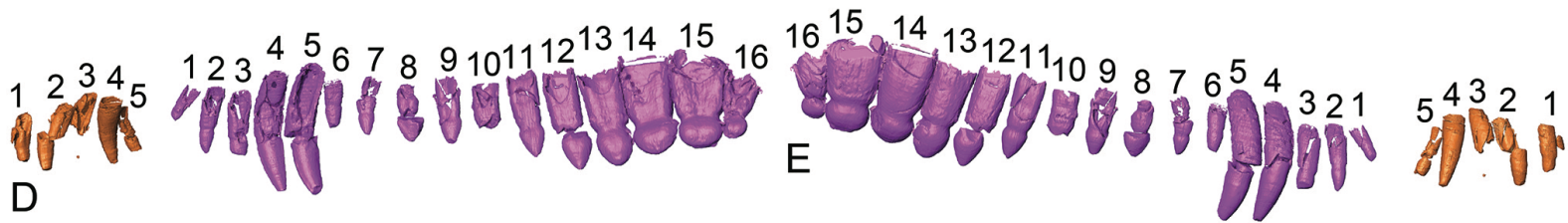
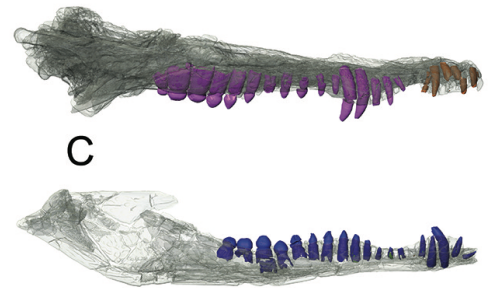
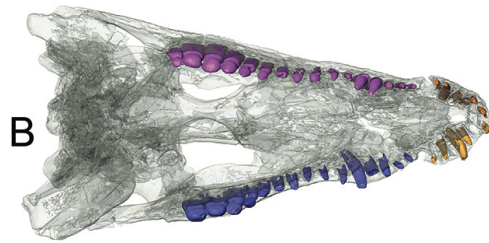
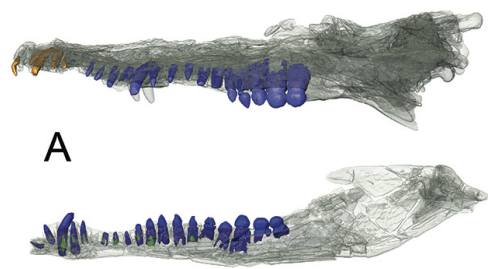




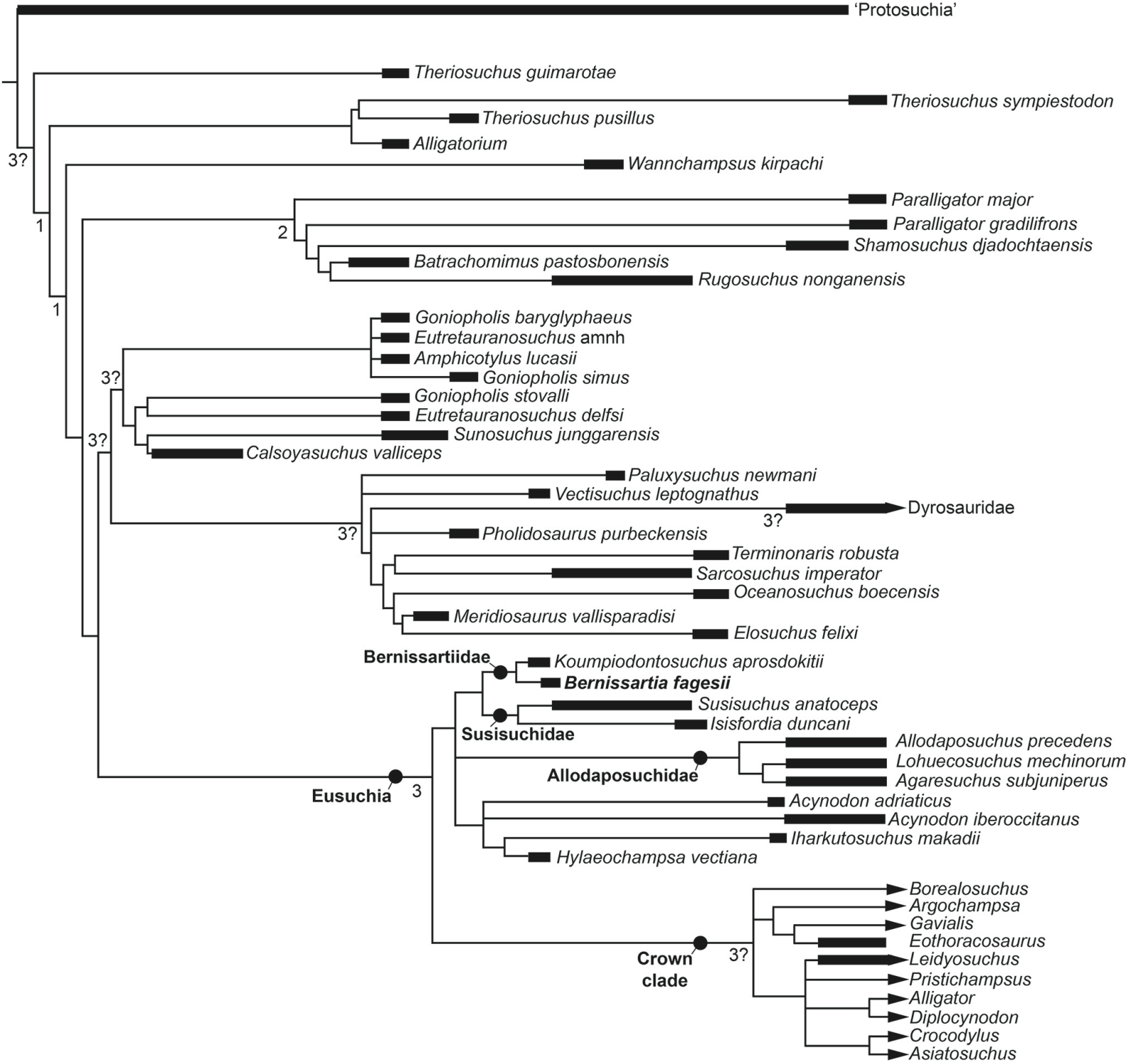


3 cm





Heft. Sinem. Pliensb. Toarcian Aal. Bath. Oxf. Kimm. Tith. Berr. Val. Hau. Barr. Aptian Albian Cen. Tur. Con. Sant. Camp. Maa.



Zaraasuchus_shepardi

10?????????????1?01?01?1000001?10?02?????????????????????????????????3?????1?010??????????????[1234]0?
?1010?0?????????????0?????????????????????????????????1?1?????????10?????????0000?????????0?????0????
?1?????1?00?????0?????1111111111?????????????????????0?????00?????????????0?10?????????1000?00?????000
0?????????0?????????0?0?0?????????????????????????????????000

Gobiosuchus_kielanae

101000?110000011001?[01][01]?1?00001?10?0201000?0020112011111000?0????301???1?20100[01]010?0?1?
?????0?1010110[01]3013002?0000??0000[01]00001000000?00001001211?0000???1100000001?00000?1?0
010000000??00?0?01?0121000011?00?00?001111111111?000000??00000000?0000?00010?00?000?001?0
??1????10?0?0?????????000000??0?000?00000??20?????0?0?????????????????????000

Sichuanosuchus_shuhanensis

[12]01??0?1200[01]00?10010[01]1?110????1?00?021?10?00020?1?011?1100???????3?11????1?000011?1??1??
????000?????????10?12?0?1??0??100000??1??10?0???0011?[01]1210?00?????1??000?00100?00?10??000?
0?00??0?00110?111011111100?1010000100?1??0??0?00?00?000??00?001??00??00??0?????0??
000?00?1??0?0?000000??000000?00000?011??0?00?????????????????????000

Shantungosuchus_hangjinensis

2?1?????1?0?0?0?1?1??11?????????21?1[01]100020?1?011?1100?10?????????101?1?000??10?????????0????
?????????0?1??????1?????00000?????00?10?00??11211??001?????00000000?0?????1??10?00?0?????0?
?????0??1011111??0?1[01]10??0????1?????????????0?????????????????0?0?????????????????????0??
00?0?00?00??00000?0?0?????????1??0?0?????????????????????000

Zosuchus_davidsoni

201??0?1200000?001010[01]110?001110?02211010012?1??011?11000?0?1?0311110?????0?01111?????????
??????????10?13?3??1?????00000011011?0001?0?0010112?[01]?0001??0?0?0010001[01]000?[01]111????0
??0?00??000?1000111?1011?10110100000100??0?000?000?0000000?0?00?0?000100?00??10?10????0
??0?0?00??000000000000?0??0000000000011?01?????????????????????000

Fruitachampsia_callisoni

201??001200100010000100100000110010221?11?0120112?1????0?0?0??1?3?31?????1?0111101011?1?00011
112?0??1?0??[12]00??1?1001?000?0?0100100??101?0012?01110?0?00?10?????001?00?0???000?0000?0??
??0?????110??000????101??0?00000?000?0?00??0?00?????0??????0?100?00????00110?????????00100
0??1?0000000000?000?0000000?000111?11?0?0?????????????????????000

Rhabdognathus

202?????200??11100010011011010011012110100[01]01112011?1011010?1?11?302?????????0?????????????
?????????????1?10?00?????????000?????00?000?0[01]10020?001?00?????1?????0?01[01]22000?0?0?00000
0?????0?00?1010010?01?1000001?0000?????0??000??112?1??010?00000000?11????0000111?0??00
00000??1?0?0?00000?1?01?0002000?000011?01?00?????????????????????000

Sokotosuchus_janwilsoni

2?2??21112??10????001001??101001?012?1?????1112?11?1?11?0??0?1?1?0?????????01?????????????????
?????????2?0?????????0?????????0?????????0?10?????????0?????????????0?????????????1?????????0?????
?0?????????????1?????????0?????????2?000?????0?001?0?11?????????????????????????????????0
000?????????????1?0?????????????????????????????000

Dyrosaurus

202?12?102?010?11??010011??101001?012?101000?1112011?1011?10?101113021??00?2?000?????????00
?????????????1?10?00?????????00?????00?00?0010020?0??0?????1000?00001?0200?????0?0?00?0????00
000010?0?000?1?00?001??000000??0?0?0?00?11201000010?000000?0??1????0010011100??00000?0?
?????00000001?0110002000?000010?11?00?????????????????????001

Hyposaurus_rogersii

?02?12?102??1??????1?????0?101??????2??????1?12011?101??10?1?1??3?????0??2?
000??112?????00?????????01??0??0??1?0100?????????????????0?1002??0??00??1?1000100?0??00??0?

Goniopholis_stovalli

203?121111??101?1000100111?0010001001?1??000?1110011?10?0?0?0?1?021312?410????02?????????????
?????????00200?00??????001??1?1100?000?0010001?1??00?????0?????0001022?00?????0?1??0?11??00?
?00?10?0?0?0?0?1?1100001000000?????0?0000000?1?00000000??0?000100?00?????0?0010?100??000?0001
0??0000??00001?0??00?0000000?0????????????????????????????????????111

Amphicotylus_lucasii

203?121111??101?1000100111?0010001001?1??000?1110011?10?0?0?0?1?021312?410????02?????????????????
?????????00100?00??????001??1?1100?000?0010001?1??00?????0?????0001022?00?????0?1??0?11??00?
?00?10?0?0?0?0?1?1100001000000?????0?0000000?1?00000000??0?000100?00?????0?0010?120??020?0001
01?00000?00?00001?00?000000010110??1?000????????????????????????????111

Calsoyasuchus_valliceps

203?0201110?10?110?01021111001000?001?1??00?1110?11??0?0?0?1?0?111[12]?????????01????????????????
?????????0?0100?00??????01??11110?0??0?0010001?1??00?????????????001022?001?????1??0?01??0?
??00??????????????1100?0100000?????0?00000000??0000000?0?100?0?100?00?????0?1010?0?0?1000??0??
0?0?0?0?0?0?0?0?0??00000?000?????0?0????????????????????????????111

Sunosuchus_junggarensis

203?0201111?10?1100010011110010001002110100011110011110100?0?11011312?41000110201??1111?0?2
0001200?11??
??1??0?011??00?00?1000??1?000
0000?000?01?????00000?0200?01??00????????????????????????????111

Eutretauranosuchus_delfsi

203??????10010111000100111?00?0001001110?000?1110011?1010?0?0?1?0?121204?00001020111??1?0?0?
?1??????3??100?00??0?001????110?????????0?00????1??0????11??[012]?1??01022100?1????10?0??1??
?00000010?0?000?1?110??01?0000000??0?000?00??100?0?000?00?0?00100?00?0?1010010?0??00010
00?0??000?0000001?01000?0000000011??1??00????????????????????????????111

Eutretauranosuchus_amnh

203??????100??1110?01001111001000100111010000?11001111010010?110??312????????????0?????????????
12?????????0?00?00??????001????10??00?1??100011100?00?????0?????0?01022100?????0?001?1??0?
?????01?010??1?111?00??0?00?00?0?0000001?0?0?????????0000?100?00?????0?00?????2?0?0?0??1
?0?0??000?0?0?0??0000000011??1??0????????????????????????????111

Goniopholis_baryglyphaeus

20??1????10010111000?0?11110010?0??02?101??001110??????10?0??0?0?131??4??01?102?????????0?000
1200?11??00?0?0?0??????0?0?0?1011??????0?00100??????00??????31?00010?2?0??1????1?????1?????
???10??????0????10??10????????????????????????000?000?????000?????0?????????????????????????
0?000?0?0?0?000?000000?10??1????????????????????????????111

Alligatorium

?0?????1?0000?1000010?111??0?100?1?????00??11??1??1000??????20?1???00101?101?0
11211000??1?00100??????????10??1????????????????????0?????????????????????1?????????????????
?????0????????????????????????0????????????????????????????0?????????????1??00????????????????
??0??????????????0??0?0000??10????????????????????????????000

Theriosuchus_pusillus

201101111201001100001101111001100110211010001?11?01111000?????1?20211?410010102011011211000
11[12]1200100130?1002?0?10?110100[01]001?1100?00?0?00120??01??0?00??10[01]00210100[01]02200?100
?0?10001110[01]?0?0?0101?0100001?100000?00000?20??000?00000?100?0000000?000??100?00?0?0?00
11?1??0?1000000001?0000?0000000?00?0000?000110011?01??00????????????????????000

Theriosuchus_sympiestodon

2?1?????1?2?????????01101??????0110?1101001????0??????0?0?????311?????????1?????????????????
?????????00?????????????0?0?????????????00????????????????????????0??2?????????0??01??0?????1?

1?0?0???1?00???0???0????0????????1?0????0????00001????????0?0?0????????0????0????????00
00?0?0?????00?0100?????1?0?????????????????????000

Theriosuchus guimarotae

201101?1121?00??01?011?11?????10?00??101??1??????1?00??????202110??00??1101??1????0100?1
20??01??100??0?10?1?0?100001??00??000?12?00?0?0??010?????1?1011022?011?0?0??0??11??0??
0??10??01000?1?000??00?00????0??1?0?00?0?00??0?0??1?0?00?1010?0????1??01000?000????
????????????0??00?000?1?0????1?0?????????????????????000

Wannchampsus kirpachi

203?0??121?0011000011111000100011021101001111201111000000?1?0??310??100111?211?????????1
1????????300?0021001??101100??1100?000?00?100010001?00??100?13101?0?022011?00?0?10001100
01000?001010010?00101000001??000020??0??000?00100?0??000?00000100?00??1?20001?00????0001
000??11000010000001?010000?00?1?010??11?00?????????????????????000

Paralligator major

213??[12]1102??00???0011?1??0010001002?101?01?1?????1?10000?0?1?0??312??????????2??1??????????
??1??????0[12]00??0?0?????001?111100?0000?0010????????????????????00010?2??1??0?1?00?11??
0?????101??0??1?1000??0??2??0?0?00?000?100??00000??0?000100?0????00????0??1?11?0?
11?0?1?000000000????000000110????01?100?????????????????????000

Shamosuchus djadochtaensis

203????10?1?0111000110111000100011021101?001110?1111000000?110??310?4100101?1??????1101[34
]11[01][13]1?0?10?[03]00[123]002?00[01]????01000??1?11?0?000000100011101?00000?0?0?10?000021[01]
?0?1??0?1000?100000?0?001010010?001?10?0001000200200?10??000?0?100?0?00?00?000001?0?0001?1?
0?01101?0001111011?1?001000000001?01000?0000001?110??01?00?????????????????????000

Paralligator gradilifrons

20301[12]11020000??1000110111?00100011021101001111001111000000?110?0312?1100101020?????21??
[234]000[13]1??10?000100??00[01]0??0100101111100?000000100010101000??010000001001021?11?10
?0?1000?110000000010100100001110000010?0200200?10?0?00000?10000000?00?00000100?00??1?10001
0001?000110111?110001?00000001000?0000000011110001?100?????????????????????000

Rugosuchus nonganensis

203??[12]?1?20?00??1?0110111????00011[01]2110?000?110?11?1000000?1?0??31??4?0010102?????????
?????21[12]0?0?0[03]0?100??0????01?01??1?1000?0?00?0100?1?1??00??100?0?1?100??2??0?10??10
??110000?0?0??0?100001?100?0010?000020??0?0?00000?1?0?000000?00000100?01????0?????????
??1111??1?0000?000001?0?000000000?0011?0?0?00?????????????????????000

Glen_Rose_Form

2030001112??0011??0100111?001100??2110?001??11??11?10?00?0?1?030310??01?10211?????????????
????????3??100??00????01000?0131?00?0000??010?0??01?????10??13101001022??1?10?0?10?0?1000?0
00??01?1?010?0?1?1000??000?0?2??0?0000000100000000?0?00?00100?00??200011001??101?1000
??1?0000100000?00?0??0000?110100011-1?0?????????????????????000

Batrachomimus pastosbonensis

2030??1021?00??100010?11100010????21101000011?0????????????????03?2?410?10102?????????????
????????100?0?0????01001?11?1000??0000012101?10??0?????0?0??00000110?????0?100??110000??
1??1?001000?1?100?00?0002?000??01??000?0?100?00000100?0??1?0?00??????????1?0??1101110??1
?0000?0000?0?0?000000?00?00?01??00?????????????????????000

Hylaeochampsia vectiana

00??????21??11??1?01??0???002?1?1012????0??101??1?1????310?????????????????????????
????????????0?????00????????????0?0?0?????0????????????????00022?01?????00?1????0?????
????????????????????????0?????0?1??0?????????00?0?0?????001110?????0000?0??1?0?0?000
????0?0??110111?0?0000??11?10?????????????????????000

lharkutosuchus_makadii

203?1211021?0011?10010?101?001?0?1002110101201110011?1010010?110013?0?0?01?0?1?????????????
?????????0?100??10?000000?14100?000010110000000000?0?10?011?1000002001?0?0000?0?0?1?
20??0010000100011?10000000?000000??0000000?1000000000?0000010?00?????2?0?00011????000001
0??10000?0000101?010111110000000021?11010????????????????????000

Acynodon_iberoccitanus

203?021102?00?210?0100111?0010001002110?012?1110011?10100?0?1?001310?3??11?10200????????????
?????????3?1100?00??0?1000?14110?00000?010101?1???00??00??1?001021?00?0?00?0?00?0??0?
00?0?1010?1000?1?100?0010?000?00??0?0000000?100?1000010?0?000100?00??0?0?0?0?0?0?01?1100
??1?00?00000?01?01?111110000001110?10010????????????????????000

Acynodon_adriaticus

203?02?1020000??0?01001110011000?0021101012?11?0?1??1??0??1?001310?3?011?0000?2?????????1?
?2110?0?301100??0??0010000?141?0??00000012111?1??00??000??0??000002110????0?0000?0??00
0??0?1[01]10?1000?1110?000?0?00000?0?0?0?0?0000100?00000??000001?0?0?????????00?11??010001
000?0?00??0000?0?01?1111?1100000110??11?10????????????????????000

Allodaposuchus_precedens

203??2?11?0??1?0?10[01]1111001000?00?11?????1??110?11?1?00?0?1?0?131?????????2?????????????11
????????????0?0?0??0??001?????0?00?000100?1?1?1?00????????????00?022?01?????1?00?????0??
?0??010?1??0?0?10?001??0000????0?0??000?1?[01]0?000?0?00000?0?0?0??0000101?????0?????
?????????0?0000?01?00010000000?1110?1?100????????????????????000

Agaresuchus_subjuniperus

203?1211120000?0000101111?0110?0??0211010120?110011010000?0?11?01?10?????????02????????????????
?????????0200?00?0??00101131100?0000001000101?1000??????????0001??110??1??0?1000?11????0?
??0?1010010??1?1000?010?1000??0?0000000?1?0?1000000?0000?100?10????00000?1?????2011????
??0?0?000?0?0?0?000000?00?1111?1?100????????????????????000

Lohuecosuchus_mechinorum

203?1211120000??1100101111?001000?0021101?12?1110?11?1?00?0?1?001310?????????02????????????????
?????????0200?00?????00101131100?00000010111?1??00????????????001022?01?1??0?1000?11????0?
??0?1010010??1?1000010?0000??0?00000?0010001000000?00000100?00????00000011????02010?0?
?100??00000?00?0?000100000001111?10?00????????????????????000

Susisuchus_anatoceps

203?12?10?1?00?11000100111?001000100?????1??11?2?????????????1?0?131??3?0?0?00??1????????0002
020110????100?10?00?1?000??1?11?0??000012011?0??00????????0????0?1022?01?0??0?10??0?0??0?
??0??0?1?00?110?00?0?000000000?0?0000??0000000?0?0?0?1?0000??0?0?11?0??0?10000?00?0?
00?0??0000?1?????0?00100?0112????????????????????????????000

Isisfordia_duncani

203?12010200001110001001111001000100211010011112011?1010010?1?101312?310001000001?1?????1
000[12]010000?010100?1001?00?0?0010?131100?0?000012101?1?1000010?0?00000000022101?1??0?00?0
00??00?00001?11010001111000010?0000000?0?0000000?100?0000000?000001000001????011000?20??
100?11000010000?00000001100?000000010010112??1?01????????????????????000

Borealosuchus_formidabilis

203?1211120010111000100111?00100010021101011111211111010010?110?1310031000110201111211113
111?110?10?300100210?100100?001?11110??000000010001?1??0000110000310?00?022101????1000[12
]11?0000?00101001000011100000100000000000?000??0?100??000000?00?001000000?0100010?111?00
?000000001?000000000001101?00?000000101000?10000????????????????000

Argochampsia_krebsi

202?121112001011????110[01]101?0010001012110?012??112?11?10110?0?1?0?1300????????00????????????
????????????0100??00????001??111100??000?010?0[12]0?0?00????????0001022?01?1??0?00?020??

??0??0??1?010????1000??10?0?0?????0?0?0000?0?000?0010?0?000100??1??????1001?0????0000??
0??100?0?0?0?00?0?00000?000101100?1?000????????????????????000

Pristichampsus_vorax

200?02?112000011100010111100010001002110??1211112011?10100?0?1?1?1310?3???0?102011?112??0?31
1?1?????1?3?0100??001??1?1101??1?1100?0000000120010100?000?[01]0??0300100002??01?1000?[01]001
?1?00?000?001010010??111000001000000?0?0?0000000?10000000000?00000100?000011000111111??
?000??00?1?000??0000000?01?00?000000101110?10000????????????????????000

Eothoracosaurus_mississippiensi

[12]02?1211120010??11?[01]100111?0010001002110??1?011?2??1?1?11??1?0?131??3100??20000????????
?[1234]111[12]1?????1?3001002?0?1?0?01?01??121100?0000?00100?1?????00??0000010?001022101????
?0000??000000?00101?0?000?1?10000010?000?00?0?0000?00??00010000100??000100?00??01010?11
0??0000000?1?000000000000?00000?0000000100010?10000????????????????????000

Gavialis_gangeticus

212?12111200111111011011111001000100211010120111201111011010111001310031000120000011121101
31112111100?300100210?10010[01]?001??121100?00000001000101?1?00001?00000100001022101?1?00000
00[12]1??00000?001010010000111000001?00000000000?000?00?100010000[12]00?00000100010111001011
0110?001000001000100000000000?1011000000000101000?10001????????????????????000

Leidyosuchus_canadensis

203112111200[01]01110001001111001000?0021101012?1112111110100?0?1?0?1310031000110201????????
????20??10?300100?00?????01001??111100?00000001000101?1?00??1[01]??31?1001022100?1000?1000
211?0000?0010100100001?10000010?00000??0?0000000?100000000000?00000100?00??1001101111??
?00010?0??1?000000000001?0010000000000101011?10000????????????????????000

Asiatosuchus_germanicus

203?1211120000111000101111?0010001002?10?012111?2?1??1?0????1?0?131003?000110?012?1?21??1?11
????????300100?10????1101001??1[12]1100??00001000101??000??10000?10?001022?01?1????10?0?110
00000?0?1?1001000?11100?0010?0000?0??0?000000?1?000000?000?0?000100?00101100010?111?0?000
?000001?00000??000?0?00000000?0101??1?0????????????????????000

Crocodylus_niloticus

203012111200[01]011100010211110010001002110?01211112011110100101110013100310001002012111211
0131112021100?3001002100100100?001??121100?0000000100010101?00001?0000310?001022101?1000110
00211??0000000101001000011100000100000000000?000000?10000000?00?000001000001011000101111
?0010000000001?0000000000001010000000000101000?10000????????????????????000

Diplocynodon_hantonensis

203?1211120010111000101111?0010001002110?01211112011110100?0?110?13100310001002011111211013
1112021110?3001002?001??1?01001??111[01]00??0000001000101?1?0000110000310?001022001?10?0?1000
?11?00000?00101001000?11100?0010?0000000?0?0000000?100?00?0000?00000100?000011001101111?00
10001100001?00000??0000010?0000000000101010?10000????????????????????000

Alligator_mississippiensis

203112?102?0001110001021111001000?002110101211112011110100101110003120310001002012111211113
1112021100?30010021001001001001??111000?00000001000[12]0101?000011?0003101001022000?10001100
0211??0000000101001000011100000100000000000?0000000?100000000000?0000010000000111011111110
0010001100001?000000000001101?0000000000100010?10000????????????????????000

Koumpiodontosuchus

2	0	3	1	?	1	?	1	1	2	0	0
	1	0	?	?	1	?	?	0	0	0	0
	1	1	?	?	?	?	?	0	0	0	1
	0	0	2	1	1	0	1	?	1	1	1
	?	?	1	0	?	0	?	?	?	?	?

0	0	?	1	?	1	?	0	0	1	3
1	0	?	?	1	0	0	1	?	1	0
2	1	0	?	?	?	?	?	?	?	?
?	?	?	?	?	?	?	?	?	?	?
?	?	3	?	0	?	0	0	?	?	1
0	?	?	?	?	?	0	1	0	0	1
0	1	1	?	0	2	0	1	?	?	?
0	?	?	0	?	1	2	0	?	1	?
1	0	?	?	?	?	?	?	?	1	0
?	?	0	3	1	0	1	0	0	0	0
2	1	1	?	0	?	?	?	?	0	?
1	0	?	1	?	1	1	1	0	?	0
?	0	?	?	0	?	?	?	0	0	1
0	?	?	?	1	?	0	0	0	?	0
0	1	0	?	?	0	0	0	?	?	?
?	0	0	?	0	?	0	0	?	0	0
0	1	1	0	0	0	?	?	0	0	0
0	0	?	0	?	0	0	0	1	?	0
?	0	0	?	?	?	?	?	0	?	1
1	?	0	0	?	?	?	?	?	0	0
0	0	0	?	0	?	?	1	0	?	0
0	0	?	0	0	0	0	0	0	1	?
1	?	?	?	0	0	?	?	1	0	0
0	0	?	0	1	0	?	?	1	0	?
?	?	?	?	?	?	?	?	?	?	?
?	?	?	?	?	?	?	?	?	?	?
?	1	0								

Bernissartia_CTScan

2	0	3	1	1	1	1	1	2	0	0
	0	0	1	?	1	0	?	1	0	0
	1	1	1	1	0	1	1	1	0	1
	0	0	2	1	1	0	1	?	0	1
	0	1	1	0	?	0	1	?	1	1
	?	?	1	1	?	1	?	0	0	1
	1	?	?	3	1	0	0	1	0	1
	2	0	0	?	?	?	1	?	0	?
	?	?	0	0	0	2	1	1	0	1
	0	?	3	0	?	1	0	0	?	0
	?	?	?	0	?	?	0	1	0	1
	0	0	0	?	0	2	0	1	?	0
	0	0	0	0	?	1	2	0	?	?
	1	0	?	?	0	1	?	?	?	0
	0	0	0	3	1	0	1	0	0	0
	2	2	?	0	0	?	?	0	0	0
	1	0	0	1	2	1	1	1	0	0
	0	0	?	0	0	0	0	0	0	1
	0	0	0	?	1	?	0	0	?	?
	0	1	0	?	?	0	0	0	0	0
	0	0	0	?	0	0	0	0	0	0
	0	0	0	?	0	0	0	0	0	0
	0	?	1	0	0	0	0	0	0	?
	?	0	?	1	?	0	0	0	1	?
	0	0	0	?	?	?	?	0	0	1
	1	1	0	0	0	?	1	?	1	0
	0	0	?	0	0	0	?	1	0	?
	0	0	0	0	0	0	0	0	?	?
	1	1	1	0	0	0	1	0	1	0
	0	0	?	0	1	1	1	0	1	0

0	?	?	?	?	?	?	?	?	?	?	?
?	?	?	?	?	?	?	?	?	?	?	?
0	1	0									

;

Ccode

+[/1 0	-[/1 1	+[/1 2	-[/1 3	-[/1 4
+[/1 5	-[/1 6	-[/1 7	-[/1 8	+[/1 9
-[/1 10	-[/1 11	-[/1 12	-[/1 13	-[/1 14
-[/1 15	-[/1 16	-[/1 17	-[/1 18	-[/1 19
-[/1 20	-[/1 21	+[/1 22	-[/1 23	-[/1 24
-[/1 25	-[/1 26	-[/1 27	-[/1 28	-[/1 29
-[/1 30	-[/1 31	-[/1 32	-[/1 33	-[/1 34
-[/1 35	+[/1 36	-[/1 37	-[/1 38	-[/1 39
-[/1 40	-[/1 41	+[/1 42	+[/1 43	+[/1 44
-[/1 45	-[/1 46	-[/1 47	+[/1 48	-[/1 49
-[/1 50	-[/1 51	-[/1 52	-[/1 53	-[/1 54
-[/1 55	-[/1 56	-[/1 57	-[/1 58	-[/1 59
-[/1 60	-[/1 61	-[/1 62	-[/1 63	+[/1 64
-[/1 65	+[/1 66	-[/1 67	+[/1 68	-[/1 69
-[/1 70	-[/1 71	+[/1 72	-[/1 73	-[/1 74
-[/1 75	+[/1 76	-[/1 77	+[/1 78	-[/1 79
-[/1 80	-[/1 81	-[/1 82	-[/1 83	-[/1 84
+[/1 85	-[/1 86	-[/1 87	-[/1 88	+[/1 89
+[/1 90	-[/1 91	-[/1 92	-[/1 93	-[/1 94
+[/1 95	+[/1 96	-[/1 97	-[/1 98	-[/1 99
-[/1 100	-[/1 101	-[/1 102	+[/1 103	+[/1 104
+[/1 105	-[/1 106	+[/1 107	-[/1 108	-[/1 109
-[/1 110	-[/1 111	-[/1 112	-[/1 113	-[/1 114
-[/1 115	-[/1 116	-[/1 117	-[/1 118	-[/1 119

-[/1 120 -[/1 121 -[/1 122 -[/1 123 -[/1 124
+[/1 125 -[/1 126 -[/1 127 -[/1 128 -[/1 129
-[/1 130 -[/1 131 -[/1 132 -[/1 133 -[/1 134
-[/1 135 -[/1 136 -[/1 137 -[/1 138 +[/1 139
-[/1 140 +[/1 141 +[/1 142 -[/1 143 -[/1 144
-[/1 145 -[/1 146 -[/1 147 +[/1 148 -[/1 149
-[/1 150 -[/1 151 -[/1 152 -[/1 153 -[/1 154
-[/1 155 -[/1 156 -[/1 157 -[/1 158 -[/1 159
-[/1 160 -[/1 161 -[/1 162 -[/1 163 -[/1 164
-[/1 165 +[/1 166 -[/1 167 -[/1 168 -[/1 169
-[/1 170 -[/1 171 -[/1 172 -[/1 173 -[/1 174
-[/1 175 -[/1 176 -[/1 177 -[/1 178 -[/1 179
-[/1 180 +[/1 181 -[/1 182 -[/1 183 -[/1 184
-[/1 185 -[/1 186 -[/1 187 -[/1 188 -[/1 189
-[/1 190 -[/1 191 -[/1 192 -[/1 193 -[/1 194
-[/1 195 +[/1 196 -[/1 197 -[/1 198 -[/1 199
-[/1 200 -[/1 201 -[/1 202 -[/1 203 -[/1 204
-[/1 205 -[/1 206 -[/1 207 -[/1 208 -[/1 209
-[/1 210 -[/1 211 -[/1 212 -[/1 213 -[/1 214
-[/1 215 -[/1 216 -[/1 217 -[/1 218 -[/1 219
-[/1 220 -[/1 221 -[/1 222 -[/1 223 -[/1 224
+[/1 225 -[/1 226 -[/1 227 -[/1 228 -[/1 229
-[/1 230 -[/1 231 -[/1 232 -[/1 233 -[/1 234
-[/1 235 -[/1 236 -[/1 237 -[/1 238 -[/1 239
-[/1 240 -[/1 241 -[/1 242 -[/1 243 -[/1 244
-[/1 245 -[/1 246 -[/1 247 -[/1 248 -[/1 249
-[/1 250 -[/1 251 -[/1 252 -[/1 253 -[/1 254
-[/1 255 -[/1 256 -[/1 257 -[/1 258 -[/1 259

-[/1 260 -[/1 261 -[/1 262 -[/1 263 -[/1 264
-[/1 265 -[/1 266 -[/1 267 -[/1 268 -[/1 269
-[/1 270 -[/1 271 -[/1 272 -[/1 273 -[/1 274
-[/1 275 -[/1 276 -[/1 277 -[/1 278 -[/1 279
-[/1 280 -[/1 281 -[/1 282 -[/1 283 -[/1 284
-[/1 285 -[/1 286 -[/1 287 -[/1 288 -[/1 289
-[/1 290 -[/1 291 +[/1 292 -[/1 293 -[/1 294
-[/1 295 -[/1 296 -[/1 297 -[/1 298 -[/1 299
-[/1 300 -[/1 301 -[/1 302 -[/1 303 -[/1 304
-[/1 305 -[/1 306 -[/1 307 -[/1 308 -[/1 309
-[/1 310 -[/1 311 -[/1 312 -[/1 313 -[/1 314
-[/1 315 -[/1 316 -[/1 317 -[/1 318 -[/1 319
-[/1 320 -[/1 321 -[/1 322 -[/1 323 -[/1 324
-[/1 325 -[/1 326 -[/1 327 -[/1 328 -[/1 329
-[/1 330 -[/1 331 -[/1 332 -[/1 333 -[/1 334
-[/1 335 -[/1 336 -[/1 337 -[/1 338 -[/1 339
-[/1 340 -[/1 341 -[/1 342 -[/1 343 -[/1 344

;

cnames

{0 External_surface_of_dorsal_cranial_bones smooth slightly_grooved
heavily_ornamented_with_deep_pits_and_grooves;

{1 Skull_expansion_at_orbits gradual abrupt;

{2 Rostrum_proportions_narrow_oreinirostral broad_oreinirostral nearly_tubular playtrostral;

{3 Premaxilla_participation_in_internarial_bar_forming_at_least_the_ventral_half with_little_participation;

{4 Premaxilla_anterior_to_nares_narrow broad;

{5 External_nares_orientation_facing anterolaterally
dorsally_not_separated_by_premaxillary_bar_from_anterior_edge_of_rostrum
dorsally_separated_by_premaxillary_bar;

{6 Palatal_parts_of_premaxillae_extent_of_contact_do_not_meet_posterior_to_incisive_foramen
meet_posteriorly_along_contact_with_maxillae;

{7 Premaxilla_maxilla_contact_nature_of_contact_
premaxilla_loosely_overlies_maxilla_i.e._posterodorsal_process_of_the_premaxilla_overlaps_the_anterodorsal_s
urface_of_the_maxilla_sutured_together_along_a_butt_joint;

{8 Ventrally_opened_space_on_ventral_edge_of_rostrum_at_premaxilla_maxilla_contact_absent
present_as_a_notch present_as_a_large_fenestra;

{9 Posterior_palatal_branches_of_maxillae_anterior_to_palatines_nature_of_contact_do_not_meet
meet_extensively_but_posterior_most_parts_do_not_meet meet_entirely;

{10 Nasal_lacrimal_contact_present absent;

{11 Lacrimal_contact_with_nasal_location_of_contact_only_along_medial_edge_of_nasal
along_medial_and_anterior_edges_of_nasal;

{12 Nasal_contribution_to_narial_border_present absent;

{13 Nasal_premaxilla_contact_present absent;

{14 Descending_process_of_prefrontal_contact_with_palate_does_not_contact_palate contacts_palate;

{15 Postorbital_jugal_contact_configuration_of_contact_postorbital_anterior_to_jugal
postorbital_medial_to_jugal postorbital_lateral_to_jugal;

{16 Dorsoventral_size_of_anterior_part_of_jugal_with_respect_to_posterior_part_as_broad twice_as_broad;

{17 Jugal_bar_beneath_infratemporal_fenestra_shape_flattened rod_shaped;

{18 Quadratojugal_dorsal_process_width_and_contact_with_postorbital_
narrow_contacting_only_a_small_part_of_the_postorbital broad_extensively_contacting_postorbital;

{19 Frontal_width_between_orbits_narrow_as_broad_as_nasals broad_twice_as_broad_as_nasals;

{20 Frontals_paired unpaired;

{21 Dorsal_surface_of_frontal_and_parietal_flat with_midline_ridge;

{22 Parietao_postorbital_suture_absent_from_dorsal_surface_of_skull_roof_and_supratemporal_fossa
absent_from_dorsal_surface_of_skull_roof_but_broadly_present_with_supratemporal_fossa
present_within_supratemporal_fossa_and_on_dorsal_surface_of_skull_roof;

{23 Supratemporal_roof_conformation_of_dorsal_surface_complex
dorsally_flat_skull_table_developed_with_postorbital_and_squamosal_with_flat_shelves_extending_laterally_bey
ond_quadrate_contact;

{24 Postorbital_bar_external_texture_sculpted_if_skull_is_sculpted_unsculpted;

{25 Postorbital_bar_shape_transversely_flattened cylindrical;

{26 Vascular_opening_in_dorsal_surface_of_postorbital_bar_absent present;

{27 Postorbital_anterolateral_process_absent_or_poorly_developed well_developed_long_and_acute;

{28 Dorsal_part_of_postorbital_shape_in_dorsal_view_with_anterior_and_lateral_edges_only
with_anterolaterally_facings_edge;

{29 Dorsal_end_of_the_postorbital_bar_shape_nearing_skull_table_
broadens_dorsally_continuous_with_dorsal_part_of_postorbital
dorsal_part_of_the_postorbital_bar_constricted_distinct_from_the_dorsal_part_of_the_postorbital;

{30 Bar_between_orbit_and_supratemporal_fossa_shape_
broad_and_solid_with_broadly_sculpted_dorsal_surface_if_sculpture_is_present_on_skull
bar_narrow_sculpting_restricted_to_anterior_surface;

{31 Parietal_occipital_portion_with_broad_occipital_portion without_broad_occipital_portion;

{32 Parietal_with_broad_sculpted_region_separating_fossae
with_sagittal_crest_between_supratemporal_fossae;

{33 Postparietal_dermosupraoccipital_a_distinct_element not_distinct_fused_with_parietal ;

{34 Posterodorsal_corner_of_the_squamosal_shape_squared_off_lacking_extra_lobe_with_unsculpted_lobe ;

{35 Posterodorsal_process_of_squamosal_shape_
poorly_developed_and_projected_horizontally_at_the_same_level_of_the_skull
elongated_thin_and_posteriorly_directed_not_ventrally_deflected
elongated_posterolaterally_directed_and_ventrally_deflected;

{36 Palatines_extent_of_contact_on_palate_do_not_meet_on_palate_below_the_narial_passage
form_palatal_shelves_that_do_not_meet
meet_ventrally_to_the_narial_passage_forming_part_of_secondary_palate;

{37 Pterygoid_location_
restricted_to_palate_and_suspensorium_joints_with_quadrate_and_basisphenoid_overlapping
pterygoid_extends_dorsally_to_contact_laterosphenoid_and_form_ventrolateral_edge_of_the_trigeminal_foram
en_strongly_sutured_to_quadrate_and_laterosphenoid;

{38 Choanal_opening_conformation_in_palate_
continuous_with_pterygoid_ventral_surface_except_for_anterior_and anterolateral_borders
opens_into_palate_through_a_deep_midline_depression_choanal_groove ;

{39 Palatal_surface_of_pterygoids_smooth sculpted;

{40 Pterygoids_posterior_to_choanae_separated fused;

{41 Depression_on_primary_pterygoidean_palate_posterior_to_choana_
absent_or_moderate_in_size_being_narrower_than_palatine_bar;

{42 Primary_pterygoidean_palate_role_in_forming_choanal_opening_does_not_enclose_choana
completely_encloses_choana;

{43 Anterior_edge_of_choanae_location_situated_between_the_suborbital_fenestra_or_anteriorly_
situated_near_the_posterior_edge_of_suborbital_fenestra near_posterior_edge_of_pterygoid_flange;

{44 Quadrate_fenestration_without_fenestrae with_single_fenestrae
with_three_or_more_fenestrae_on_dorsal_and_posteromedial_surfaces;

{45 Posterior_edge_of_quadrate broad_medial_to_tympanum_gently_concave
posterior_edge_narrow_dorsal_to_otoccipital_contact_strongly_concave;

{46 Dorsal_primary_head_of_quadrate_articulates_with_squamosal_otoccipital_and_prootic
with_prootic_and_laterosphenoid;

{47 Ventrolateral_contact_of_otoccipital_with_quadrate_very_narrow broad;

{48 Quadrate_squamosal_and_otoccipital_formation_of_cranioquadrate_passage_
do_not_meet_to_enclose_cranioquadrate_passage_enclose_passage_near_lateral_edge_of_skull
meet_broadly_lateral_to_the_passage;

{49 Pterygoid_ramus_of_quadrate_ventral_edge_with_flat_ventral_edge
with_deep_groove_along_ventral_edge;

{50 Ventromedial_part_of_quadrate_contact_with_otoccipital_does_not_contact_otoccipital
contacts_otoccipital_to_enclose_carotid_artery_and_form_passage_for_cranial_nerves_IX_XI;

{51 Eustachian_tubes_relationship_with_basioccipital_and_basisphenoid_
not_enclosed_between_basioccipital_and_basisphenoid_entirely_enclosed;

{52 Basisphenoid_rostrum_cultriform_process_slender dorsoventrally_expanded;

{53 Basisphenoid_process_shape_prominent_forming_movable_joint_wiht_ptyergoid
small_or_absent_with_basisphenoid_joint_suturally_closed;

{54 Basisphenoid_ventral_surface_size_relative_to_basioccipital_shorter_than_the_basioccipital
wide_and_similar_to_or_longer_in_length_than_basioccipital;

{55 Basisphenoid_exposure_on_braincase_exposed_on_ventral_surface_of_braincase
virtually_excluded_from_ventral_surface_by_ptyergoid_and_basioccipital;

{56 Basioccipital_without_well_developed_bilateral_tuberosities with_large_pendulous_tubera;

{57 Otoccipital_without_laterally_concave_descending_flange_ventral_to_subcapsular_process with_flange;

{58 Cranial_nerves_IX_XI_passage_through_braincase_
pass_through_common_large_foramen_vagi_in_otoccipital
cranial_nerve_IX_passes_medial_to_nerves_X_and_XI_in_separate_passage;

{59 Otoccipital_ventral_to_parooccipital_process_without_large_ventrolateral_part with_large_ventrolateral_part;

{60 Crista_interfenestralis_between_fenestrae_pseudorotunda_and_ovalis_orientation_nearly_vertical horizontal;

{61 Supraoccipital_participation_in_foramen_magnum_forms_dorsal_edge_of_the_foramen_magnum
otoccipitals_broadly_meet_dorsal_to_the_foramen_magnum_separating_supraoccipital_from_foramen;

{62 Mastoid_antrum_location_does_not_extend_into_supraoccipital
extends_through_transverse_canal_in_supraoccipital_to_connect_middle_ear_regions;

{63 Posterior_surface_of_supraoccipital_nearly_flat with_bilateral_posterior_prominences;

{64 Palpebrals_number_absent one_small_palpebral_present_in_orbit one_large_palpebral
two_large_palpebrals;

{65 External_nares_divided_by_a_septum confluent;

{66 Antorbital_fenestra_size_as_large_as_orbit about_half_the_diameter_of_the_orbit
much_smaller_than_the_orbit absent;

{67 Supratemporal_fenestrae_extension_relatively_large_covering_most_of_surface_of_skull_roof
relatively_short_fenestrae_surrounded_by_a_flat_and_extended_skull_roof;

{68 Choanal_groove_ undivided partially_septated completely_septated;

{69 Dentary_relative_to_mandibular_fenestra_extends_posteriorly_beneath_mandibular_fenestra
does_not_extend_beneath_fenestra;

{70 Retroarticular_process_absent_or_extremely_reduced very_short_broad_and_robust
with_an_extensive_rounded_wide_and_flat_or_slightly_concave_surface_projected_posteroventrally_and_facing
_dorsomedially posteriorly_elongated_triangular_shaped_and_facing_dorsally
posteroventrally_projecting_and_paddle_shaped;

{71 Prearticular_present absent;

{72 Articular_medial_process_without_medial_process with_short_process_not_contacting_braincase
with_process_articulation_with_occipital_and_basisphenoid;

{73 Dorsal_edge_of_surangular_flat arched_dorsally;

{74 Mandibular_fenestra_present absent;

{75 Insertion_area_for_M.pterygoideous_posterior_does_not_extend_onto_lateral_surface_of_angular
extends_onto_lateral_surface_of_angular;

{76 Splenial_involvement_in_symphysis_in_ventral_view_not_involved involved_slightly_in_symphysis
extensively_involved;

{77 Posterior_premaxillary_teeth_size_similar_in_size_to_anterior_teeth
longer_but_does_not_form_an_enlarged_caniniform_tooth;

{78 Maxillary_teeth_waves_absent_no_tooth_size_variation one_wave_of_teeth_enlarged
enlarged_maxillary_teeth_curved_in_two_waves_festooned_;

{79 Anterior_dentary_teeth_opposite_premaxilla_maxilla_contact_
no_more_than_twice_the_length_of_other_dentary_teeth more_than_twice_the_length;

{80 Dentary_teeth_posterior_to_tooth_opposite_premaxilla_maxilla_contact_equal_in_size
enlarged_dentary_teeth_opposite_to_smaller_teeth_in_maxillary_toothrow;

{81 Anterior_and_posterior_scapular_edges_symmetrical_in_lateral_view
anterior_edge_more_strongly_concave_than_posterior_edge dorsally_narrow_with_straight_edges;

{82 Coracoid_length_up_to_two_thirds_of_the_scapular_length subequal_in_length_to_scapula;

{83 Anterior_process_of_iliac_length_relative_to_posterior_process_similar_in_length
one_quarter_or_less_of_the_length;

{84 Pubis_shape_rodlike_without_expanded_distal_end with_expanded_distal_end;

{85 Pubis_contribution_to_acetabulum_forms_anterior_half_of_ventral_edge_of_acetabulum
pubis_contacts_the_iliac_but_partially_excluded_from_the_acetabulum_by_the_anterior_process_of_the_ischium
pubis_completely_excluded_from_the_acetabulum_by_the_anterior_process_of_the_ischium;

{86 Distal_end_of_femur_lateral_facet_for_fibula_large very_small;

{87 Fifth_pedal_digit_phalanges_present absent;

{88 Atlas_intercentrum_size_broader_than_long_as_long_as_broad;

{89 Cervical_neural_spines_shape_all_anteroposteriorly_large only_posterior_spines_rodlike all_spines_rodlike;

{90 Hypapophyses_in_cervicodrsal_vertebrae_absent present_only_in_cervical_vertebrae
present_in_cervical_and_the_first_two_dorsal_vertebrae present_up_to_the_third_dorsal_vertebra
present_up_to_the_fourth_dorsal_vertebrae;

{91 Cervical_vertebrae_amphicoelous_or_amphyplatian procoelous;

{92 Trunk_vertebrae_amphicoelous_or_amphyplatian procoelous;

{93 All_caudal_vertebrae_amphicoelous_or_amphyplatian first_caudal_biconvex_with_other_procoelous
procoelous;

{94 Dorsal_osteoderms_shape_rounded_or_ovate rectangular_broader_than_long square
rectangular_longer_than_broad;

{95 Dorsal_osteoderms_anterior_margin_without_articular_anterior_process
with_a_discrete_convexity_on_anterior_margin
with_a_well_developed_process_located_anterolaterally_in_dorsal_parasagittal_osteoderms;

{96 Rows_of_dorsal_osteoderms_two_parallel_rows more_than_two more_than_four;

{97 Osteoderms_contact_with_one_another_some_or_all_imbricated sutured_to_one_another;

{98 Tail_osteoderms_dorsal_only completely_surrounded_by_osteoderms;

{99 Osteoderms_on_ventral_part_of_trunk_absent present;

{100 Osteoderms_longitudinal_keels_on_dorsal_surface_present absent;

{101 Jugal_relationship_with_antorbital_fossa_participates_in_margin_of_antorbital_fossa separated_from_it;

{102 Mandibular_symphysis_in_lateral_view_shallow_and_tapering_anteriorly deep_and_tapering_anteriorly
deep_and_anteriorly_convex shallow_and_anteriorly_convex;

{103 Articular_facet_for_quadrate_condyle_size_equal_in_length_to_the_quadrate_condyles slightly_longer;

{104 Jaw_joint_location_placed_at_level_with_basioccipital_condyle
below_basioccipital_condyle_about_above_level_of_lower_toothrow below_level_of_toothrow;

{105 Premaxillary_tooth_number_six five four three;

{106 Unsculptured_region_along_alveolar_margin_on_lateral_surface_of_maxilla_absent present;

{107 Maxilla_number_of_teeth_eight_or_more seven six five four;

{108 Coracoid_posteromedial_or_ventromedial_process_absent elongate_posteromedial_process_present
distally_expanded_ventromedial_process_present;

{109 Radiale_and_ulnare_size_short_and_massive elongate;

{110 Prefrontals_anterior_to_orbits_elongated_oriented_parallel_to_anteroposterior_axis_of_the_skull
short_and_broad_oriented_posteromedially_anterolaterally;

{111 Basioccipital_and_ventral_part_of_otoccipital_orientation_facing_posteriorly posteroventrally;

{112 Vertebral_centra_shape_cylindrical spool_shaped;

{113 Transverse_process_of_posterior_dorsal_vertebrae_shape_dorsoventrally_low_and_laminar dorsoventrally_high;

{114 Number_of_sacral_vertebrae two;

{115 Supra_acetabular_crest_present absent;

{116 Proximal_end_of_radiale_shape_expanded_symmetrically_similarly_to_the_distal_end more_expanded_proximolaterally_than_proximomedially;

{117 Lateral_surface_of_the_anterior_region_of_surangular_and_posterior_region_of_dentary_ without_a_longitudinal_depression with_a_longitudinal_depression;

{118 Ventral_exposure_of_splenials_absent present;

{119 Tooth_margin_carinae_without_carinae_or_with_smooth_or_crenulated_carinae with_homogeneous_denticulate_carinae_denticles_are_small_and_symmetrical_in_form_as_in_zipodont_teeth ;

{120 Lateral_surface_of_anterior_process_of_jugal_flat_or_convex with_broad_shelf_below_the_orbit_with_triangular_depression_underneath_it;

{121 Jugal_extension_below_the_orbit_does_not_exceed_the_anterior_margin_of_orbit exceeds_margin_of_orbit;

{122 Notch_in_premaxilla_on_lateral_edge_of_external_nares_absent;

{123 Dorsal_border_of_external_nares_formed_mostly_by_the_nasals formed_by_both_the_nasals_and_premaxilla;

{124 Posterodorsal_process_of_premaxilla_absent present_extending_posteriorly_wedging_between_maxilla_and_nasals;

{125 Premaxilla_maxilla_suture_in_palatal_view_medial_to_alveolar_region_orientation_of_suture_ anteromedially_directed sinusoidal_posteromedially_directed_on_its_lateral_half_and_anteromedially_directed_along_its_medial_region posteromedially_directed straight posteromedially_curved_U_shaped_;

{126 Nasal_lateral_border_posterior_to_external_nares_laterally_concave straight;

{127 Nasal_lateral_edges_nearly_parallel oblique_to_each_other_converging_anteriorly oblique_to_each_other_diverging_anteriorly;

{128 Palatine_anteromedial_margin_ exceeding_the_anterior_margin_of_the_palatal_fenestrae_extending_anteriorly_between_the_maxillae;

{129 Dorsoventral_height_of_jugal_antorbital_region_with_respect_to_infraorbital_region equal_or_lower antorbital_region_more_expanded_than_infraorbital_region_of_jugal;

{130 Maxilla_lacrimal_contact_partially_included_in_antorbital_fossa completely_included;

{131 Lateral_eustachian_tube_openings_location_located_posteriorly_to_the_medial_opening aligned_anteroposteriorly_and_dorsoventrally;

{132 Anterior_process_of_ectopterygoid_developed reduced_absent;

{133 Posterior_process_of_ectopterygoid_developed_reduced_absent;

{134
Small_foramen_located_in_the_premaxillo_maxillary_suture_in_lateral_surface_not_for_big_mandibular_teeth_absent_present;

{135 Jugal_posterior_process_extent_of_process_exceeding_posteriorly_the_infratemporal_fenestrae_does_not_exceed_infratemporal_fenestrae;

{136 Compressed_crown_of_maxillary_teeth_orientation_oriented_parallel_to_the_longitudinal_axis_of_skull;

{137 Large_and_aligned_neurovascular_foramina_on_lateral_maxillary_surface_absent_present;

{138 External_surface_of_maxilla_and_premaxilla_general_shape_with_a_single_plane_facing_laterally_with_ventral_region_facing_laterally_and_dorsal_region_facing_dorsolaterally;

{139 Maxillary_teeth_lateral_compression_absent
present_compression_asymmetrically_occurring_only_along_distal_margin_giving_teeth_a_teardrop_shape
present_lateral_compression_symmetrically_developed;

{140 Posteroventral_corner_of_quadrate_reaches_the_quadrate_condyles
does_not_reach_the_quadrate_condyles;

{141 Base_of_postorbital_process_of_jugal_orientation_directed_posterodorsally directed_dorsally
directedanterodorsally;

{142 Postorbital_process_of_jugal_location_on_jugal_anteriorly_placed_in_the_middle posteriorly_places;

{143 Postorbital_ectopterygoid_contact_present_absent;

{144 Quadrate_ornamentation_absent_ornamented_on_the_base;

{145 Prefrontal_maxillary_contact_in_the_inner_anteromedial_region_of_orbit_absent_present;

{146 Basisphenoid_exposure_on_braincase_without_lateral_exposure_with_lateral_exposure;

{147 Quadrate_process_of_ptyergoids_well_developed;

{148 Quadrate_major_axis_direction_of_orientation_posteroventrally;

{149 Quadrate_distal_end_with_only_one_plane_facing_posteriorly
with_two_distinct_faces_in_posterior_view_a_posterior_one_and_anterior_one_bearing_the_foramen_aereum;

{150 Anteroposterior_development_of_neural_spine_in_axis_well_developed_covering_all_the_neural_arch_length;

{151 Prezygapophyses_of_axis_development_relative_to_neural_arch_not_exceeding_edge_of_neural_arch
exceeding_the_anterior_margin_of_neural_arch;

{152 Postzygapophyses_of_axis_well_developed_curved_laterally_poorly_developed;

{153 Shape_of_dentary_symphysis_in_ventral_view_tapering_anteriorly_forming_an_angle
U_shaped_smoothly_curving_anteriorly;

{154 Unsculpted_region_in_the_dentary_below_the_tooth_row_absent_present;

{155 Suranglur_contribution_to_the_glenoid_fossa_forms_only_the_lateral_wall_of_glenoid
forms_approximately_one_third_of_the_glenoid;

{156 Femur_anterior_margin_linear_bears_flange_for_coccygeofemoralis_musculature;

{157 Dentary_lateral_surface_smooth_lateral_to_seventh_alveolous
with_lateral_concavity_for_the_reception_of_the_enlarged_maxillary_tooth;

{158 Dorsal_edge_of_dentary_slightly_concave_or_straight_and_subparallel_to_the_longitudinal_axis_of_skull
straight_with_an_abrupt_dorsal_expansion_being_straight_posteriorly
with_a_single_dorsal_expansion_and_concave_posterior_to_this_sinusoidal_with_two_concave_waves;

{159 Dentary_compression_and_lateroventral_surface_anterior_to_mandibular_fenestra_
compressed_and_vertical_not_compressed_and_convex;

{160 Splenial_posterior_to_symphysis_thin_robust_dorsally;

{161 Cheek_teeth_not_constricted_at_base_of_crown_constricted;

{162 Ventral_edge_of_premaxilla_location_relative_to_maxilla_
at_the_same_height_as_the_ventral_edge_of_maxilla
located_deeper_with_the_dorsal_contour_of_anterior_part_of_dentary_strongly_concave;

{163 Maxillary_dental_implantation_teeth_in_isolated_alveoli_located_on_a_dental_groove;

{164 Caudal_tip_of_nasals_converge_at_sagittal_plane
caudally_separated_by_anterior_sagittal_projection_of_frontals;

{165 Relative_length_between_squamosal_and_postorbital_squamosal_is_longer_postorbital_is_longer;

{166 Jugal_portion_of_postorbital_bar_relative_to_lateral_surface_of_jugal_flush_with_lateral_surface
anteriorly_continuous_but_posteriorly_inset
medially_displaced_and_a_ridge_separate_postorbital_bar_from_lateral_surface_of_jugal;

{167 Outer_surface_of_squamosal_laterodorsally_oriented_extensive_reduced_and_sculpted
reduced_and_unsculpted;

{168 Quadratojugal_spine_at_caudal_margin_of_infratemporal_fenestra_absent_present;

{169 Quadrate_condyles_poorly_developed_intercondylar_groove
medial_condyle_expands_ventrally_being_separate_from_the_lateral_condyle_by_a_deep_intercondylar_groove
;

{170 Exposure_of_supraoccipital_in_skull_roof_absent_present;

{171 Nasal_participation_in_antorbital_fenestra_present_absent;

{172 Anterior_opening_of_temporo_orbital_canal_in_dorsal_exposed
hidden_in_dorsal_view_and_overlapped_by_squamosal_rim_of_supratemporal_fossa;

{173 Foramen_intramandibularis_oralis_small_or_absent;

{174 Coronoid_size_short_and_located_below_the_dorsal_edge_of_the_mandibular_ramus;

{175 Width_of_root_of_teeth_with_respect_to_crown_narrower_or_equal_wider;

{176 Gap_in_cervico_thoracic_dorsal_armor_absent_present;

{177 Lateral_contour_of_snout_in_dorsal_view_straight sinusoidal;

{178 Pterygoidean_flanges_laminar_and_expanded;

{179 Ectopterygoid_medial_process_shape_single_process;

{180 Skull_roof_shape_in_dorsal_view_rectangular trapezoidal;

{181 Prefrontal_pillars_when_integrated_in_palate_pillars_transversely_expanded
transversely_expanded_in_their_dorsal_part_and_columnar_ventrally
longitudinally_expanded_in_their_dorsal_part_and_columnar_ventrally;

{182 Ventral_edge_of_maxilla_in_lateral_view_straight_or_convex sinusoidal;

{183 Position_of_first_enlarged_maxillary_teeth_second_or_third_alveoli fourth_or_fifth;

{184 Splenial_dentary_suture_at_symphysis_on_ventral_surface_v_shaped transversal;

{185 Posterior_peg_at_symphysis_absent present;

{186 Posterior_ridge_on_glenoid_fossa_of_articular_present absent;

{187 Cusps_of_teeth_number_and_conformation_one_unique_cusp
one_main_cusp_with_smaller_cusps_arranged_in_one_row
one_main_cusp_with_smaller_cusps_arranged_in_more_than_one_row
several_cusps_of_equal_size_arranged_in_more_than_one_row;

{188 Dorsal_surface_of_mandibular_symphysis_flat_or_slightly_concave;

{189 Medial_surface_of_splenials_posterior_to_symphysis_flat_or_slightly_convex;

{190 Choanal_septum_shape_narrow_vertical_bony_sheet T_shaped_bar_expanded_ventrally;

{191 Cross_section_of_distal_end_of_quadrate_mediolaterally_wide_and_anteroposteriorly_thin
subquadrangular;

{192 Lateral_surface_of_dentaries_below_alveolar_margin_at_mid_to_posterior_region_of_tooth_row_
vertically_oriented_continuous_with_rest_of_lateral_surface_of_the_dentaries
flat_surface_exposed_laterodorsally_divided_by_a_ridge_from_rest_of_the_lateral_surface_of_the_dentaries;

{193 Palatine_ptyergoid_contact_on_palate_palatines_overlies_ptyergoids
palatines_firmly_sutured_to_ptyergoids;

{194 Ectopterygoid_main_axis_orientation_laterally_or_slightly_anterolaterally
anteriorly_subparallel_to_the_skull_longitudinal_axis;

{195 Squamosal_descending_process_absent present;

{196 Development_of_distal_quadrate_body_ventral_to_otoccipital_quadrate_contact_distinct
incipiently_distinct indistinct;

{197 Pterygoid_flanges_size_thin_and_laminar dorsoventrally_thick_with_pneumatic_spaces;

{198 Postorbital_participation_in_infratemporal_fenestra_almost_or_entirely_excluded
bordering_infratemporal_fenestra;

{199 Palatines_contribution_to_suborbital_fenestra_form_margin_of_suborbital_fenestra excluded_from_margin_of_suborbital_fenestra;

{200 Angular_posterior_to_mandibular_fenestra_location_on_mandible_ widely_exposed_on_lateral_surface_of_mandible shifted_to_the_ventral_surface_of_mandible;

{201 Posteroventral_edge_of_mandibular_ramus_shape_straight_or_convex markedly_deflected;

{202 Quadrate_ramus_of_pterygoid_width_in_ventral_view_narrow broad;

{203 Pterygoids_contact_on_palate_not_in_contact_anterior_to_basisphenoid_on_palate pterygoids_in_contact;

{204 Olecranon_well_developed absent;

{205 Cranial_table_width_with_respect_to_ventral_portion_of_skull_as_wide_as_ventral_portion narrower_than_ventral_portion_of_skull;

{206 Depression_on_posterolateral_surface_of_maxilla_absent present;

{207 Paired_anterior_palatal_fenestra_absent present;

{208 Paired_ridges_located_medially_on_ventral_surface_of_basisphenoid_absent present;

{209 Ventral_margin_of_infratemporal_bar_of_jugal_straight dorsally_arched;

{210 Posterolateral_end_of_quadratejugal_shape_and_relationship_with_quadrate_ acute_or_rounded_tightly_overlapping_the_quadrate with_sinusoidal_ventral_edge_and_wide_and_rounded_posterior_edge_slightly_overhanging_the_lateral_surface_of_the_quadrate;

{211 Quadrate_body_distal_to_otoccipital_quadrate_orientation_of_contact_in_posterior_view_ ventrally_oriented ventrolaterally_oriented;

{212 Wedge_like_process_of_the_maxilla_in_lateral_surface_of_premaxilla_maxilla_absent;

{213 Palpebrals_separated_from_the_lateral_edge_of_the_frontal extensively_sutured_to_each_other_and_to_the_lateral_margin_of_the_frontals;

{214 External_surface_of_ascending_process_of_jugal_exposed_laterally exposed_posterolaterally;

{215 Longitudinal_ridge_on_lateral_surface_of_jugal_below_infratemporal_fenestra_absent present_running_entire_length_of_of_posterior_process_of_jugal present_running_entire_length_of_jugal;

{216 Dorsal_surface_of_posterolateral_region_of_squamosal_without_ridges with_three_curved_ridges_oriented_longitudinally;

{217 Ridge_along_dorsal_section_of_quadrate_quadratejugal_contact_absent present;

{218 Sharp_ridge_on_the_surface_of_the angular_absent present_on_the_ventral_most_margin present_along_the_lateral_surface;

{219 Longitudinal_ridge_along_the_dorsolateral_surface_of_surangular_absent present;

{220 Dorsal_surface_of_osteoderms_ornamented_withanterolaterally_andanteromedially_directed_ridges_fleur_delys_pattern_of_Osmolska_et_al._1997_absent present;

{221 Cervical_region_surrounded_by_lateral_and_ventral_osteoderms_sutured_to_the_dorsal_elements_absent present;

{222 Appendicular_osteoderms_absent present;

{223 Supratemporal_fenestra_present absent;

{224 Flate_ventral_surface_of_internal_nares_septum_parallel_sided tapering_anteriorly;

{225 Perinarial_fossa_restricted_extension;

{226 Premaxillary_palate_circular_paramedian_depressions_absent present_located_anteriorly_on_the_premaxilla;

{227 Nasals_shape_of_posterolateral_region_flat_surface_facing_dorsally;

{228 Lacrimal_posterior_extent_and_relationship_with_jugal_extends_ventroposteriorly_widely_contacting_the_jugal tapers_ventroposteriorly_does_not_contact_or_contacts_the_jugal_only_slightly;

{229 Jugal_large_foramen_on_the_lateral_surface_near_the_anterior_margin_absent;

{230 Procumbent_premaxillary_alveoli_absent;

{231 Palatines_orientation_run_parasagittally_along_midline;

{232 Ectopterygoid_participation_in_the_palatine_bar_absent;

{233 Choanal_opening_opened_posteriorly_and_continuous_with_pterygoid_surface closed_posteriorly_by_an_elevated_wall_formed_by_the_pterygoids;

{234 Ectopterygoid_extent_of_medial_projection_on_the_ventral_surface_of_pterygoid_flanges_barely_extended widely_extended_covering_approximately_the_lateral_half_of_the_ventral_surface_of_the_pterygoid_flanges;

{235 Evaginated_maxillary_alveolar_edges_absent present_as_a_continuous_sheet present_as_discrete_evaginations_at_each_alveoli;

{236 Premaxilla_foramen_in_perinarial_depression_absent;

{237 Frontal_anterior_ramus_with_respect_to_the_tip_of_the_prefrontal_ending_posteriorly ending_anteriorly;

{238 Premaxilla_anterior_alveolar_margin_orientation_vertical inturned;

{239 Premaxillary_tooth_row_orientation_arched_posteriorly_from_midline angled_posterolaterally_at_120_degree_angle;

{240 Last_premaxillary_tooth_position_relative_to_tooth_row_anterior anterolateral;

{241 Posterior_teeth_with_rings_of_undulated_enamel_absent;

{242 Maxilla_palatine_suture_shape_of_palatines_palatine_anteriorly_rounded palatine_anteriorly_pointed palatine_invaginated;

{243 Postorbital_bar_lateral_surface_formed_by_postorbital_and_jugal;

{244 Surangular_groove_enlarged_foramen_at_anterior_end_absent;

{245 Shape_of_antorbital_fossa_subcircular_or_subtriangular elongated_low_and_oriented_obliquely;

{246 Prefrontal_lateral_development_reduced;

{247 Foramen_for_the_internal_carotid_artery_reduced_similar_in_size_to_the_openings_of_cranial_nerves_IX_XI;

{248 Squamosal_posterolateral_region_lateral_to_paroccipital_process_narrow;

{249 Posteromedial_branch_of_squamosal_orientation_transversely_oriented posterolaterally_oriented;

{250 Squamosal_dorsal_margin_of_occipital_flange_straight;

{251 Sculpture_in_external_surface_of_rostrum_absent present;

{252 Longitudinal_depressions_on_palatal_surface_of_maxillae_and_palatines_absent;

{253 Angle_between_medial_and_anterior_margins_of_supratemporal_fossa_approximately_90_degrees;

{254 Sacral_vertebrae_direction_of_transverse_processes_laterally;

{255 Prefrontal_and_lacrimar_around_orbits_forming_flat_rims evaginated_forming_elevated_rims;

{256 Nasal_bones_paired_partially_or_completely_fused;

{257 Axial_neural_spines_width_of_posterior_half_wide narrow;

{258 Axial_hypophysis_deep_fork_present absent;

{259 Ulna_width_of_olecranon_process_narrow_and_subangular wide_and_rounded;

{260 M.teres_major_and_M.dorsalis_scapulae_insert_separately_on_humerus_scars_can_be_distinguished_dorsal_to_deltpectoral_crest insert_with_common_tendon_single_insertion_scar;

{261 Dentary_projection_of_anterior_alveoli_anterodorsally weakly_procumbent strongly_procumbent;

{262 Squamosal_dorsal_and_ventral_rims_of_squamosal_groove_for_external_ear_valve_musculature_parallel_or_squamosal_groove_flares_anteriorly;

{263 Ectopterygoid_contact_with_maxilla_near_toothrow_ectopterygoid_abuts_maxillary_toothrow maxilla_broadly_separates_ectopterygoid_from_maxillary_toothrow;

{264 Shallow_fossa_at anteromedial_corner_of_supratemporal_fenestra_present absent_anteromedial_corner_of_supratemporal_fenestra_smooth;

{265 Lateral_margins_of_the_frontal_relative_to_the_skull_surface_flush_with_skull_surface elevated_forming_ridged_orbital_margins;

{266 Laterosphenoid_orientation_of_capitate_process_laterally_oriented anteroposteriorly_oriented_toward_midline;

{267 Exoccipital_development_of_boss_and_paroccipital_process_boss_prominent_on_paroccipital_process_process_lateral_to_cranioquadrate_opening_short boss_small_or_absent_on_paroccipital_process_process_lateral_to_cranioquadrate_opening_long;

{268 Ectopterygoid_extent_along_lateral_pterygoid_flange_at_maturity_
extends_to_posterior_tip_of_lateral_pterygoid_flange does_not_extend_to_posterior_tip_of_lateral_pterygoid;

{269 Incisive_foramen_location_relative_to_premaxillary_toothrow_
foramen_situated_far_from_premaxillary_toothrow_at_the_level_of_the_second_or_third_alveolus
abuts_premaxillary_toothrow projects_between_first_premaxillary_teeth;

{270 Ventral_surface_of_choanal_septum_smooth_to_slightly_depressed marked_by_a_acute_groove
vomeral_septum_divided_by_into_bilateral_laminae;

{271 Proximal_most_portion_of_fibular_head_straight_sided_to_weakly_developed_posteriorly
very_sharply_projecting_posteriorly_forming_distinct_extension;

{272
Cervical_rib_shaft_posterior_process_posterodorsally_projecting_spine_at_the_junction_with_the_tubercular_pr
ocess_absent;

{273 Longitudinal_keels_on_dorsal_surface_of_osteoderms_restricted_to_the_posterior_edge_of_osteoderm
not_restricted_to_the_posterior_edge;

{274 Jugal_anteriorly_on_lateral_surface_below_orbits_lacks_a_depression possesses_a_depression;

{275 Transverse_ridge_crossing_the_frontal_anteromedial_to_the_orbits_absent present_as_a_ridge
present_as_prominent_anteriorly_curved_shelf_transverse_interorbital_crest_sensu_Andrade_and_Hornung_20
11_;

{276
Shallow_hemispherical_depression_on_the_lacrimal_and_or_prefrontal_anterior_to_the_orbital_margin_not_arti
culation_facet_for_palbebral_absent present;

{277 Anterior_half_of_interfenestral_bar_between_suborbital_fenestrae_
lateral_margins_are_parallel_to_subparallel flared_anteriorly;

{278 Posterior_half_of_interfenestral_bar_between_suborbital_fenestrae_
lateral_margins_are_parallel_to_subparallel flared_posteriorly;

{279 Angular_shape_of_posteroventral_margin_straight_or_gently_arched_dorsally strongly_arched_dorsally;

{280 Squamosal_lateral_margin_of_dorsal_surface_squared_off_with_continuous_ear_valve_groove
bears_a_prominent_depressed_area_just_anterior_to_the_posterior_lobe_of_the_squamosal_groove_for_ear_v
alve_discontinuous;

{281 Fibula_shaft_distal_to_iliofibularis_trochanter_straight bowed_posteriorly;

{282 Scapular_blade_width_no_more_than_twice_the_length_of_the_scapulocoracoid_articulation
scapular_blade_very_broad_and_greater_than_twice_the_length_of_the_scapulocoracoid_articulation;

{283 Vomer_exposure_on_palate_exposed unexposed;

{284 Supraoccipital_when_present_on_dorsal_skull_roof_
with_narrow_exposure_parietal_forms_portion_of_occipital_surface
with_broad_exposure_parietal_does_not_form_portion_of_occipital_surface;

{285 Jugal_anterior_and_posterior_processes_inline_dorsoventrally;

{286 Lateral_expansion_of_posterodorsal_edge_of_surangular_anterior_to_glenoid_fossa_absent present;

{287

In_lateral_view_anterior_process_of_the_squamosal_extending_to_the_orbital_margin_overlapping_the_postorbital_absent present;

{288 In_lateral_view_surangular_and_dentary_suture_simple_with_little_or_no_interdigitating;

{289 Prominent_depression_on_the_palate_near_alveolar_margin_at_the_level_of_the_6th_or_7th_alveolus_absent present;

{290 Pterygoid_ventral_surface_of_ptyerygoid_flanges_parachanal_fossae_absent;

{291 Pterygoid_in_ventral_view_participation_in_the_suborbital_fenestra_ptyerygoid_forms_margin_of_suborbital_fenestra;

{292 Maxilla_lateral_surface_along_alveolar_margin_conformation_of_the_neurovascular_foramina_foramina_absent_or_form_a_single_continuous_row;

{293 Surface_of_tooth_enamel_smooth_or_slightly_crenulated;

{294 Posterior_molariform_teeth_wear_facets_absent present;

{295 Tooth_with_transitional_morphology_present_at_premax_max_contact absent;

{296 Basioccipital_midline_crest_on_basioccipital_plate_below_occipital_condyle absent present;

{297 Dorsal_osteoderms_accessory_ranges_of_osteoderms_sensu_Frey_1988_absent present;

{298 Maxillary_tooth_size_relative_to_maxillary_palatal_surface_in_palatal_view_proportionally_small_teeth_occupying_only_marginal_portion_of_ventral_surface_of_maxilla_proportionally_well_developed_teeth_occupying_large_area_of_maxillary_palatal_surface;

{299 Ventral_lamina_of_jugal_extends_far_anterior_to_the_ectopterygoid_ends_at_the_level_of_the_ectopterygoid;

{300 Surangular_extension_toward_posterior_end_of_retroarticular_process_along_entire_length_pinned_off_anterior_to_posterior_tip;

{301 Muscle_attachment_scars_on_ventral_surface_of_quadrate_ramus_form_modest_crests_prominent_knobs;

{302 Pterygoid_flange_shape_mediolaterally_broad_reaching_laterally_beyond_medial_margin_of_quadrate_condyles_relatively_narrow_does_not_reach_laterally_to_medial_margin_of_quadrate_condyles;

{303 In_ventral_view_posterior_process_of_maxilla_relative_to_ITF_excluded_from_ITF_forms_part_of_ITF;

{304 Highly_modified_ectopterygoid_mediolaterally_broad_and_flattened_with_greatly_expanded_absent_present_robust_anterior_process_larger_than_posterior_process_present_anterior_and_posterior_process_roughly_equal_in_size;

{305 In_ventral_view_palate_medial_to_toothrow_forms_a_single_continuous_surface_ridge_running_on_the_palate_medial_to_toothrow_formed_by_maxilla_and_ectopterygoid;

{306

Maxillary_tooth_row_penultimate_and_ultimate_maxillary_teeth_enlarged_and_highly_modified_crushing_tooth_absent present;

{307 Prefrontals do_not_meet_at_midline meet_at_midline;

{308 Pear_shaped_external_naris absent present;

{309 Skull_dorsal_surface_at_parietal_squamosal_contact surface_continuous_across_suture
suture_marked_by_groove_or_sulcus;

{310

Maxilla_lateral_surface_continuous_groove_or_sulcus_extending_from_orbital_margin_to_near_orbital_margin_to
wards_narial_opening absent present;

{311 Maxilla_posteromedial_process_curving_posteriorly_onto_palatine_formed_nasopharyngeal_passage
absent present;

{312 Squamosal_posterior_half_dorsal_and_ventral_rims_of_groove_for_external_ear_valve_musculature_
thin_or_parallel_sided flared_posteriorly;

{313 Lacrimal_in_dorsal_view_anterior_extent_on_rostrum_relative_to_prefrontal
prefrontal_extends_further_anteriorly lacrimal_extends_further_anteriorly
lacrimal_and_prefrontal_subequal_in_anterior_extent;

{314 Lacrimal_in_dorsal_view_mediolateral_width_relative_to_prefrontal
equal_to_or_less_than_width_of_prefrontal wider_than_prefrontal;

{315 Incisive_foramen_size small moderate large;

{316 Premaxillae_degree_of_contact_posterior_to_the_incisive_foramen extensive_contact narrow_contact;

{317 Posterior_margin_of_the_palatines_where_they_form_the_floor_of_the_nasopharyngeal_passage_shape
V_or_U_shaped straight;

{318 Posterior_margin_of_the_choanal_groove_location anteriorly_on_the_ptyergoids
posteriorly_on_the_ptyergoids_near_the_posterior_margin_of_ptyergoids;

{319 Pterygoid_palatine_contact_ventral_aspect_of_palate_shape_of_the_suture_transverse_or_nearly_so
prong_of_ptyergoid_projects_anteriorly;

{320 On_palate_foramen_located_on_premaxilla_maxilla_suture_near_the_alveolar_border absent present;

{321 Ectopterygoid_ptyergoid_contact_in_ventral_view
complex_anterior_part_of_ectopterygoid_forming_suture_whereas_posterior_part_of_ectopterygoid_overlaps_t
he_ptyergoid sutured_along_entire_contact_no_part_of_ectopterygoid_overlapping_ptyergoid;

{322 Palatines_mediolateral_width_anterior_to_the_suborbital_fenestrae wide
narrow_constricted_between_the_palatal_processes_of_the_maxilla;

{323 Ventral_tubercle_of_proatlas_width_relative_to_dorsal_crest;

{324 Fused_proatlas_shape;

{325 Proatlas_anterior_process;

{326 Proatlas_dorsal_keel_size;

{327 Atlas_intercentrum_shape_in_lateral_view_;

{328 Atlantal_rib_shape_of_dorsal_margin;

{329 Atlantal_rib_medial_laminae;

{330 Atlantal_ribs_articular_facet;

{331 Axila_rib_width_of_tuberculum;

{332 Axial_rib_tuberculum_diapophysis_contact;

{333 Axis_neural_spine_orientation_of_anterior_half;

{334 Axis_neural_spine_shape;

{335 Axis_neural_spine_posterior_half_shape;

{336 Axis_neural_arch_lateral_process_diapophysis_;

{337 Axis_location_of_hypapophysis;

{338 Axis_hypapophysis_with_deep_fork;

{339 Axis_hyapophyseal_keels_present_up_to;

{340 Third_cervical vertebra_first_postaxial_presence_of_prominent_hypapophysis;

{341 Choana_at_maturity_projects;

{342 posterior_margin_of_suborbital_process_of_ectopterygoid_in_ventral_view_straight_or_concave_convex;

{343
large_laterally_displaced_and_adjoining_maxillary_and_dentary_alveoli_holding_double_caniniform_dentition_absent_present;

{344
posterior_margin_of_the_pterygoid_wing_mediolaterally_oriented_or_posterolaterally_oriented_being_straight_or_concave;

;

Ancstates

-0 -1 -2 -3 -4 -5 -6 -7 -8 -9

-10 -11 -12 -13 -14 -15 -16 -17 -18 -19

-20 -21 -22 -23 -24 -25 -26 -27 -28 -29

-30 -31 -32 -33 -34 -35 -36 -37 -38 -39

-40 -41 -42 -43 -44 -45 -46 -47 -48 -49

-50 -51 -52 -53 -54 -55 -56 -57 -58 -59

-60 -61 -62 -63 -64 -65 -66 -67 -68 -69

-70 -71 -72 -73 -74 -75 -76 -77 -78 -79

-80 -81 -82 -83 -84 -85 -86 -87 -88 -89
-90 -91 -92 -93 -94 -95 -96 -97 -98 -99
-100 -101 -102 -103 -104 -105 -106 -107 -108 -109
-110 -111 -112 -113 -114 -115 -116 -117 -118 -119
-120 -121 -122 -123 -124 -125 -126 -127 -128 -129
-130 -131 -132 -133 -134 -135 -136 -137 -138 -139
-140 -141 -142 -143 -144 -145 -146 -147 -148 -149
-150 -151 -152 -153 -154 -155 -156 -157 -158 -159
-160 -161 -162 -163 -164 -165 -166 -167 -168 -169
-170 -171 -172 -173 -174 -175 -176 -177 -178 -179
-180 -181 -182 -183 -184 -185 -186 -187 -188 -189
-190 -191 -192 -193 -194 -195 -196 -197 -198 -199
-200 -201 -202 -203 -204 -205 -206 -207 -208 -209
-210 -211 -212 -213 -214 -215 -216 -217 -218 -219
-220 -221 -222 -223 -224 -225 -226 -227 -228 -229
-230 -231 -232 -233 -234 -235 -236 -237 -238 -239
-240 -241 -242 -243 -244 -245 -246 -247 -248 -249
-250 -251 -252 -253 -254 -255 -256 -257 -258 -259
-260 -261 -262 -263 -264 -265 -266 -267 -268 -269
-270 -271 -272 -273 -274 -275 -276 -277 -278 -279
-280 -281 -282 -283 -284 -285 -286 -287 -288 -289
-290 -291 -292 -293 -294 -295 -296 -297 -298 -299
-300 -301 -302 -303 -304 -305 -306 -307 -308 -309
-310 -311 -312 -313 -314 -315 -316 -317 -318 -319
-320 -321 -322 -323 -324 -325 -326 -327 -328 -329
-330 -331 -332 -333 -334 -335 -336 -337 -338 -339
-340 -341 -342 -343 -344 ;

xgroup

;

agroup

;

taxcode

+0 +1 +2 +3 +4 +5 +6 +7

+8 +9 +10 +11 +12 +13 +18 +19

+20 +21 +22 +23 +24 +25 +26 +27

+28 +29 +30 +31 +32 +33 +34 +35

+36 +37 +38 +39 +40 +41 +42 +43

+44 +45 +46 +47 +48 +49 +50 +51

+52 +53 +54 +55 +56 +57 +58 +59

+60 +61 +62 +63

;